

USING MODAL ANALYSIS TO INVESTIGATE BAT-BALL  
PERFORMANCE OF BASEBALL BATS

BY

ANDREW D. SUTTON  
B.S. UNIVERSITY OF MASSACHUSETTS LOWELL (2008)

SUBMITTED IN PARTIAL FULFILLMENT OF THE REQUIREMENTS  
FOR THE DEGREE OF MASTER OF SCIENCE  
DEPARTMENT OF MECHANICAL ENGINEERING  
UNIVERSITY OF MASSACHUSETTS LOWELL

Signature of Author: \_\_\_\_\_

ANDREW D SUTTON

Date: \_\_\_\_\_

Signature of Thesis

Supervisor: \_\_\_\_\_

JAMES A. SHERWOOD, PH.D. MECHANICAL ENGINEERING DEPARTMENT, UMASS  
LOWELL

Committee Member Signature: \_\_\_\_\_

PETER AVITABILE, PH.D. MECHANICAL ENGINEERING DEPARTMENT, UMASS  
LOWELL

Committee Member Signature: \_\_\_\_\_

DANIEL A. RUSSELL, PH. D PHYSICS DEPARTMENT, KETTERING UNIVERSITY

USING MODAL ANALYSIS TO INVESTIGATE BAT-BALL  
PERFORMANCE OF BASEBALL BATS

BY

ANDREW D. SUTTON  
B.S. UNIVERSITY OF MASSACHUSETTS LOWELL (2010)

SUBMITTED IN PARTIAL FULFILLMENT OF THE REQUIREMENTS  
FOR THE DEGREE OF MASTER OF SCIENCE  
DEPARTMENT OF MECHANICAL ENGINEERING  
UNIVERSITY OF MASSACHUSETTS LOWELL

Signature of Author:

ANDREW D SUTTON

Date: MAY 14, 2010

Signature of Thesis Supervisor:

JAMES A. SHERWOOD, PH.D. MECHANICAL ENGINEERING DEPARTMENT, UMASS LOWELL

Committee Member Signature:

PETER AVITABILE, PH.D. MECHANICAL ENGINEERING DEPARTMENT, UMASS LOWELL

DANIEL A. RUSSELL, PH. D     PHYSICS DEPARTMENT, KETTERING UNIVERSITY

USING MODAL ANALYSIS TO INVESTIGATE BAT-BALL  
PERFORMANCE OF BASEBALL BATS

BY

ANDREW D. SUTTON

SUBMITTED IN PARTIAL FULFILLMENT OF THE REQUIREMENTS  
FOR THE DEGREE OF MASTER OF SCIENCE  
DEPARTMENT OF MECHANICAL ENGINEERING  
UNIVERSITY OF MASSACHUSETTS LOWELL  
2010

Thesis Supervisor: James A. Sherwood, Ph.D.  
Professor, Department of Mechanical Engineering

## ABSTRACT

The relationship between the vibration response of wood and nonwood baseball bats and batted-ball performance was investigated for a representative set of collegiate and major league bats of various lengths. The nonwood bats had hollow barrels of either aluminum or fiber-reinforced composite. The bats were performance tested using a high-speed air cannon where the baseball was projected at a stationary bat. Performance metrics of Ball Exit Speed Ratio (BESR), Batted-Ball Speed (BBS) and Bat-Ball Coefficient of Restitution (BBCOR) were calculated using the speeds measured in the air cannon tests and the appropriate physical properties of the bats and balls. Modal analysis was performed on the bats to measure the first and second bending mode frequencies for the wood and nonwood bats and to measure the first and second hoop mode frequencies of the nonwood bats. The hoop modes were used to examine the trampoline effect of the hollow nonwood bats. A nonlinear mass-spring-damper model was used to explore the effect of the hoop-mode frequency on performance. For wood bats, it was found that the performance increases as the frequency of the first bending mode increases. For nonwood bats, it was observed that the performance increases as the frequency of the first hoop mode approaches the optimal value which is ~1250 Hz.

## ACKNOWLEDGMENTS

I would like to acknowledge the NCAA (Ty Halpin and Todd Petr) for allowing me to use baseball bats submitted for certification testing to be used for study in this thesis.

In addition, I would like to thank the following individuals for their support and help with this research.

- Prof. James Sherwood, my graduate advisor, for allowing me to have the opportunity to perform this research at the Baseball Research Center and for lending his expertise and support throughout my college career.
- Prof. Peter Avitabile, for all his help and support with modal analysis and vibrations studies.
- Prof. Daniel Russell, for all his support and help of modeling the bat-ball collision.
- Patrick Drane, for all of his support and advice on testing and analysis.
- Glen Bousquet for allowing the use of mechanical engineering laboratory equipment.
- All of the graduates and undergraduates from the UMLBRC and ACMTRL and Modal lab for giving me their support: Josh Jones, Matt Broe, Brian Munroe, Tim Connelly, Renzo Colossimo, Evan Gauthier, Steve Natoli, Jacqueline Buckley, Zeke Radik, Nicole Rondo, Dr. Samira Farboodmanesh, John Fitek, Joe Sargent, Konstantine Fetfatsidis, Dave Cloutier, and Chris Warren
- I must thank my Father Charlie, Mother Mary, Sister Elizabeth, and most importantly I must thank my Wife Julie, for their continuous support and encouragement throughout my life.

## Terminology

**BESR: Ball Exit Speed Ratio;** Bat performance test based on inbound and rebound speeds of the baseball.

**BBCOR: Bat Ball Coefficient Of Restitution;** Bat performance test based on inbound and rebound speeds of the baseball, physical properties of the bat, and the mass of the baseball.

**BBS: Batted-Ball Speed;** Calculation of the projected speed of the baseball in the field based on data from an inbound/rebound performance test and an empirical swing-speed model.

**COR: Coefficient Of Restitution;** Measure of the liveliness of the baseball by comparing the inbound and rebound speeds of a ball impacting a stationary wall.

**CCOR: Cylindrical Coefficient Of Restitution;** Measure of the liveliness of the baseball by comparing the inbound and rebound speeds of a ball impacting a steel cylindrical surface.

**MOI: Moment Of Inertia;** Often referred to as the ‘swing weight’ of the bat.

**DROP:** The numerical difference between the weight of the bat in ounces and the length of the bat in inches.

## Table of Contents

1	INTRODUCTION .....	1
2	BACKGROUND .....	4
2.1	BAT PROPERTIES.....	4
2.1.1	Bat Construction .....	4
2.1.2	Drop .....	5
2.1.3	Moment of Inertia (MOI).....	6
2.2	SWING SPEED.....	6
2.3	PERFORMANCE METRICS .....	8
2.3.1	Ball Exit Speed Ratio (BESR) .....	8
2.3.2	Batted-Ball Speed (BBS) .....	10
2.3.3	Bat-Ball Coefficient of Restitution (BBCOR).....	10
2.4	DYNAMIC RESPONSE OF BASEBALL BATS.....	11
2.4.1	Previous Research on the Vibration Response of Bats.....	13
2.5	SUMMARY .....	17
3	METHODOLOGY .....	18
3.1	BAT IDENTIFICATION .....	18
3.2	BASEBALL BAT PROFILING .....	19
3.2.1	Bat Profiling – Moment of Inertia .....	20
3.3	LAB CONDITIONS .....	21
3.4	BASEBALL CONDITIONS.....	22
3.5	PERFORMANCE TESTING .....	23
3.6	MODAL ANALYSIS .....	26
3.7	SUMMARY .....	30
4	RESULTS .....	31
4.1	WOOD BAT DATA .....	32
4.1.1	Performance versus MOI .....	32
4.1.2	Performance vs. Drop .....	35
4.1.3	Correlation of Wood Bat Dynamic Response to Performance .....	38
4.2	PERFORMANCE VS. MOI FOR NONWOOD BASEBALL BATS.....	43
4.2.1	BESR vs. MOI for Nonwood Bats.....	43
4.2.2	BBS vs. MOI for Nonwood Baseball Bats .....	47

4.2.3	BBCOR vs. MOI for Nonwood Baseball Bats .....	51
4.3	PERFORMANCE VS. BENDING FREQUENCY FOR NONWOOD BASEBALL BATS.....	55
4.3.1	BESR vs. Bending Frequencies .....	55
4.3.2	BBS vs. First Bending Frequency.....	58
4.3.3	BBCOR versus First Bending Frequency.....	61
4.4	MODELING THE TRAMPOLINE EFFECT OF A HOLLOW BASEBALL BAT .....	64
4.4.1	Bat Model.....	64
4.5	PERFORMANCE VS. THE FIRST HOOP FREQUENCY FOR NONWOOD BASEBALL BATS	
	68	
4.5.1	BESR vs. the First Hoop Frequency for Nonwood Bats .....	70
4.5.2	BBS versus the First Hoop Frequency for Nonwood Bats .....	73
4.5.3	BBCOR versus Hoop Frequency for Nonwood Bats .....	76
4.6	MONITORING A BASEBALL BAT GOING THROUGH AN ACCELERATED BREAK-IN	
	(ABI) PROCEDURE.....	78
4.7	THE EFFECT OF THE BASEBALL ON THE HOOP FREQUENCY DURING THE COLLISION	
	81	
4.8	SUMMARY.....	83
5	CONCLUSIONS.....	86
6	RECOMMENDATIONS.....	89
7	LITERATURE CITED.....	91
	APPENDIX A.....	A1
	APPENDIX B:.....	B1
	APPENDIX C.....	C1
	APPENDIX D.....	D1
	APPENDIX E:.....	E1



## List of Figures

Figure 1: Bending modes of baseball bats .....	12
Figure 2: Hoop modes of baseball bats.....	13
Figure 3: Mass-spring model of the ball-bat collision [8] .....	15
Figure 4: Normalized collision efficiency versus hoop frequency [8] .....	16
Figure 5: Hoop frequency versus batted ball speed [8] .....	17
Figure 6: MOI fixture.....	21
Figure 7: LVSports cannon.....	23
Figure 8: Light gate box.....	25
Figure 9: Baseball bat placed in the free-free condition .....	27
Figure 10: Accelerometer placements on the barrel of the bat .....	27
Figure 11: Coherence function of two accelerometers .....	28
Figure 12: Overlaid FRF from both accelerometers .....	28
Figure 13: BESR vs. MOI for wood bats.....	32
Figure 14: BBS vs. MOI for wood bats .....	34
Figure 15: BBCOR vs. MOI for wood bats .....	35
Figure 16: BESR vs. Drop for wood bats .....	36
Figure 17: BBS vs. Drop for wood bats.....	37
Figure 18: BBCOR vs. Drop for wood bats.....	38
Figure 19: BESR vs. First bending frequency for wood bats .....	40
Figure 20: Batted-ball speed vs. First bending frequency for wood bats .....	41
Figure 21: Bat-Ball COR vs. First bending frequency for wood bats .....	42
Figure 22: BESR vs. MOI for 31-in. nonwood bats .....	44
Figure 23: BESR vs. MOI for 32-in. nonwood bats .....	45
Figure 24: BESR vs. MOI for 33-in. nonwood bats .....	45
Figure 25: BESR vs. MOI for 34-in. nonwood bats .....	46
Figure 26: BESR vs. MOI for all lengths of nonwood bats.....	46
Figure 27: BBS vs. MOI for all 31-in. nonwood bats.....	48
Figure 28: BBS vs. MOI for all 32-in. nonwood bats.....	49
Figure 29: BBS vs. MOI for all 33-in. nonwood bats.....	49
Figure 30: BBS vs. MOI for all 34-in. nonwood bats.....	50
Figure 31: BBS vs. MOI for all nonwood bats .....	50
Figure 32: BBCOR vs. MOI for all 31-in. nonwood bats.....	52
Figure 33: BBCOR vs. MOI for all 32-in. nonwood bats.....	53
Figure 34: BBCOR vs. MOI for all 33-in. nonwood bats.....	53
Figure 35: BBCOR vs. MOI for all 34-in. nonwood bats.....	54
Figure 36: BBCOR vs. MOI for all nonwood bats .....	54
Figure 37: BESR vs. First bending frequency for all 31-in. nonwood bats.....	56

Figure 38: BESR vs. First bending frequency for all 32-in. nonwood bats.....	56
Figure 39: BESR vs. First bending frequency for all 33-in. nonwood bats.....	57
Figure 40: BESR vs. First bending frequency for all 34-in. nonwood bats.....	57
Figure 41: BESR vs. First bending frequency for all nonwood bats .....	58
Figure 42: BBS vs. First bending frequency for all 31-in. nonwood bats .....	59
Figure 43: BBS vs. First bending frequency for all 32-in. nonwood bats .....	59
Figure 44: BBS vs. First bending frequency for all 33-in. nonwood bats .....	60
Figure 45: BBS vs. First bending frequency for all 34-in. nonwood bats .....	60
Figure 46: BBS vs. First bending frequency for all nonwood bats.....	61
Figure 47: BBCOR vs. First bending frequency for all 31-in. nonwood bats .....	62
Figure 48: BBCOR vs. First bending frequency for all 32-in. nonwood bats .....	62
Figure 49: BBCOR vs. First bending frequency for all 33-in. nonwood bats .....	63
Figure 50: BBCOR vs. First bending frequency for all 34-in. nonwood bats .....	63
Figure 51: BBCOR vs. First bending frequency for all nonwood bats.....	64
Figure 52: Mass-spring-damper model of the baseball/bat collision.....	65
Figure 53: Analytical CCOR data compared to experimental data .....	67
Figure 54: Normalized collision efficiency versus Hoop frequency .....	68
Figure 55: BESR vs. Hoop frequency for all 31-in. nonwood bats .....	71
Figure 56: BESR versus Hoop frequency for all 32-in. nonwood bats .....	71
Figure 57: BESR versus Hoop frequency for all 33-in. nonwood bats .....	72
Figure 58: BESR versus Hoop frequency for all 34-in. nonwood bats .....	72
Figure 59: BBS versus Hoop frequency for all 31-in. nonwood bats.....	74
Figure 60: BBS versus Hoop frequency for all 32-in. nonwood bats.....	74
Figure 61: BBS versus Hoop frequency for all 33-in. nonwood bats.....	75
Figure 62: BBS versus Hoop frequency for all 34-in. nonwood bats.....	75
Figure F63: BBCOR versus Hoop frequency for all 31-in. nonwood bats.....	76
Figure F64: BBCOR versus Hoop frequency for all 32-in. nonwood bats.....	77
Figure F65: BBCOR versus Hoop frequency for all 33-in. nonwood bats.....	77
Figure 66: BBCOR versus Hoop frequency for all 34-in. nonwood bats.....	78
Figure 67: BESR vs. Hoop frequency for ABI test of one bat .....	79
Figure 68: BBS vs. Hoop frequency for ABI test of one bat.....	80
Figure 69: BBCOR vs. Hoop frequency for ABI test of one bat.....	80
Figure 70: (a) Baseball impacting an aluminum baseball bat (b) Finite element model of a baseball impacting an aluminum baseball bat.....	83
Figure A1: Aluminum cylinder in a simulated free-free condition with points labeled....	1
Figure A2: ME-Scope animation of the first mode shape of the aluminum cylinder.....	2
Figure A3: Measured FRF of aluminum cylinder using two accelerometers.....	3
Figure A4: Labeled barrel of baseball bat.....	4
Figure A5: ME-Scope animation of the first hoop mode of a baseball bat barrel .....	5
Figure A6: Accelerometers mounted on the barrel of the bat approximately 90 degrees apart.....	5
Figure A7: Baseball bat barrel FRF of two accelerometers overlaid.....	6
Figure C1 BBS vs. MOI for 32-in. nonwood bats with BBCOR certification bats.....	1
Figure C2: BBS vs. MOI for 33-in. nonwood bats with BBCOR cert bats .....	2
Figure C3: BBS vs. MOI for 34-in. nonwood bats with BBCOR cert bats .....	2
Figure E1: Roller used in ABI procedure .....	1

## List of Tables

Table 1: Swing-speed equation constants .....	7
Table 2: Inputs for spring-mass-damper model .....	65

## **1 INTRODUCTION**

Nonwood baseball bats were introduced to amateur baseball in the 1970s. The first nonwood bats were aluminum. These bats had an initial higher cost than wood baseball bats but were more durable than wood and could last an entire season or more. Youth leagues, high schools and colleges were drawn to the cost-saving potential offered by replacing their wood bats with aluminum bats. Bat designers soon found another potential in these bats over wood—increased batted-ball speeds (BBS). Over the past 40 years, these nonwood bats have become a majority of the bats sold in the baseball market and the cost advantage has been overshadowed by the performance advantage.

In the 1990s, aluminum baseball bats started to increase in performance as manufacturers began to understand how to take advantage of the additional design options that were available with a hollow bat design over that of solid wood. By reducing the weight of the bat, a player was able to swing the bat faster and make contact with the ball more consistently. Manufactures were able to increase the barrel size from wood, which had been typically around 2½ in., to 2¾ in. without adding

swing weight. It was soon realized that thin walls in the barrel could develop a “trampoline effect” on the barrel of the baseball bat. The trampoline effect is only found in hollow-barrel baseball bats and can be recognized by the pinging sound heard when the bat-ball collision takes place on aluminum-barrel bats.

In the past decade, manufacturers have also been producing bats made of composite materials, using carbon and glass fibers embedded in a resilient polymer matrix. Composites can exhibit good damping and, hence, can be used to help reduce the stinging sensation a player feels in his hands when the baseball is not hit on the “sweet spot” location of the barrel. However, the biggest advantage composites have is the ability to design and control the properties of the bat more than what can be done with aluminum. In contrast to the ping of aluminum bats, composite-barrel bats make a “thud” sound during the impact with the ball.

The trampoline effect and the stinging sensation are due to modal characteristics of the bat. The stinging sensation can be attributed to the bending modes over the length of the bat, in which the bat bends and flexes much like a guitar string. The trampoline effect is a dynamic response of the barrel of the bat where the barrel moves in and out, as in a trampoline, during the collision between the bat and the ball. The trampoline effect is also known as a hoop mode (or bell mode) of the barrel of the bat.

Previous research has been performed to investigate the “inertial properties” (length, weight, moment of inertia) of the bats as they relate to and affect the performance characteristics of baseball bats. This previous research has helped bat companies to understand how to produce a high-performing baseball bat and has

given the governing bodies insight as to what properties need to be regulated to ensure the balance of the game does not become compromised by increased offense. For example, the NCAA has placed regulations on the minimum weights, the minimum moment of inertia, and maximum performance for the baseball bats used in its games [1, 2]. Some research has been directed toward studying the relationship between the modal properties of baseball bats and batted-ball performance [3-8], but there has been no comprehensive modal study for a representative set of bats that are currently used in collegiate and high school baseball. The goal of this thesis is to perform such a comprehensive study.

The scope of this thesis is to investigate the relationship among bending and hoop modes and batted-ball performance for wood and nonwood bats. Modal analysis is used to measure the natural frequencies of the bending and hoop modes of a representative sample of baseball bats. Models of the bat-ball collision are used to determine the effects of hoop mode frequencies on performance. The effect the baseball has on the hoop mode, while in contact with the bat, is investigated using finite element models of a bat-ball collision. Various performance metrics are measured using a high-speed air cannon. This research will give an improved understanding of the dynamic effects that the bat and baseball contribute to the overall performance of the baseball bat.

## **2 BACKGROUND**

This chapter will discuss the different materials used to make baseball bats and their relevance to bat performance. The performance metrics of Ball Exit Speed Ratio (BESR), Bat-Ball Coefficient of Restitution (BBCOR), and Batted-Ball Speed (BBS) will be presented. The importance of moment of inertia (MOI) and swing speed will be discussed. Previous models used in research describing the relationship of the natural frequencies of softball bats to performance will be reviewed.

### **2.1 Bat Properties**

Brief descriptions of various bat properties are presented in the following sections.

#### **2.1.1 Bat Construction**

A traditional baseball bat used in the major leagues is required to be made from a single piece of solid wood, while bats used in college and high school baseball are allowed to be constructed of more than one piece of wood, e.g. laminated strips of wood,

and several different materials. The most common materials used in college and high school bats are aluminum and composites. Composite baseball bats are comprised of either carbon or glass fibers or a combination of the two. The most common barrel construction is a single-walled barrel, but there are also multi-walled bats.

According to the NCAA specifications, a baseball bat can be composed of multiple pieces or sections, e.g. a composite handle paired with an aluminum barrel. To prohibit any modifications to the bat by the end user, the bat is required to be tamperproof.

### 2.1.2 Drop

The NCAA bat specifications prescribe a maximum allowable drop. The intent of the NCAA drop rule is to ensure that the overall weight of the nonwood bat is not significantly different from that of a typical solid wood bat. The drop of a bat is defined by:

$$Drop = weight - length \quad (1)$$

where the *weight* is measured in ounces and the *length* is measured in inches. The most common drop is the largest drop that is allowed for an NCAA certified bat, i.e. -3. Most companies produce and sell -3 drop bats because the lighter the bat the easier it is to swing. However, manufacturers are able to distribute weight in the bat to affect the Moment of Inertia, which in turn influences the swing speed. In this thesis, only -3 (by classification) drop bats were considered for nonwood bats. Any bat with a drop between



2.1 and 3.0 oz from its length in inches is classified as a -3 drop bat. The MOI is specified with respect to an axis located 6 in. from the base of the knob.

### **2.1.3 Moment of Inertia (MOI)**

The NCAA baseball rules also specify a minimum allowable MOI (weight moment of inertia). The intent of the minimum allowable MOI is to ensure that the swing weight of a nonwood bat is not significantly different from that of a solid wood bat. The drop of the bat and how the bat is weighted, i.e. mass added by putting a polymer or similar filler in the handle and the barrel ends of the bat, affects the total MOI of the bat. The MOI is best considered to be the effective swing weight of the bat. As the MOI of the bat increases, the harder it is for the bat to be swung. The MOI of a solid wood bat is a result of the wood used, and thus there is little that can be done to vary the MOI of a wood bat other than by varying the profile of the bat, i.e. diameters of the barrel, handle and taper. Because the weight distribution of a nonwood bat can potentially be varied for any location along the bat by changes in diameter, wall thickness and addition of mass, the NCAA has imposed regulations stating minimum allowable MOI values for each length of bat.

## **2.2 Swing Speed**

The swing speed is a result of the combination of the bat MOI and the strength of the player. Several different swing-speed models have been developed based on MOI by Fleisig [9], Adair [10], Nathan [11] and Bahill [12].

One of the most comprehensive swing-speed studies was by Crisco and Greenwald [13]. They used high school and collegiate level bats and players in a batting cage, where

the conditions were very controlled and repeatable. A laser system was used to track ball speed and trajectory along with the angular speed of the bat. Nathan [11] subsequently analyzed the data to produce an empirical swing-speed model. This model is based upon a “standard bat” with a given MOI and length, with the bat pivoting six inches from the base of the knob. The model calculates the linear speed as a function of MOI at the impact location. The speed of the bat at the point of impact can be determined by:

$$v_{bat} = v_{bat0} \left( \frac{Length - Band}{Length_0} \right) \left( \frac{MOI_0}{MOI} \right)^{exp} \quad (2)$$

where the *Length* is the length of the baseball bat in inches, *Band* is the distance from the impact location to the tip of the barrel in inches, and *MOI* is the moment of inertia of the bat about the 6-in. pivot location measured in oz-in<sup>2</sup>. The constants used in Equation 2 are summarized in Table 1.

Table 1: Swing-speed equation constants

$v_{bat0}$	$Length_0$	$exp$	$MOI_0$
40 mph	28 in.	0.3	15000 oz-in <sup>2</sup>

The exponent can be thought of as the player’s ability to swing the bat. An exponent of 0.3 was used in the swing-speed model but can range from 0.08 to 0.37 based upon a swing-speed study of softball players performed by Smith [14].

## 2.3 Performance Metrics

This research will consider several different metrics to quantify bat performance. The Ball Exit Speed Ratio, Batted-Ball Speed, and Bat-Ball Coefficient of Restitution are the metrics currently used to quantify the performance of a baseball bat. Each of these metrics analyzes the effectiveness of the bat-ball collision in its own particular manner.

### 2.3.1 Ball Exit Speed Ratio (BESR)

The BESR test is the metric used to certify bats for the NCAA for bats used between 2000 and 2010. This metric was first used in September 1999 in preparation for bats used in 2000. The test involves the measurements of the inbound (pitched) and rebound (batted) speeds of the baseball. The BESR test can be used for any combination of bat-ball scenarios from a moving bat and stationary ball (tee test), to a moving bat and ball, to a moving ball and stationary bat. In the currently implemented test setup for measuring BESR, the moving ball and stationary bat is method is used. The bat is initially at rest but is allowed to pivot about the 6-in. location on the handle—as measured from the base of the knob. A ball is “pitched” at the bat at a speed that combines the velocity of a pitched ball with the velocity of a swinging bat. In its simplest form, the BESR equation is:

$$BESR = \frac{V_{out}}{V_{in}} + 0.5 \quad (3)$$

where:  $V_{out}$  = rebound velocity of the baseball

$V_{in}$  = inbound velocity of the baseball

To account for different swing velocities at the different locations of the barrel of the bat, Equation 3 has been modified for use in the NCAA bat performance standard.

The NCAA form of the BESR equation is:

$$NCAA\_BESR = \frac{V_{out} - \delta V}{V_{in} + \delta V} + 0.5 \quad (4)$$

$$\text{where } \delta V = V - V_{contact}$$

The value of  $V_{in}$  is the measured inbound velocity, and  $V_{out}$  is the rebound velocity off of the bat. The baseball is “pitched” toward the 6-in. location of the barrel at a speed of 136 mph, which is the value of  $V$ . This velocity correlates to an 80-mph pitch (by an actual pitcher) that slows to 70 mph when reaching the batter and a 66-mph swing speed as measured 6 in. from the tip of the barrel. This 66-mph speed at the 6-in. location corresponds to a bat tip speed of 85 mph. The value of  $V_{contact}$  is defined by

$$V_{contact} = V_{swing} \left( \frac{L - 6 - z}{L - 12} \right) + V_{pitch} \quad (5)$$

where  $L$  = the length of the bat (in.)

$z$  = the impact location measured from the barrel end of the bat (in.)

$V_{pitch}$  = pitch speed of the baseball as it crosses the plate (70 mph)

$V_{swing}$  = swing speed of the bat at the point of contact. This speed is determined using a swing-speed model.

### 2.3.2 Batted-Ball Speed (BBS)

The batted-ball speed is the speed of the ball immediately after the batter has hit the ball with the bat. This metric quantifies bat performance on the field of play, where the speed of the baseball as it comes off the bat can be measured. The BBS accounts for the total momentum of the collision between the ball and the bat. The BBS equation is given by:

$$BBS = V_{pitch}(BESR - 0.5) + V_{swing}(BESR + 0.5) \quad (6)$$

where:  $V_{pitch}$  = the speed of the pitch as it crosses the plate

$V_{swing}$  = the speed of the bat at the contact point.

The BBS values calculated in this thesis use the swing-speed model developed by Nathan [11] as described in Section 2.2.

### 2.3.3 Bat-Ball Coefficient of Restitution (BBCOR)

The Bat-Ball Coefficient of Restitution (BBCOR) is a performance metric that accounts for the inertial effects of the bat and ball. This metric correlates the effect of MOI of the bat based on the impact location of the ball and the pivot location. The BBCOR equation is given by:

$$BBCOR = (BESR - 0.5)(1 + k) + k \quad (7)$$

where:  $k = \frac{m_{ball}x^2}{MOI}$

and where  $m_{ball}$  is the mass of the ball in oz,  $x$  is the distance between the pivot location and the impact location in inches and the  $MOI$  is the moment of inertia about the pivot location.

## 2.4 Dynamic Response of Baseball Bats

A baseball player can feel the dynamic response of a wood baseball bat when the bat makes contact with the ball. The dynamic response of a wood baseball bat during the collision excites the bending modes of the bat. The most predominant modes noticed by a player are the first and second bending modes, in which the player will notice a sting in their hands. In a nonwood hollow bat, hoop modes (also known as bell modes) exist in the barrel, and these modes are excited during the collision along with the bending modes. The presence of the hoop modes is most noticeable to the casual observer by the pinging sound that is heard after contact of the ball with an aluminum bat.

Figure 1 shows the first three bending modes that a baseball bat exhibits. The knob of the baseball bat is on the left-hand side. The frequencies shown above each bending mode are an approximate typical value for wood baseball bats. The dots located on each of the modes represent the nodes of the modes. The nodes of the modes are locations on the bat where if an input excitation is placed at a node location, that mode will not be excited. The node for the first bending mode on the barrel is located approximately 6 in. from the end cap. The node on the barrel for the second bending mode is approximately 5 in. from the end cap. The region between the nodes for the first and second mode is related to the “sweet zone” location as defined by Cross [3]. This area will cause little excitation of both modes and have a good feel to a player when a baseball is hit in this section of the bat.

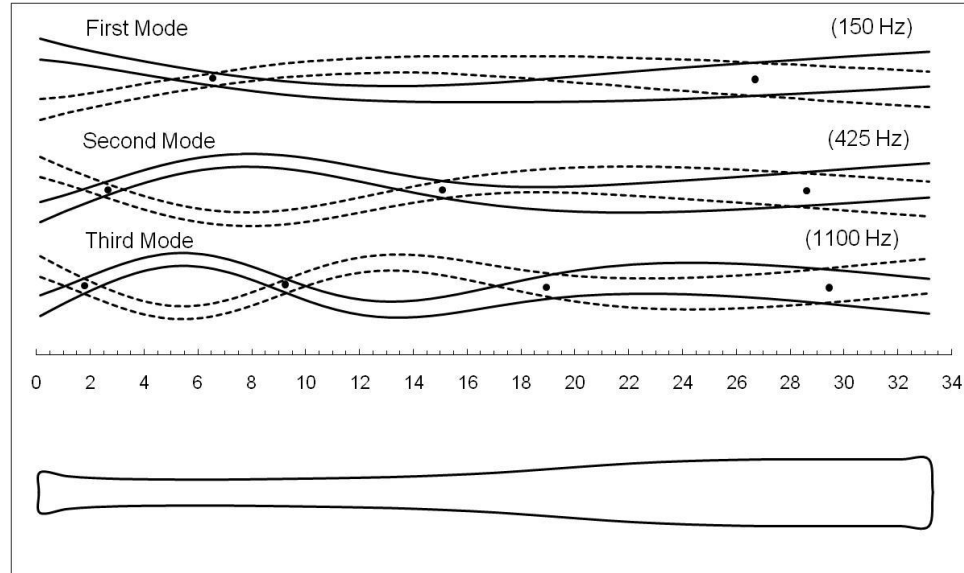


Figure 1: Bending modes of baseball bats

Figure 2 shows the first two hoop modes that a baseball bat will exhibit. The first hoop mode is responsible for the trampoline effect and exhibits the most deformation in the barrel of the bat of all the hoop modes as it deforms from a circle to an ellipse. The first hoop mode will be present over the barrel of the bat typically from the end cap into the taper region. This length is approximately 13 in. long and can vary as function of the bat profile. The most deformation will occur in the middle of the 13-in. region which corresponds to 5- to 7-in. area on the barrel as measured from the tip of the end cap. The first hoop mode will have the largest amplitude when the ball impacts the antinode. The node of the second hoop mode is located around the circumference at approximately the 7-in. location from the end cap. The frequencies above each of the modes are an approximate value at which that mode would occur for a typical aluminum baseball bat.

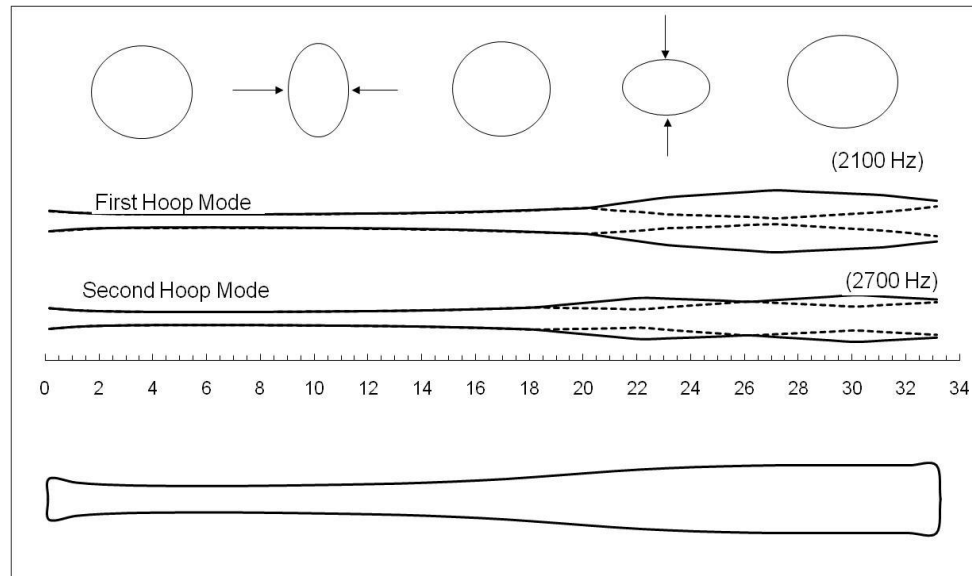


Figure 2: Hoop modes of baseball bats

#### 2.4.1 Previous Research on the Vibration Response of Bats

Naro and Sato [4] performed modal and COR-performance tests on reinforced plastic tubes. They showed that increasing the first bending mode resulted in an increase in the Coefficient of Restitution (COR). They also observed that as the hoop frequency decreased the COR increased. They concluded that by raising the first bending mode while decreasing the hoop frequency the effective COR of the collision could be increased.

Tests performed by Brody [5] showed that a hand-held bat acts more like an object suspended in the free-free condition rather than being clamped at one end. Based on this observation, the modal tests of the baseball bats for this research were performed in the free-free condition to capture the dynamic response as would be observed by a hand-held bat on the field.



Noble [6] theorized that the performance of bats will increase as the bending stiffness of the bat increases thereby resulting in higher natural frequencies for the bending modes. According to Noble, manufacturers should tune the vibration characteristics of the bending and diving board modes to produce the best performing bats.

Noble [7] performed studies that looked at the “diving board mode” or “springboard” effect of softball bats where the bat was considered to be fixed at the knob end such that the bat acted like a cantilever beam. The experiments were performed using college males and females and several high-performing aluminum softball bats. A strain gauge on the handle measured the vibration response of the bat as the players hit softballs. A radar gun was used to record the rebound velocity of the ball. Noble found that the oscillation from the bat did not correlate to a cantilever boundary condition. Noble also did not find a correlation between the diving board mode and performance for the study performed.

Russell [8] studied the effect of hoop frequency as a predictor of performance for softball bats. Russell used a two degree of freedom system model from a golf ball model that was previously developed by Cochran [15]. Russell’s model predicted the performance of softball bats given different hoop frequencies. A nonlinear spring was chosen for the ball to describe the reaction of the ball coming into contact with the bat. The barrel of the bat was considered to be a simple mass, spring and dashpot system. Figure 3 depicts the two degree of freedom system.

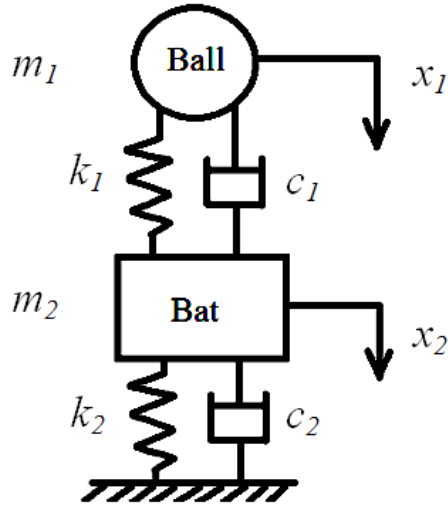


Figure 3: Mass-spring model of the ball-bat collision [8]

The equations of motion for the system shown in Figure 3 are:

$$m_1 \ddot{x}_1 = -k_1(x_1 - x_2)|x_1 - x_2|^a - c_1(\dot{x}_1 - \dot{x}_2)|x_1 - x_2|^b \quad (8a)$$

$$m_2 \ddot{x}_2 = -k_2 x_2 - c_2 \dot{x}_2 + k_1(x_1 - x_2)|x_1 - x_2|^a + c_1(\dot{x}_1 - \dot{x}_2)|x_1 - x_2|^b \quad (8b)$$

Russell found the properties for the softball to be  $m_1=0.180$  kg,  $k_1=40.6 \cdot 10^6$  N/m and  $c_1=4700$  N-s/m. The given properties for the softball bat are  $c_2=100.5$  N-s/m and  $m_2=0.16$  kg. The spring stiffness of the softball bat  $k_2$  was found through an iteration process by stepping through a set of hoop frequencies. Russell solved Equations 8a and 8b for the upward velocity of the ball for each value of  $k_2$  and calculated the normalized COR for each hoop frequency. Figure 4 shows the plot of hoop frequency versus normalized collision efficiency. Based upon this model for softball bats, a hoop frequency between 800 and 1000 Hz would be optimal, i.e. producing the greatest collision efficiency and the highest batted-ball speeds.

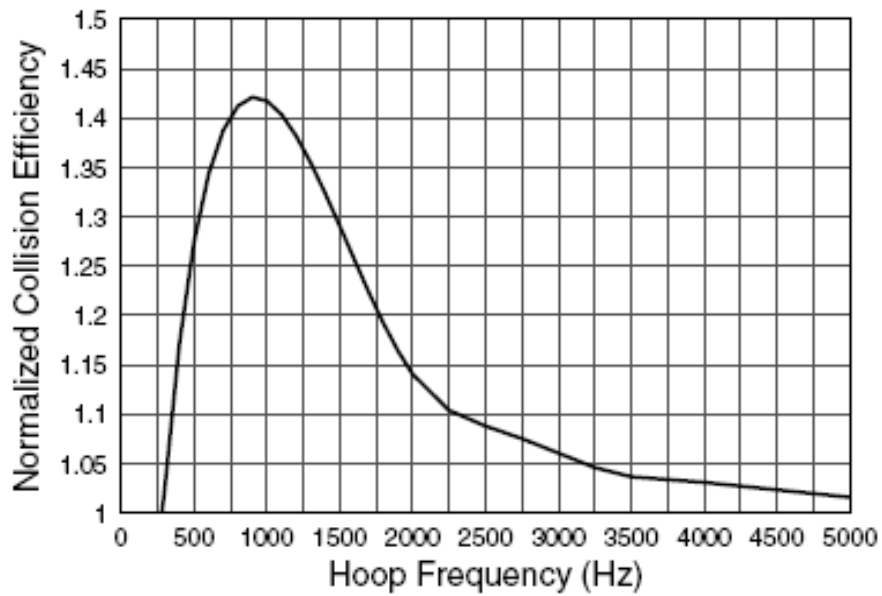


Figure 4: Normalized collision efficiency versus hoop frequency [8]

Russell compared his model to softball bat test data collected at the Sports Science Lab at Washington State University. He showed good correlation between the batted-ball speed and the hoop frequency. The data consisted of several different softball bat models with different constructions and materials. Figure 4 shows the good correlation observed by Russell between his model and the experimental data collected using a high-speed air cannon.

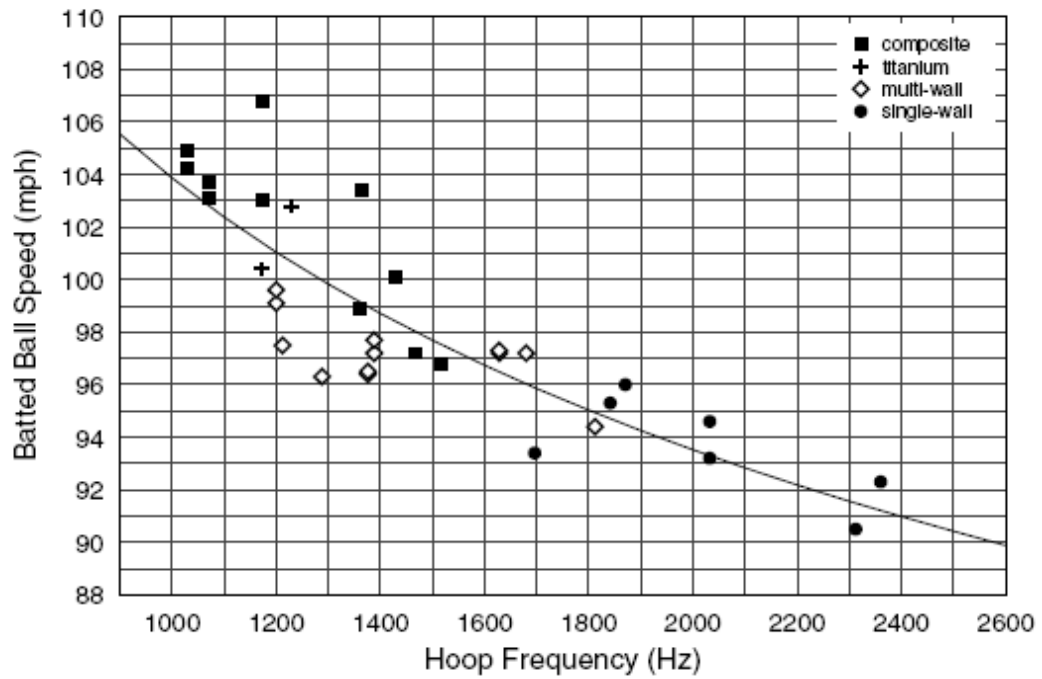


Figure 5: Hoop frequency versus batted ball speed [8]

## 2.5 Summary

Bats can range in the type of material used in their construction along with the ability to control properties such as drop and MOI. The performance-metric calculations that will be used in this thesis were outlined. Previous research exploring the dynamic response of bats was reviewed.

### **3 Methodology**

This chapter outlines the process and tests performed on the baseball bats for this research. The NCAA protocol for profiling and performance testing will be covered as it pertains to this thesis. Topics include Bat Identification, Bat Profiling for Moment of Inertia, Baseball Conditioning, Performance Testing and Modal Analysis.

#### **3.1 Bat Identification**

The bats used in this study included bats that had been submitted by various companies for NCAA certification and other bats that had been obtained by the UMLBRC for the purpose of academic studies. Each bat used in this thesis was assigned a unique Thesis ID prior to testing. The Thesis ID starts with the letters “AS” and was given to the bat during the modal testing phase of the research. The first bat identified during modal testing was AS001. The Thesis ID was assigned to each bat to remove any information about the manufacturer and model of the baseball bat for reporting purposes in this research. This blinding of the data was done so as not to disseminate information

that could help or hurt any manufacturer or aid anyone in the selection of a bat for use in play. The NCAA authorized use of the certification bats for this research.

### **3.2 Baseball Bat Profiling**

Baseball bats specified for NCAA BESR certification go through a profiling procedure according to the NCAA BESR protocol [1] prior to being tested for performance. Length measurements are taken to the nearest  $1/16^{\text{th}}$  (0.0625) in. Seven rings are drawn onto the barrel of the bat in one-inch increments starting at the 3-in. axial location as measured from the barrel end of the bat. Diameter measurements of the barrel are recorded at each of the lines using a vernier caliper to the nearest 0.001 in. A handle diameter measurement is also recorded at a point 6 in. from the base of the knob.

The overall weight is recorded to the nearest 0.005 oz. For this research, all bats tested fell within the -3 weight class. The drop of the bat is checked to ensure that the bat falls within the specified weight class. The balance point, or center of gravity (CG), is measured by balancing the bat on a knife edge and marked. The CG is measured from the tip of the barrel end of the bat to the nearest  $1/16^{\text{th}}$  in.

### 3.2.1 Bat Profiling – Moment of Inertia

The baseball bat Moment of Inertia (MOI) is measured according to ASTM F2398 [16]. The baseball bat is clamped at the 6-in. location on the handle and placed on the MOI fixture as shown in Figure 6. The bat is set to swing through a set of light gates which measure the period of oscillation and the number of periods. A LabVIEW VI is used to measure the period of oscillation and compute the MOI about an axis that is 6 in. from the base of the knob. A minimum MOI is prescribed for each length in the NCAA BESR protocol. The MOI was calculated by

$$MOI = \frac{t^2 g W a}{4\pi^2} \quad (1)$$

where:  $t$  = the average period of oscillation (sec)

$g$  = acceleration due to gravity (386.4 in/s<sup>2</sup>)

$W$  = total weight of the bat (oz)

$a$  = the distance from the CG to the pivot point (in)



Figure 6: MOI fixture

### 3.3 Lab Conditions

The Baseball Research Center environmental conditions are set at  $72\pm 4$  °F and  $50\pm 5\%$  relative humidity. The controlled conditions ensure that variation in the environmental conditions do not compromise the test data and assist in the repeatability of performing multiple tests on the same bat. Any bat used in this research was in the controlled lab environment for a minimum of two days, and any baseballs used were in the environment for at least 14 days prior to any testing.



### 3.4 Baseball Conditions

Baseballs are required to perform bat performance testing. Rawlings model R1NCAA baseballs are stored in the lab for a minimum of two weeks prior to being selected for a ball lot. Baseballs lots are typically made of 120 to 160 baseballs. The baseballs weights are required to be  $145.4 \pm 1.0$  g. Each ball is marked with a lot number and ball number. Lot preparations are performed by taking a random sample of baseballs from the lot to achieve 30 valid hits on the standard baseball bat at the 6-in. location (measured from the end cap) at a velocity, which is a target speed of  $V = 136$  mph. The rebound speed,  $v$ , is measured for each baseball. The correction factor,  $\varepsilon$ , for each ball was determined by:

$$\varepsilon = 0.231 - \frac{v}{V} \quad (2)$$

The average of the individual ball correction factors,  $\varepsilon_i$ , determines the correction factor,  $\varepsilon$ , for entire lot.

Each baseball weight is measured to the nearest 0.1 g prior to being used in the performance test. The relative moisture content of the baseball is measured by using a Delmohrst wood moisture meter by sticking the prongs into the stitches of ball. While this moisture reading is not an absolute value, it does give a relative value of the ball-moisture content from test to test and from ball to ball. The mass, moisture, and date are recorded on the side of the ball. Each baseball is allowed up to eight total impacts, twice on each ear (or face) before the ball is removed from testing.

### 3.5 Performance Testing

Performance testing of the baseball bats was completed according to the NCAA BESR protocol [1]. The air cannon used in the performance testing was the LVSports bat performance system. Figure 7 shows the LVSports cannon used to perform the testing.

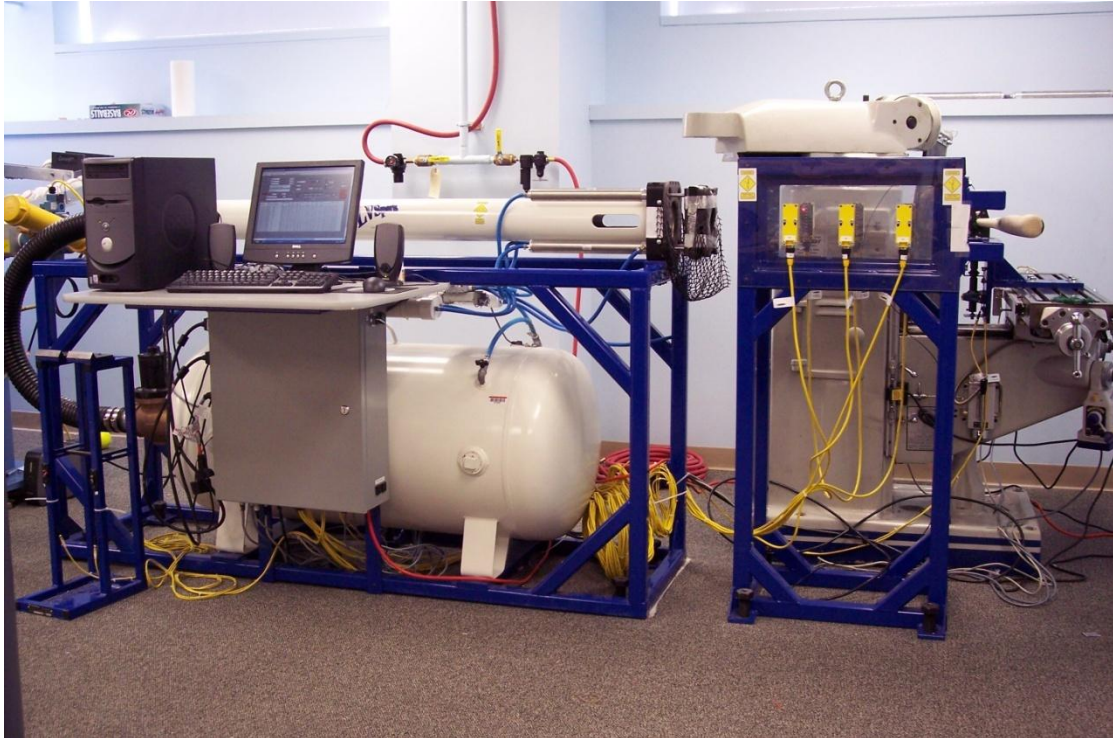


Figure 7: LVSports cannon

Astroturf is used on the grip of the bat at the point of contact with the clamp to allow the bat to rotate and to allow some flex. Each bat was clamped so the axis of rotation pivoted around the 6-in. location measured from the base of the knob. The clamp is mounted to a table of a milling-machine base used to control the horizontal and vertical position of the bat in front of the cannon. The heavy weight of the mill base makes the base an essentially rigid support.

The target speed at which the ball is fired at the 6-in. location is 136 mph. This collision velocity is based upon a bat swing velocity of 66 mph, at the 6-in. location (which corresponds to a tip speed of 85 mph), and a ball pitch velocity of 70 mph at the time of contact (which corresponds to a pitch speed as released from the pitcher of 80 mph). For other impact locations, the speed at which the ball contacts the bat is determined by

$$V_{contact} = 66mph \left( \frac{L-6-z}{L-12} \right) + 70mph \quad (4)$$

where  $L$  = the length of the bat (in.)

$z$  = impact location measured from the barrel of the bat (in.)

The velocity of the ball is measured by sets of light gates. There are three pairs of light gates evenly spaced at 6-in. apart. The time is recorded as the baseball breaks the plane of each light gate and the velocity is calculated. The velocity of the ball must be within  $\pm 2$  mph of the target velocity,  $V_{contact}$ , to be considered a valid inbound speed. The rebound velocity of the ball is measured using the same light gates. Figure 3 shows the light-gate setup.

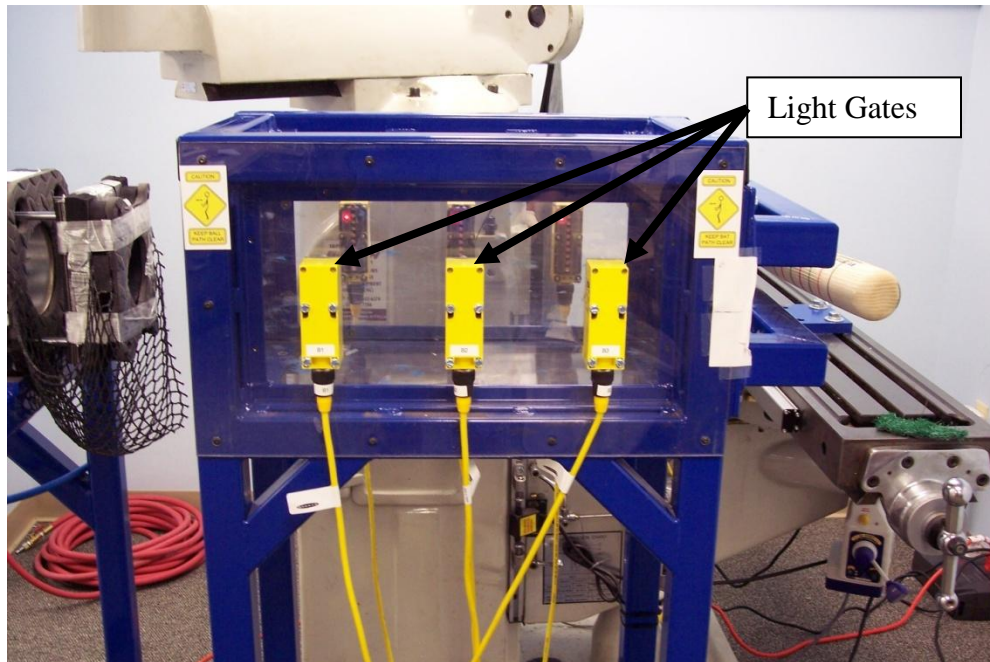


Figure 8: Light gate box

Baseballs selected from the lot are individually loaded into a sabot so the ball does not experience any rotation during the test. The sabot yields the necessary consistency in speed. The test is performed by pitching the baseballs at the desired impact velocity and by achieving six valid shots for each test location. A shot is determined valid when the ball passes back through the light gates at no more than  $\pm 5^\circ$  vertically and the difference in velocity between each pair of light is no more than  $\pm 1.5$  mph. The bat is scanned by testing locations along the barrel until the performance at one location is determined to be the maximum or “sweet spot” location. Testing begins by impacting the 6.0-in. location, measured from the barrel end, and is repeated for the 5.0- and 7.0-in. locations. Based upon the values of the performance at these three locations, either the 5.5-in. or the 6.5-in. location is tested. If the 5.0- or 7.0-in. location has a higher value, then testing moves out or in a 0.5-in. increment from that location. The sweet spot location is

considered to be isolated when the performance at a location on the barrel of the bat is 0.003 BESR points higher than the locations that are  $\pm 0.5$  in. on either side of it.

### **3.6 Modal Analysis**

The modal tests were completed on each bat before performance testing in the air cannon due to the chance that some change could occur in the barrel, e.g. cracking and/or delamination of a composite barrel, denting of an aluminum barrel or cracking of a wood barrel, that could alter the modal response of the bat. The first and second bending modes were measured for all bats, and the first and second hoop modes were measured for all hollow bats, e.g. aluminum and composite constructions. A Dactron Photon II four-channel FFT analyzer was used for the modal testing along with a PCB force gauge on an impact hammer and two PCB 303A accelerometers. An RT Pro Photon 6.06 data acquisition program analyzed the frequency response of the bat. The frequency range selected for the hollow baseball bats was 4000 Hz at 800 spectral lines of resolution. The frequency range for wood baseball bats was selected to be 1000 Hz at 800 spectral lines of resolution. No windows or weighting functions were applied to the data.

The bat was suspended in the free-free condition using Bungee cords located at the 6-in. mark on the barrel (as measured from the tip of the barrel) and the 6-in. mark on the handle (as measured from the base of the knob). The Bungee cords have a low spring constant allowing the baseball bat to vibrate as if the baseball bat was essentially floating in air. Accelerometers were placed at the 2-in. location (as measured from the tip of the barrel). Figures 9 and 10 show the bat hung in the free-free condition and the accelerometer configuration, respectively. One accelerometer was directly on top of the bat, and the second one was 90 degrees from the top, i.e. on the side of the bat.

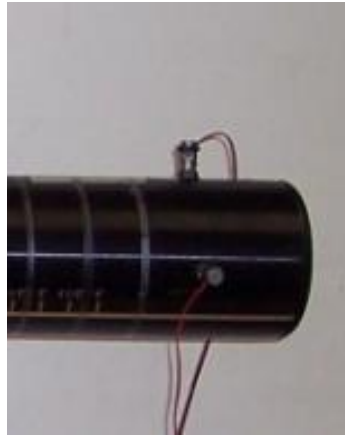


Figure 9: Baseball bat placed in the free-free condition

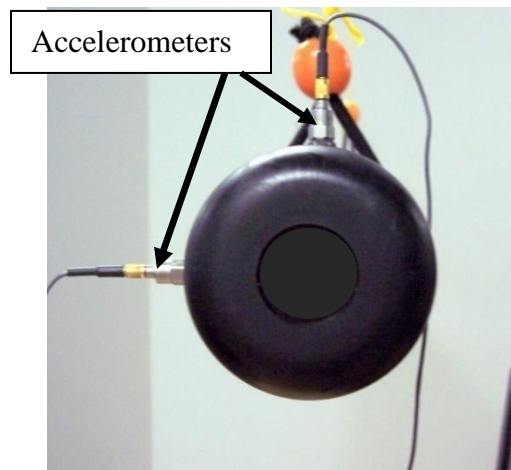


Figure 10: Accelerometer placements on the barrel of the bat

The baseball bat was excited using an impact hammer on the barrel a total of five times to average the response of the accelerometers. The frequency response function

(FRF) was computed from the time response using the Fast Fourier transform based on the ratio of acceleration output to force input. The frequency response functions were overlaid to compare the response of each accelerometer. Figures 11 and 12 show the coherence function and the FRF computed for a baseball bat, respectively.

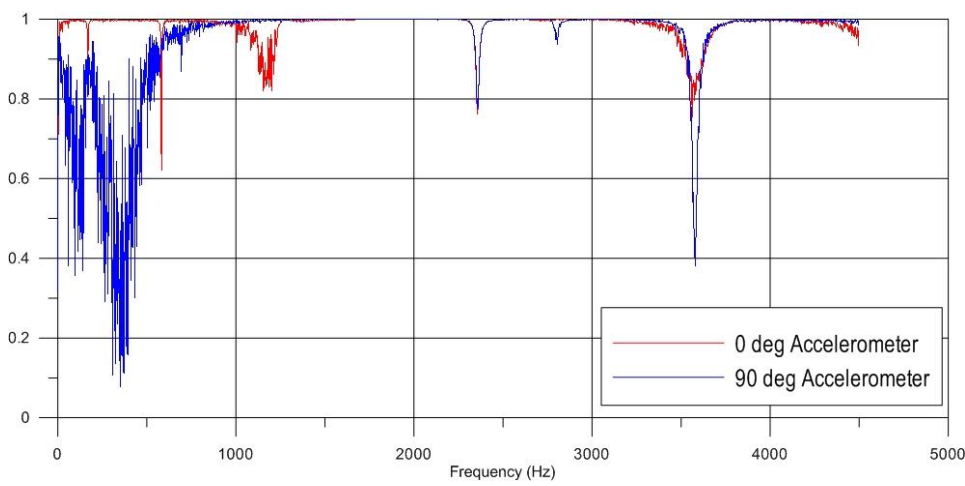


Figure 11: Coherence function of two accelerometers

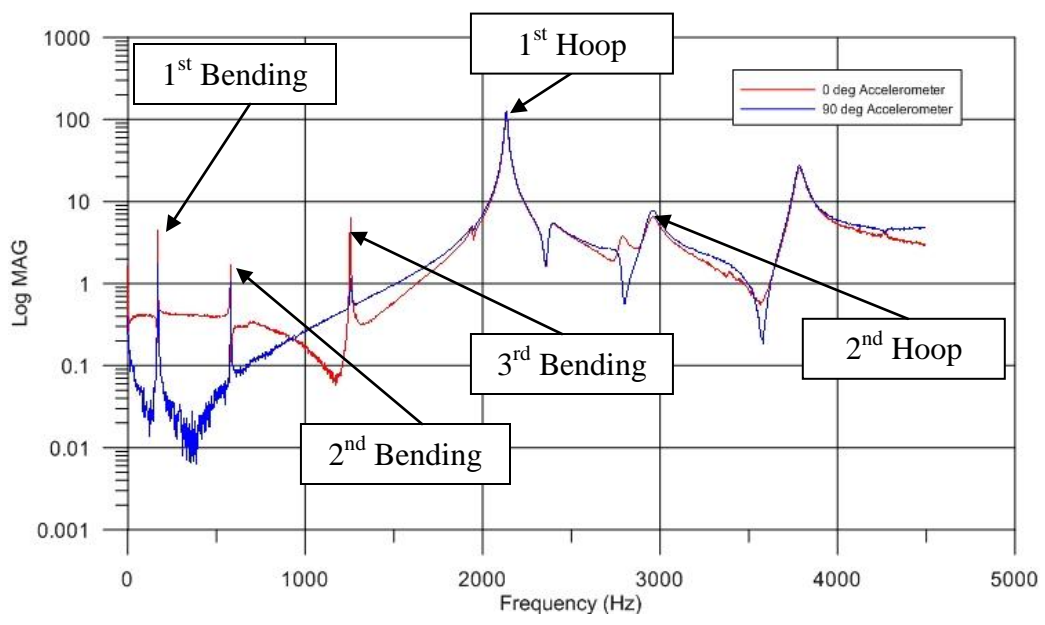


Figure 12: Overlaid FRF from both accelerometers

Figure 11 shows the coherence function and the frequency response functions for both accelerometers. The red and blue lines denote the side and top accelerometers, respectively. The coherence function describes how much the output of the accelerometer is related to the input of the impact hammer. A value of one shows direct correlation between input and output. A coherence close to zero indicates the output was not related to the input; anti-resonances are expected to have a coherence of zero and do not indicate a bad measurement.

In Figure 12, the horizontal axis is the frequency range, and the vertical axis is the magnitude of response in decibels. The red line in Figure 12 is the FRF for the accelerometer mounted horizontal and in the same direction as the impact takes place.

Each peak shown in Figure 12 corresponds to a natural frequency of the baseball bat. Moving left to right; the first peak happens at 205 Hz and is the first bending mode frequency of the baseball bat. Continuing left to right, the second and third bending modes of the baseball bat are the next two peaks. When the two frequency response functions directly overlay one another with the same magnitude then that mode is determined to be the first hoop mode. This mode is shown in Figure 12 as the fourth peak in the FRF. The second occurrence of the peaks being lined up and having the same magnitude was determined to be the second hoop mode.

In some cases, the peaks of the frequency response function would split or become double peaks. These peaks are relatively close to one another, within 25 Hz. If this occurred, the first peak of the double peak was chosen for the frequency measurement.

Double peaks can occur for multiple reasons. Manufactures may implement a tuned absorber that causes smaller response from the two peaks than a single response of a



larger magnitude. Double peaks can also be a sign that there is a crack or damage in the bat or some slight variation in the wall thickness and/or material properties that induces a measurable cylindrical asymmetry in the bat.

The nodes of the bending modes on the barrel were determined by impacting along the length from the barrel end of the bat to the taper region. Averages were not performed, and the FRF was recalculated for each impact. Impacts started at the 3-in. location on the barrel of the bat and moved in 0.25-in. increments toward the handle of the bat. The node of the mode was determined when the peak of the FRF at the first or second bending mode approached a minimum. Several impacts were then performed around the minimum location to ensure the node of the mode was determined. The node was marked and measured from the barrel end to the nearest 0.125 in.

Full modal tests were performed on several baseball bats to confirm the quick approach of determining the bending and hoop modes of baseball bats. The results of these tests can be seen in Appendix A.

### **3.7 Summary**

Bats for testing undergo a profiling procedure that gives the bat a unique Bat ID along with measurements of length, weight, barrel diameters, center of gravity and MOI. Performance testing is done using a high-speed air cannon and light-gate sensors to record the inbound and rebound velocities of the baseball. The modal analysis procedure uses two accelerometers placed on the barrel of the bat 90 degrees from one another to measure the bending and hoop modes. An overlaid plot of the FRF responses of the two accelerometers is used to identify the hoop modes.

## 4 **Results**

This chapter presents the results collected from the modal analyses, performance testing and computer models. Baseball bats are categorized as being either wood or nonwood. For nonwood bats, classifications are made by barrel material—either aluminum or composite. Baseball bats that had aluminum barrels and composite handles are identified to be made of aluminum because the objective of the research is to explore the hoop response of the hollow-barrel bats. All performance testing was done according to the NCAA protocol as specified in Section 3.5. Values of BESR, BBS, and BBCOR were calculated for all baseball bats tested and are presented in multiple ways for data analysis.

Ideally, to explore how a change in one design parameter for a bat affects the modal and batted-ball performance, all other design variables should be the same respective values. However, the samples of bats used in this research are from commercially available bats and prototypes by manufacturers, so the holding of all other design parameters constant while changing only one was not possible. Thus, this limitation must be kept in mind when exploring any one parameter.

## 4.1 Wood Bat Data

A set of wood baseball bats, ranging in length from 30 to 34 in. was investigated. The following sections will examine the relationship between performance and inertial properties, e.g. moment of inertia and drop. Later sections will examine the relationship between the bending mode frequencies and performance.

### 4.1.1 Performance versus MOI

To understand and potentially isolate how the bending frequency contributes to the performance of wood baseball bats, other characteristics of baseball bats also need to be considered as to how they contribute to performance. The MOI has been found to exhibit a correlation with several different performance metrics as observed by Jones *et al.* [17].

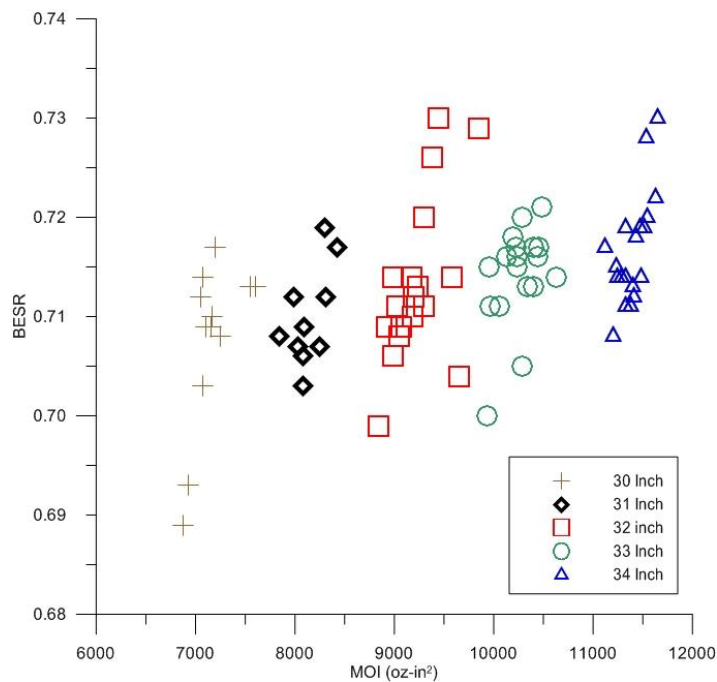


Figure 13: BESR vs. MOI for wood bats

Figure 13 shows a plot of BESR vs. MOI with a different symbol for each wood bat length. In this figure, it can be seen that the BESR value increases as the MOI of the

baseball bat increases. Trend lines through the data of each individual length classification would show that a small increase in MOI can cause a large increase in BESR. Figure 13 also shows that the MOI increases as the length increases—as evidenced by the grouping of the bats in semi-vertical clusters. This increase in MOI with increasing bat length is a result of more mass being located further from the axis of rotation as the length increases. The increasing trend in BESR with increasing MOI is similar to the coefficient of restitution, COR, for a baseball where the baseball COR is the ratio of the outbound speed over the inbound speed. As the bat MOI increases in the bat-ball collision, the initially stationary bat requires more energy to rotate on the pivot support and acts increasingly like a stationary wall, and thereby, causing an increase in the rebound speed of the ball off the bat and decreasing speed of the bat rebounding after the collision.

It should be noted that bats with the same MOI can have very different BESR values due to the contribution of other properties of the bat. Thus, while the trend of increasing BESR with increasing MOI is observed for each length class shown in Figure 13, there may be other factors contributing to the resulting BESR which could not be isolated in these data.

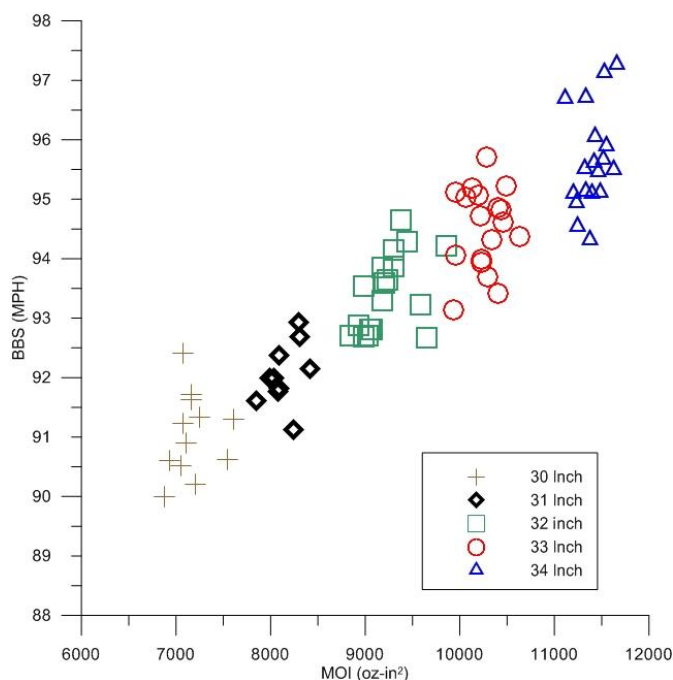


Figure 14: BBS vs. MOI for wood bats

Figure 14 is a plot of BBS vs. MOI with different symbols to sort the bats into length groups. In this figure, it can be seen that each length classification falls within an MOI range. The BBS can be seen to increase as the length of the bat increases, and within a given length group, it can also be observed that BBS increases with increasing MOI. Based on the swing-speed model in Section 2.2, the angular velocity of the swing speed decreases as the MOI of the bat increases. However, this reduction in the angular velocity contribution is offset by the increase in linear velocity resulting from the increased length of the bat. The linear speed at the point of contact is the input to the BBS calculation. In each length classification, it can be observed that some bats have similar MOI values but can have very different values of BBS. As stated previously, not all of the properties were held constant, so there may be other factors influencing BBS

that could not be isolated. However, the data in Figure 14 do imply that BBS increases with increasing MOI.

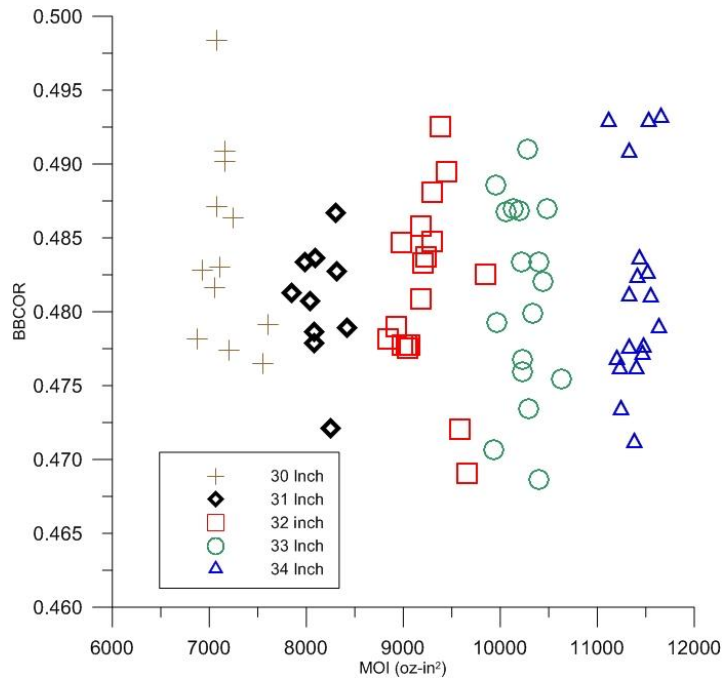


Figure 15: BBCOR vs. MOI for wood bats

Figure 15 shows the calculated BBCOR values for the wood bat data. The BBCOR values for these wood bats are fairly constant regardless of the length or MOI, and this result was also observed by Jones *et al.* [17] for youth wood bats. The relatively uniform BBCOR values are a result of the bat being a relatively rigid construction, i.e. no trampoline effect. The average BBCOR value for these wood baseball bats was found to be 0.480.

#### 4.1.2 Performance vs. Drop

Each of the performance metrics was compared against the drop for the wood baseball bats. It was shown in Section 4.1.1 that a correlation exists between the BESR and BBS performance metrics and MOI. Therefore, it is assumed that there will be a correlation between performance and drop, i.e. as the drop (weight minus length) becomes more positive, the MOI will increase. However, MOI is dependent on the total mass plus how that total mass of the bat is distributed along the length of the bat. Thus, two bats of the same mass can potentially have different MOIs, and vice versa.

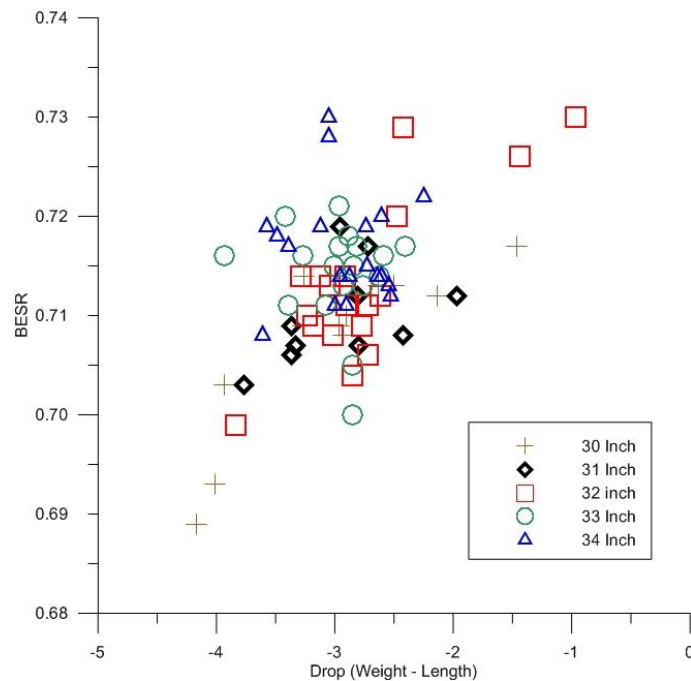


Figure 16: BESR vs. Drop for wood bats

Figure 16 is a plot of the drop of a baseball bat vs. BESR for all lengths of bats considered in this study. In this figure, it can be seen that as the drop becomes less negative the BESR increases. As the drop of the baseball bat becomes less negative, i.e. overall bat weight increases, the performance of the baseball bat increases. As the drop

for a bat becomes more negative, the weight of the bat decreases, and the MOI should also decrease. It was shown previously in Figure 13 that as the MOI for the bat increases the BESR also increases. Individual plots of BESR vs. drop for each length group of wood bats can be found in Appendix B.

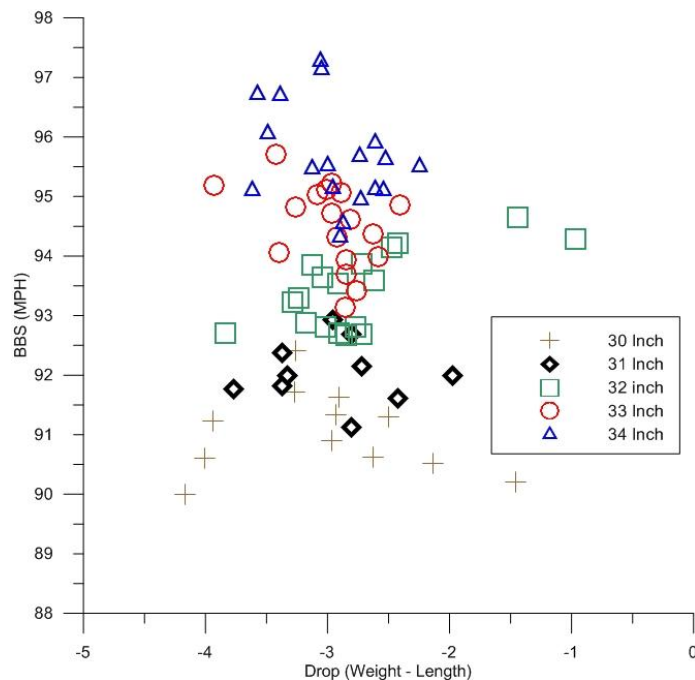


Figure 17: BBS vs. Drop for wood bats

Figure 17 is a plot of BBS vs. Drop for wood bats. In this plot, it can be seen that BBS increases with increasing bat length. This trend agrees with the trend that was previously shown in Figure 14 for BBS vs. MOI. This increasing BBS with increasing length is due to the increased linear velocity of the bat at the bat-ball contact point. It can also be seen in this plot that as the weight of the bat decreases, the performance of the baseball bat increases. As the bat weight increases, the drop will become more positive.



This observation implies that the increase in the linear speed at the point of contact is more important to the resulting BBS than the loss of mass in the barrel.

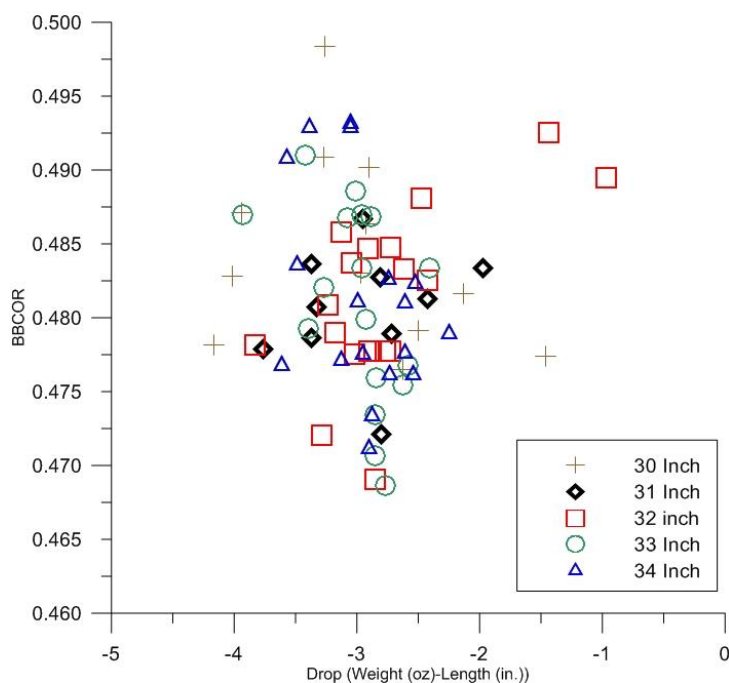


Figure 18: BBCOR vs. Drop for wood bats

Figure 17 is a plot of BBCOR vs. Drop for the wood bats. This plot shows that BBCOR is not well correlated to drop, i.e. that BBCOR is independent of the inertial properties of the wood bats (length, weight, MOI). As stated previously, wood bats can be considered essentially rigid, so the BBCOR does not vary appreciably from bat to bat due to the lack of a trampoline effect in wood bats.

#### 4.1.3 Correlation of Wood Bat Dynamic Response to Performance

Modal tests as described in Section 3.6 were performed on the wood baseball bats. Only the first and second bending modes were measured, and these were only in the

direction excited by impacting the ball impact side of the bat. The first bending modes were recorded and were compared to each of the three performance metrics. In general, the first bending frequency decreases as the length of the bat increases. The mass of the bat increases with increasing length, and the stiffness decreases with increasing length. Because the natural frequency is proportional to the square root of the stiffness divided by the mass, the modal test data agree qualitatively with theory.

An effort was made to investigate if a hoop mode was present in the solid wood bats, and thus the presence of a trampoline effect in the wood bats. It was concluded that a hoop mode did exist, but its frequency was so high that this mode required a very large mass to excite it. Thus, this mode would not be excited during a bat/ball impact and, thus, would have no influence on the resulting performance. It will be shown for the hollow bats that for a hoop mode to effect performance, the mode has to be under 2 kHz.

Figures 19 through 21 show BESR, BBS and BBCOR vs. first bending frequency, respectively, for the wood bat data. In these figures, a correlation can be seen between the first bending frequency and each of the performance metrics. As the bending frequency increases, the performance of the baseball bat increases for each of the length groups, i.e. as the first bending frequency increases for a given length class, the BESR, BBS and BBCOR all show an increase. It can also be seen that each length classification falls within a region of performance. As previously mentioned, the bending frequency decreases as the length of the baseball bat increases. The increase in length has a greater influence on bat performance than the first bending mode due to the increase in linear velocity at the bat-ball contact point. However, it can be concluded from Figure 20 that a

long baseball bat with a relatively high bending frequency will have the relatively highest batted-ball performance. Figures 19 and 21 also imply this conclusion.

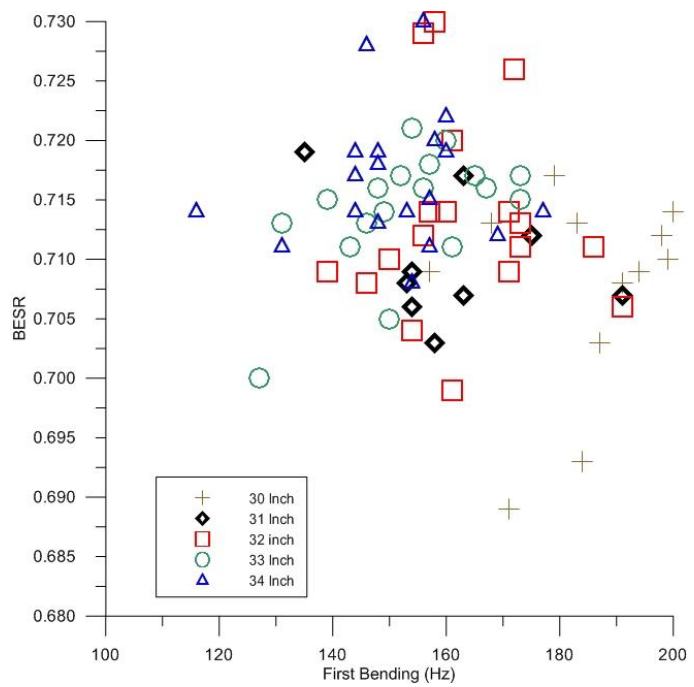


Figure 19: BESR vs. First bending frequency for wood bats

Figure 19 shows BESR vs. the first bending frequency. This figure shows that the shorter bats have will have the higher first bending frequencies. As the length increases the first bending frequency decreases. The 33-in. bats in Figure 19 show the best correlation between first bending frequency and BESR.

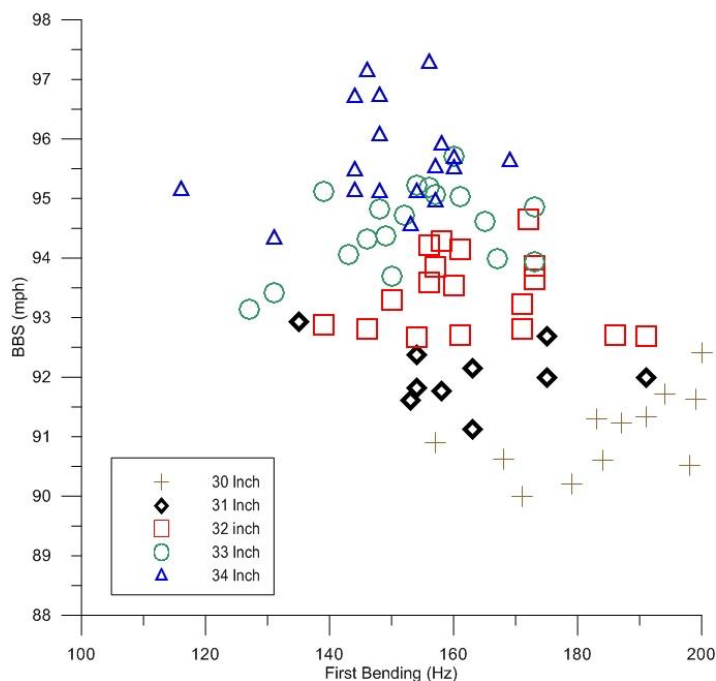


Figure 20: Batted-ball speed vs. First bending frequency for wood bats

Figure 20 shows BBS vs. first bending frequency. Initially the data look to contradict the statement that as first bending frequency increases BBS increases. However, Figure 20 clearly shows the separation between length classifications of bats. Within each length classification, it is observed that the BBS increases as the first bending frequency increases. The relative increase in performance as length classification increases is due to the increasing linear speed at the contact point with increasing bat length. Figure 20 shows the 32-in. bats have similar performance but vary in first bending frequency. As with all length classes of bats, the inertial properties were not held constant when comparing to first bending frequency to batted-ball performance, and hence there can be secondary effects that are not isolated in this interpretation of the

data. Regardless, the data do imply that BBCOR increases with increasing first bending mode frequency.

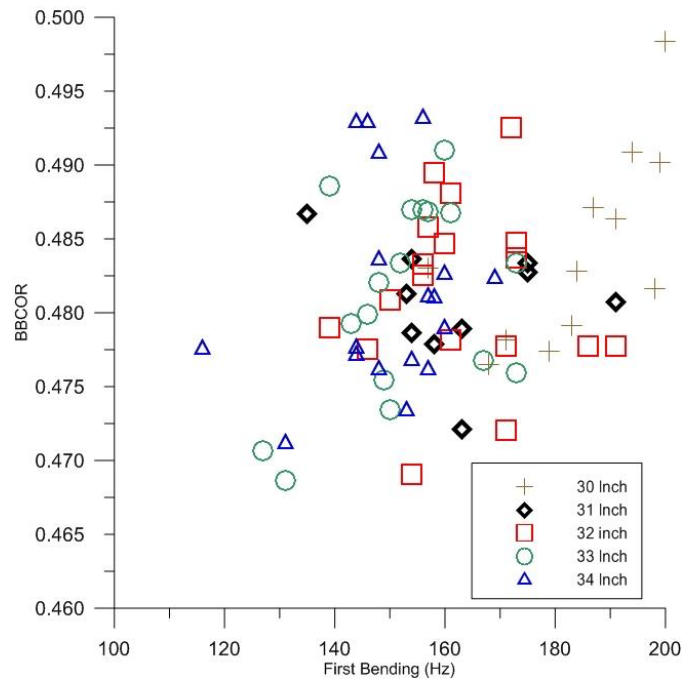


Figure 21: Bat-Ball COR vs. First bending frequency for wood bats

Figure 21 shows BBCOR vs. the first bending frequency. The 30-in. bats show the best correlation between BBCOR and first bending frequency. As the first bending frequency increases, the BBCOR increases. However, BBCOR is fairly constant for the wood barrel bats, and the other lengths do not necessarily show such a direct correlation.

## **4.2 Performance vs. MOI for Nonwood Baseball bats**

A representative sample of nonwood baseball bats comprised of aluminum and composite barrels was investigated. In the following sections, the relationship between performance to MOI and first bending frequency will be examined. The drop of the bat and how it relates to performance is not being investigated because all the nonwood bats fell within the -3 classification range. Each plot will be presented by length classification. Bats are classified by barrel material, e.g. aluminum or composite.

### **4.2.1 BESR vs. MOI for Nonwood Bats**

Figures 22 through 25 show BESR vs. MOI for nonwood bats classified by length. Different symbols distinguish the aluminum (plus signs) from the composite barrels (open diamonds). Figure 26 shows the same data for all lengths of bats. In Figures 22 through 25, it can be seen that the BESR value typically increases as the MOI of the baseball bat increases, and Figure 26 shows that the MOI increases as the length of the bat increases. Both the composite and aluminum barrel bats cover the same range in MOI. Distinct groupings by length can be observed in Figure 26 as was seen for the nonwood bats. For the nonwood bats, the MOI range associated with a length is lower than the range for the wood bats, and this lower range is due to the NCAA allowing a nonwood bat to have slightly lower MOI than a wood bat. The NCAA Baseball Bat Certification Protocol does specify a minimum allowable MOI for each length of bat. For ease of swing, manufacturers typically target to produce baseball bats that are close to the MOI lower limit—there is no upper limit.

As discussed in Section 4.1.1, the BESR performance of wood bats increases as MOI increases. As the MOI of a bat increases, the energy required to swing on the pivot in the air cannon test increases, and hence the bat acts more like a stationary wall as the MOI increases. As stated previously, nonwood bats exhibit the same phenomenon. However, nonwood bats have the added benefit of hollow construction (hoop mode), which introduces a trampoline effect. This benefit will be discussed more in later sections.

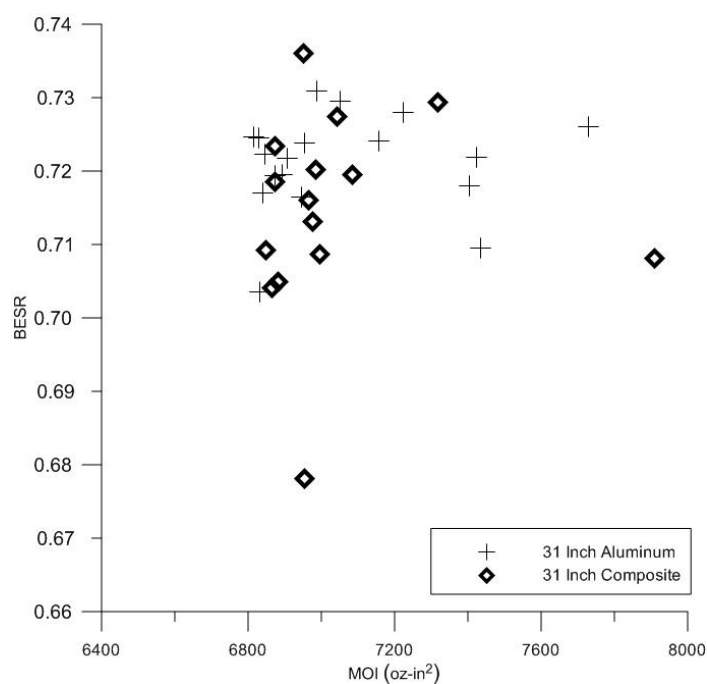


Figure 22: BESR vs. MOI for 31-in. nonwood bats

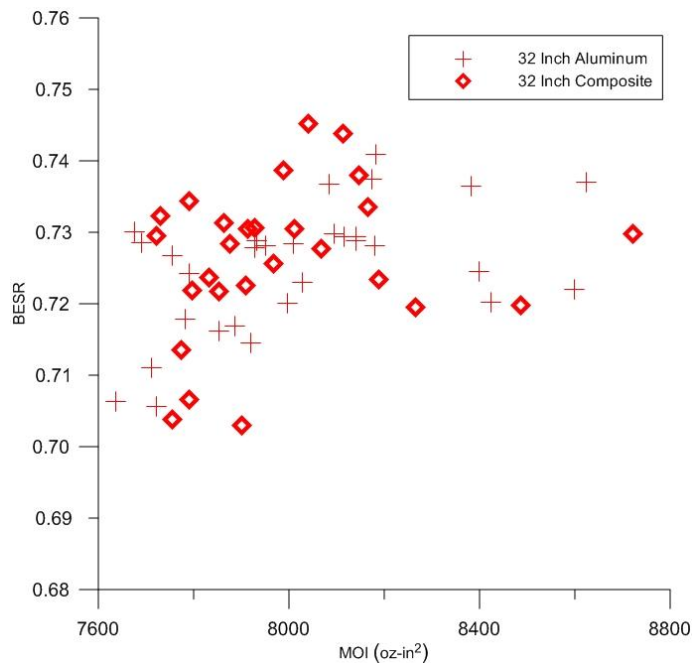


Figure 23: BESR vs. MOI for 32-in. nonwood bats

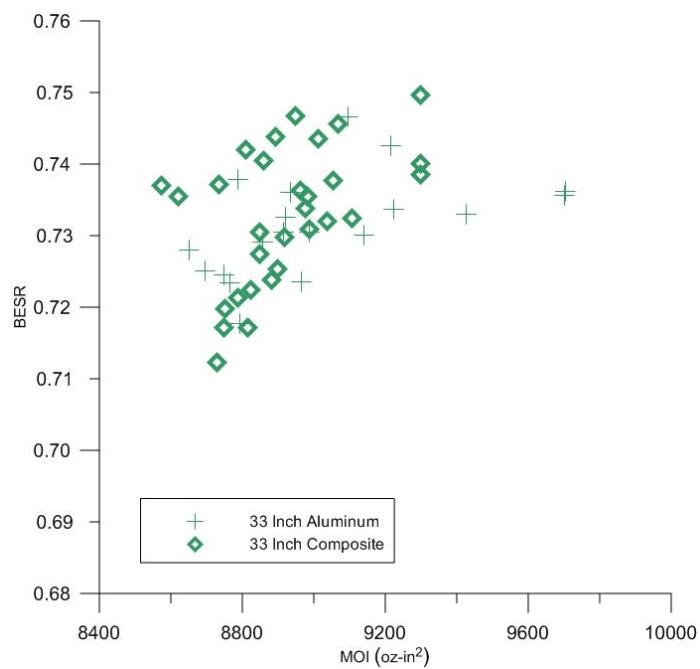


Figure 24: BESR vs. MOI for 33-in. nonwood bats



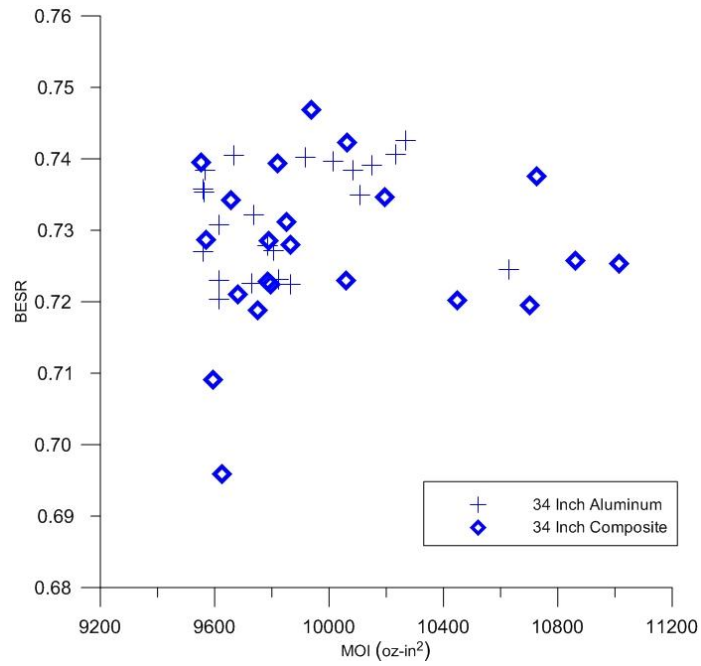


Figure 25: BESR vs. MOI for 34-in. nonwood bats

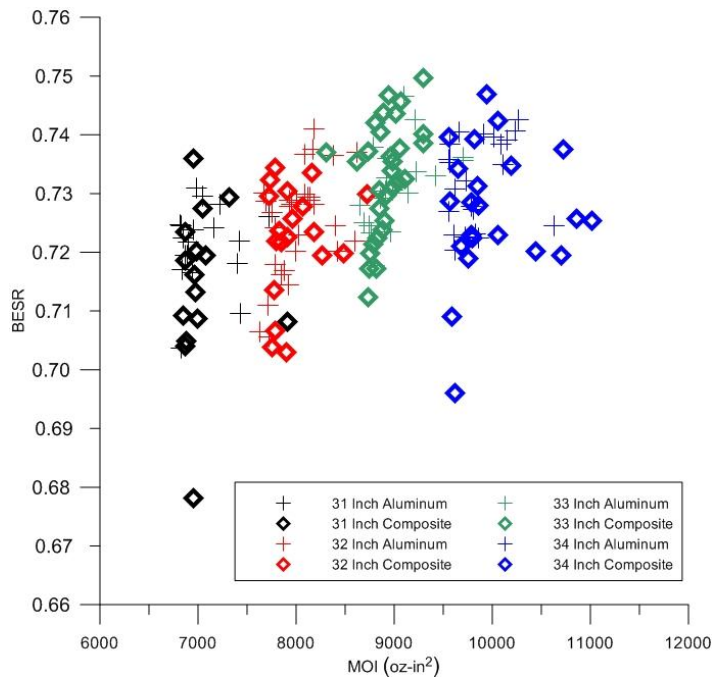


Figure 26: BESR vs. MOI for all lengths of nonwood bats

Figure 26 shows the BESR vs. MOI for all lengths of nonwood bats. This figure shows how each length falls within an MOI range. As the lengths of the bats increase, the linear velocity increases and the BESR increases.

Nonwood bats have the added benefit of hollow barrel construction and in general show better batted-ball performance than wood baseball bats as a consequence of the trampoline effect. This trampoline effect can be altered without needing to change the MOI. Thus, it is harder to conclude a trend due to MOI for hollow bats than it is for solid wood bats because of the presence of the trampoline effect, which will be shown to be a function of the hoop mode frequency.

#### **4.2.2 BBS vs. MOI for Nonwood Baseball Bats**

Figures 27 through 31 show the BBS vs. MOI for all nonwood baseball bats. These data show that for any given length of bat the BBS increases with decreasing MOI. This result is opposite of what was observed for wood baseball bats where BBS increased due to MOI increase. The result of a decrease in MOI increasing the BBS is a combination of linear speed and the trampoline effect that is present in the hollow-barrel bats. As the MOI decreases for a given length, the linear velocity of the bat increases. The increase in velocity contributes to an increase in BBS. However, unlike the wood baseball bats which have an essentially uniform BBCOR for all bats, the BBCOR of the hollow bats can vary from bat to bat due the presence of the trampoline effect.

Figure 28 shows the BBS vs. MOI for the 32-in. nonwood bats. The data set does not depict any clear trend between BBS and MOI. The aluminum baseball bats appear to have a trend of increasing MOI decreases the BBS. The composite barrel bats have

larger ranges of MOI and BBS than the aluminum bats, and there is a slight trend for the BBS to decrease with increasing MOI. The hollow construction allows for significant design freedom for the level of trampoline effect and mass distribution that contributes to the large scatter in the data.

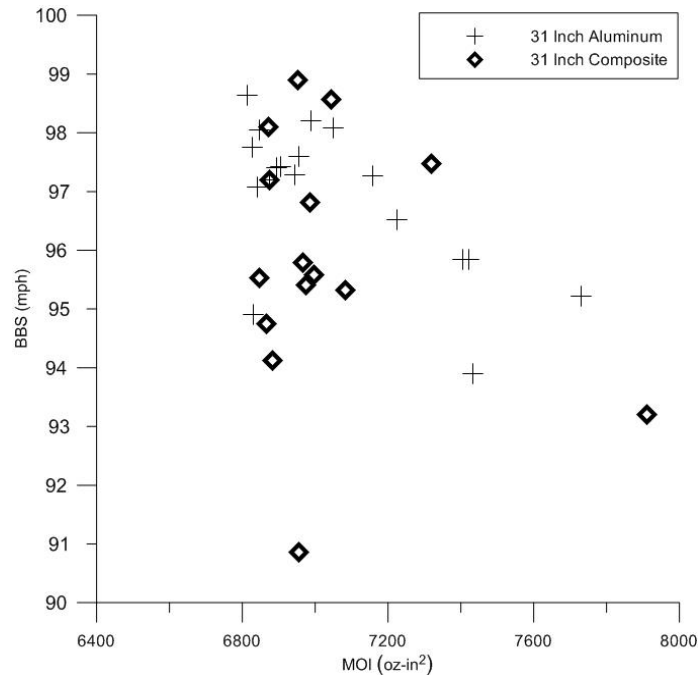


Figure 27: BBS vs. MOI for all 31-in. nonwood bats

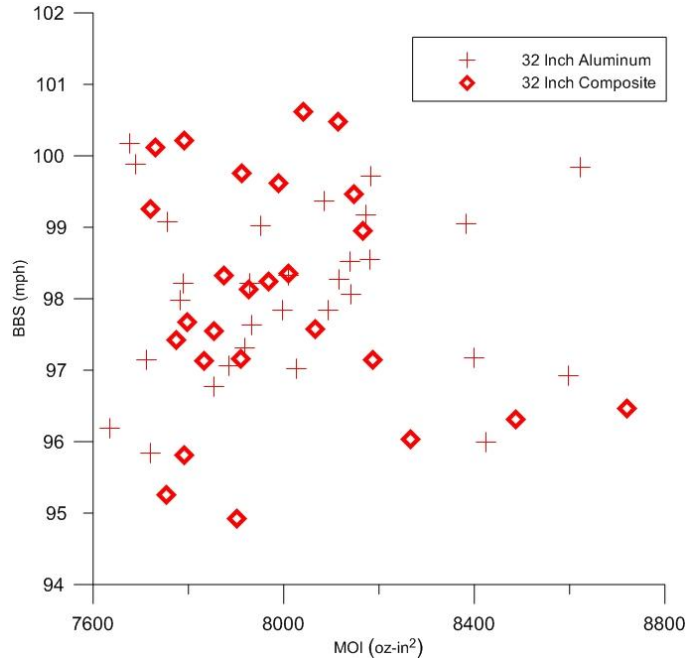


Figure 28: BBS vs. MOI for all 32-in. nonwood bats

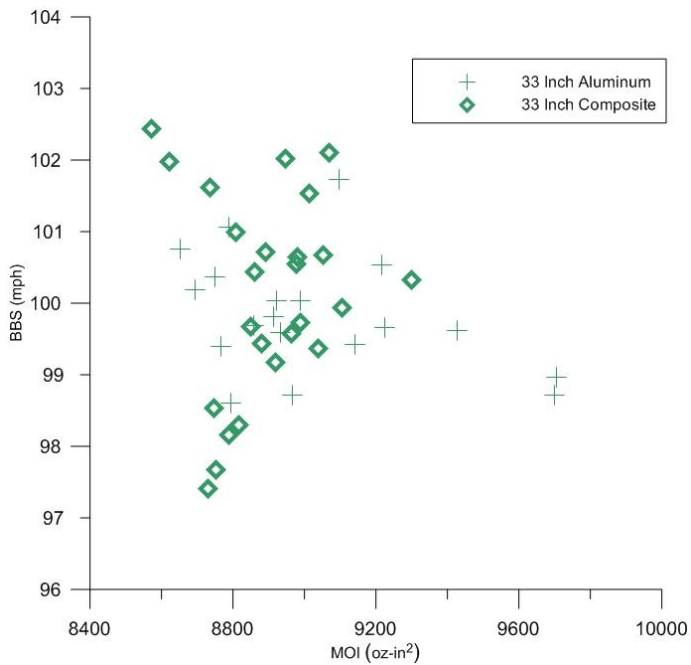


Figure 29: BBS vs. MOI for all 33-in. nonwood bats

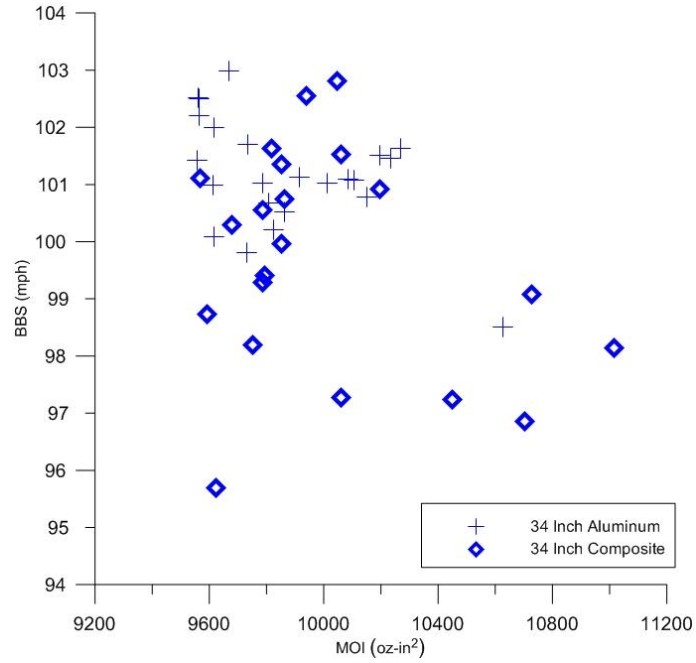


Figure 30: BBS vs. MOI for all 34-in. nonwood bats

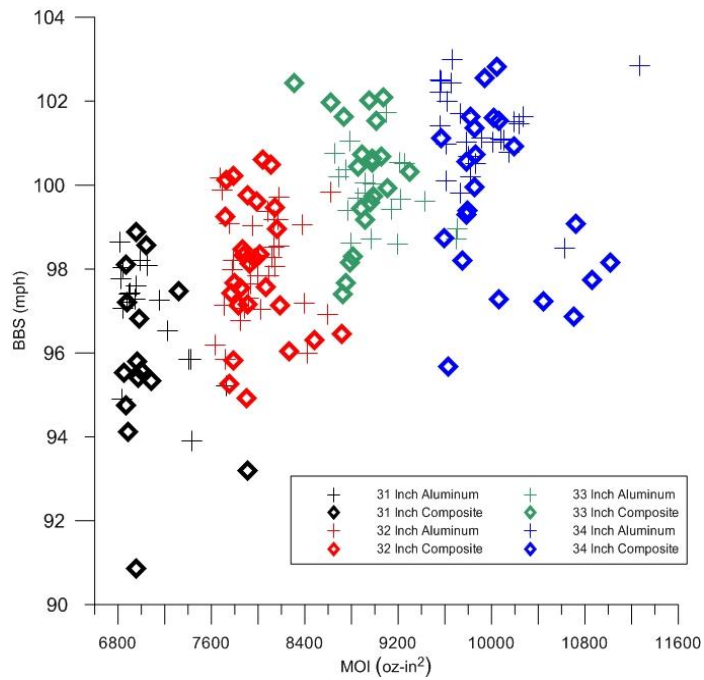


Figure 31: BBS vs. MOI for all nonwood bats

Figure 31 shows BBS vs. MOI for all lengths of nonwood bats. This figure shows again how the each length falls within an MOI range. As the length of the bat increases, the linear velocity at the point of contact increases and the BBS increases. The hollow bat construction, which introduces the trampoline effect into the performance of the bat, makes it difficult to see clearly that as the MOI increases the BBS decreases. However, the data imply the BBS vs. MOI relationship is opposite of what is observed for solid wood.

Over the course of this thesis the NCAA issued a change in performance metric from BESR to BBCOR for certification. Several of the manufacturers have submitted bats for BBCOR certification, but were not included in this set of data. Appendix C shows the previous BBCOR vs. MOI plots with the added data of the new BBCOR certification bats. These Appendix C plots show the BBCOR certification bats have relatively high MOI for their length class and have slower BBS speeds in comparison to the current BESR-certified bats.

#### **4.2.3 BBCOR vs. MOI for Nonwood Baseball Bats**

Figures 32 through 36 show BBCOR vs. MOI for all nonwood bats. Different symbols distinguish the aluminum (plus signs) from the composite barrels (open diamonds). In these, plots it can be concluded that as the MOI of the bat increases, the BBCOR decreases. Figure 36 shows the lengths of the bats fall within the MOI limits. As previously stated, the average BBCOR value for the wood bats is ~0.480. The BBCOR of nonwood bats being greater than 0.480 shows that nonwood baseball bats



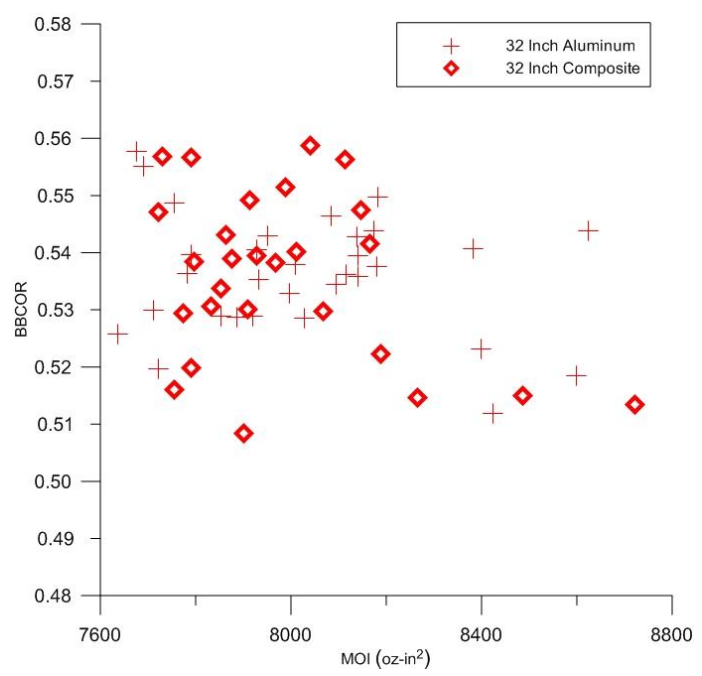


Figure 33: BBCOR vs. MOI for all 32-in. nonwood bats

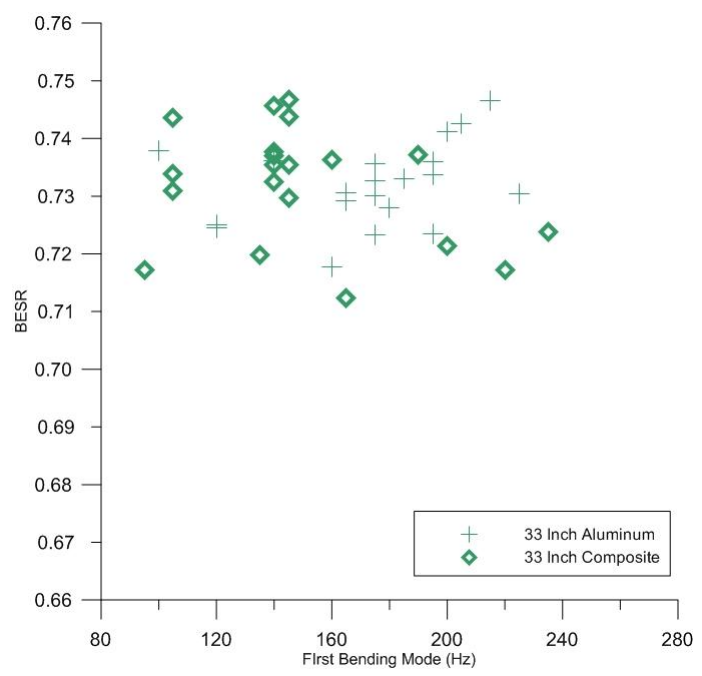


Figure 34: BESR vs. First Bending Mode for all 33-in. nonwood bats



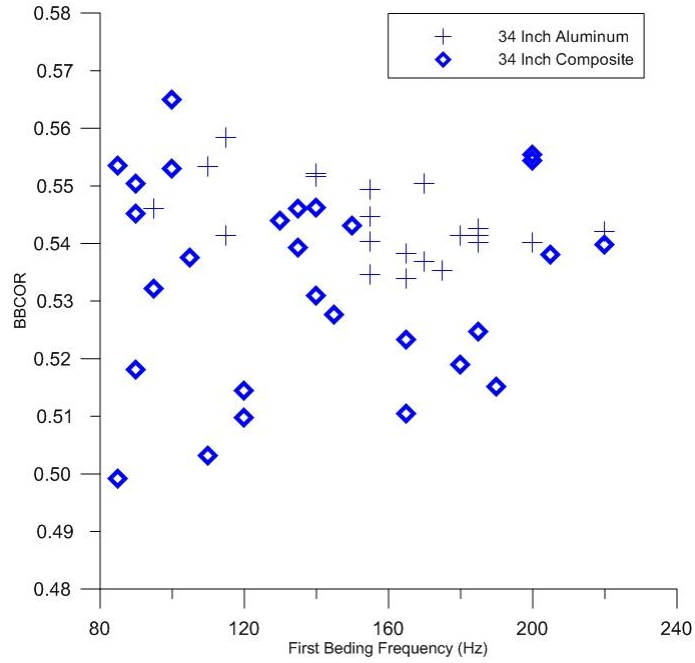


Figure 35: BBCOR vs. MOI for all 34-in. nonwood bats

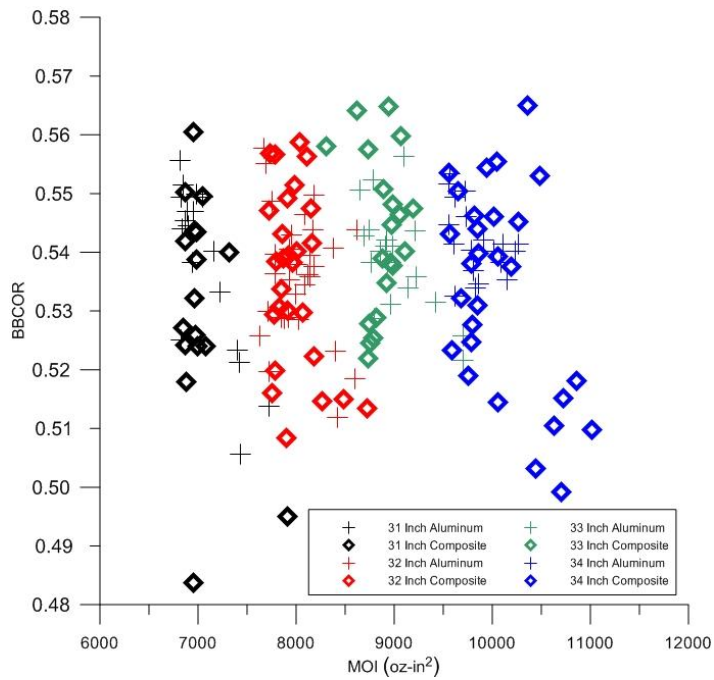


Figure 36: BBCOR vs. MOI for all nonwood bats

### **4.3 Performance vs. Bending Frequency for Nonwood Baseball Bats**

Modal tests were performed on the nonwood bats. The first bending modes were recorded and were compared to BESR, BBS and BBCOR. As discussed in Section 4.1.3 for the wood bats, as the length and mass increase, the stiffness decreases, and the first bending mode frequency decreases. The plots presented for the nonwood bats in Section 4.3 are by classification of length and barrel material.

Other parameters such as MOI, and hoop mode could not be isolated from the frequency information. Thus, the data presented in Section 4.3 are not solely a consequence of a variation in the modal variations amongst the bats. However, this limitation does not negate making some important observations as to a relationship between modal behavior and bat performance.

#### **4.3.1 BESR vs. Bending Frequencies**

Figures 37 through 41 show plots of BESR vs. the frequency of the first bending mode for the nonwood baseball bats. Similar to the wood bat data, a correlation can be seen between the first bending frequency and BESR. As the first bending frequency increases, the performance increases slightly for the nonwood bats. This slight increase in performance with increasing bending frequency is not as significant as was observed for the wood bats. The range of bending frequencies was 100 to 200 Hz for the wood baseball bats, while the range of bending frequencies was from 80 to 280 Hz for the nonwood bats. The various constructions of the nonwood bats contribute to the wide range in bending frequencies among these bats.

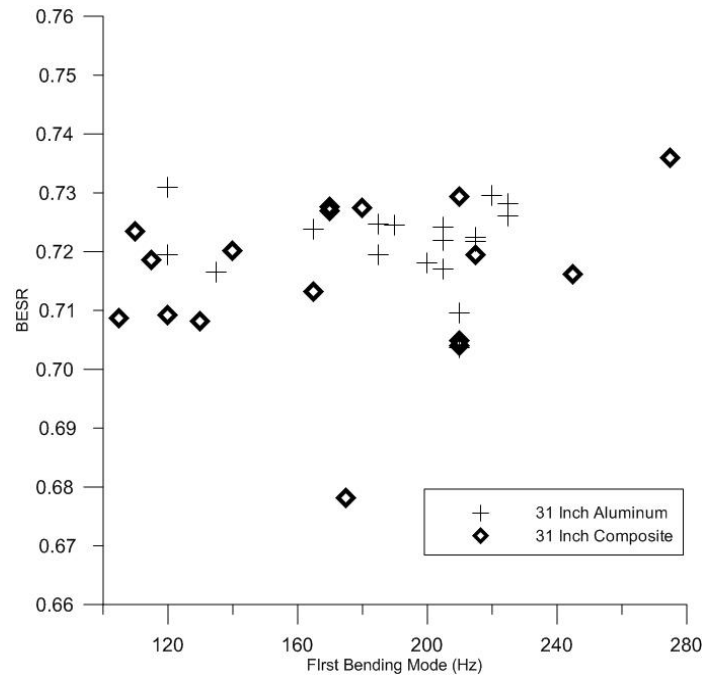


Figure 37: BESR vs. First bending frequency for all 31-in. nonwood bats

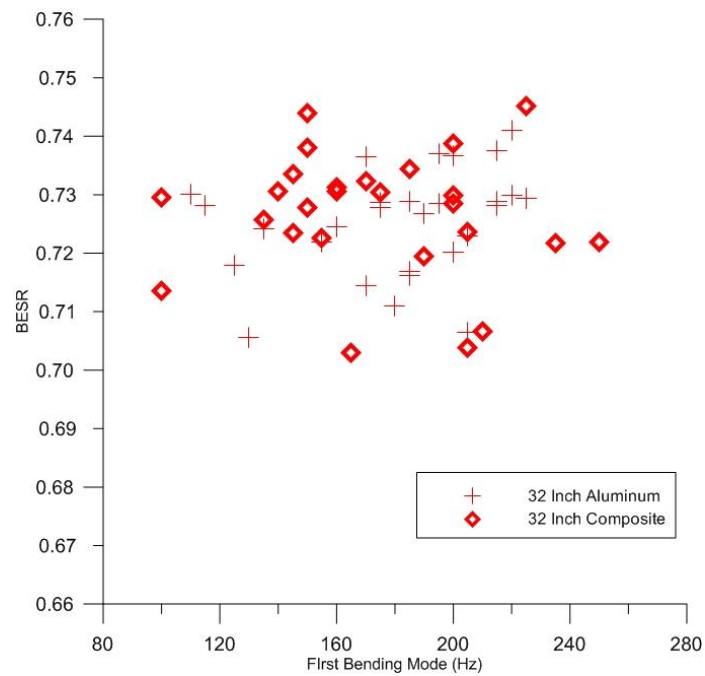


Figure 38: BESR vs. First bending frequency for all 32-in. nonwood bats

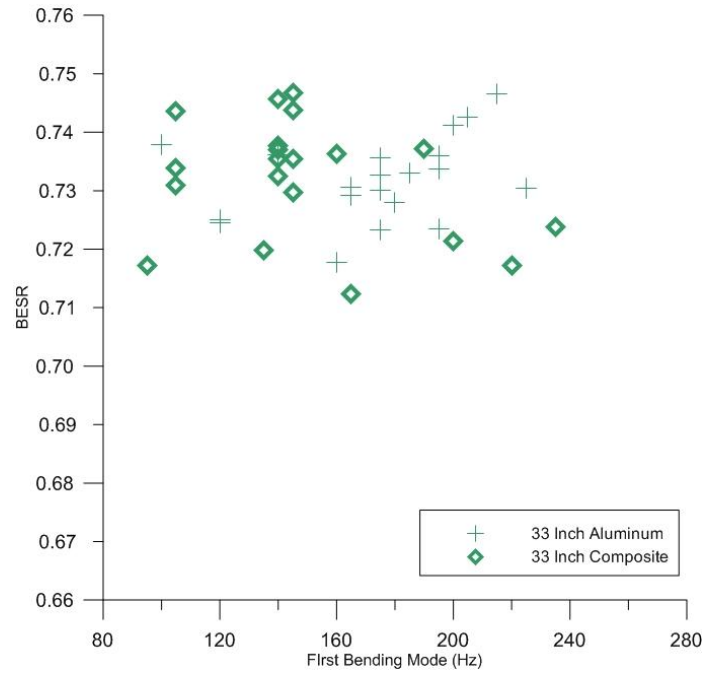


Figure 39: BESR vs. First bending frequency for all 33-in. nonwood bats

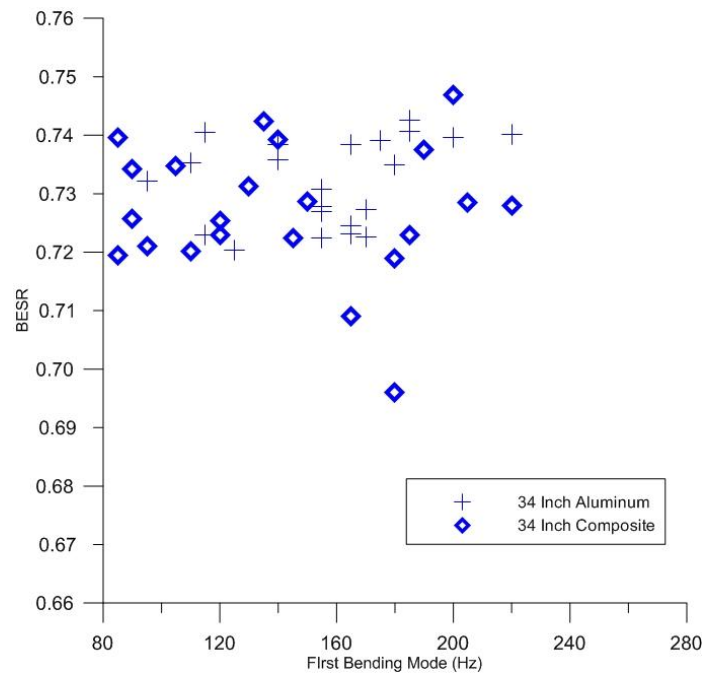


Figure 40: BESR vs. First bending frequency for all 34-in. nonwood bats

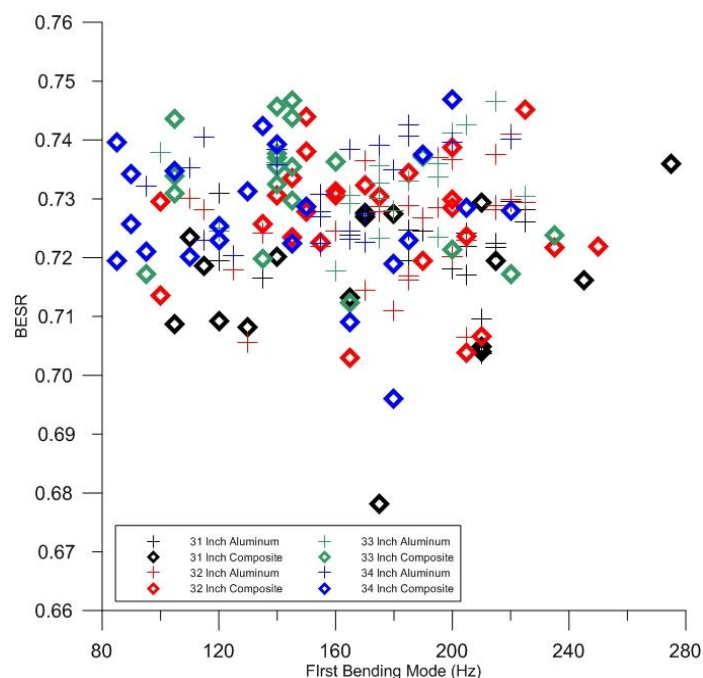


Figure 41: BESR vs. First bending frequency for all nonwood bats

#### 4.3.2 BBS vs. First Bending Frequency

Figures 42 through 46 are plots of BBS vs. first bending frequency. In these plots, it can be concluded that a small relationship exists between BBS and the first bending frequency, i.e. as the first bending frequency increases the BBS increases very slightly. As concluded from Figures 27 through 31, the range of MOIs exhibited by this set of bats has a greater effect on BBS than the range of first bending modes exhibited by these bats does. Figure 46 shows that aluminum- and composite-barrel bats fall within the same range of bending frequencies in each length classification. Figure 46 also shows as stated previously that as the length of the bat increases the BBS also increases.

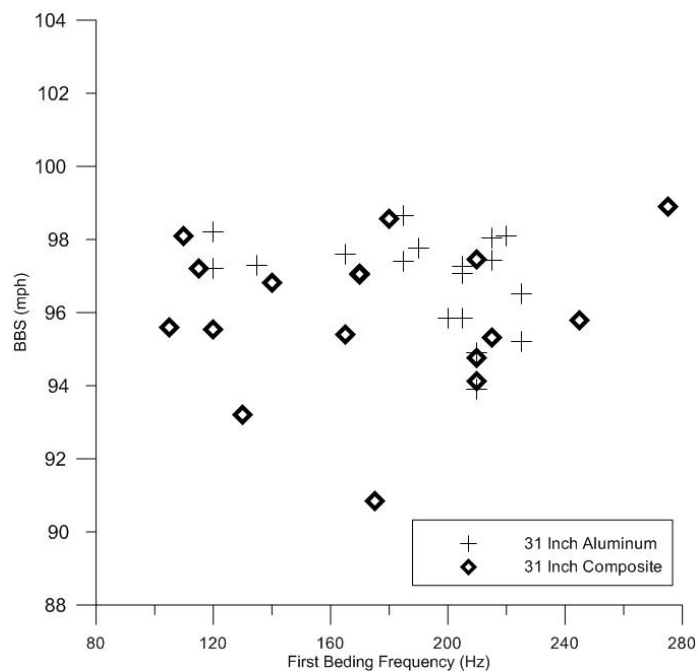


Figure 42: BBS vs. First bending frequency for all 31-in. nonwood bats

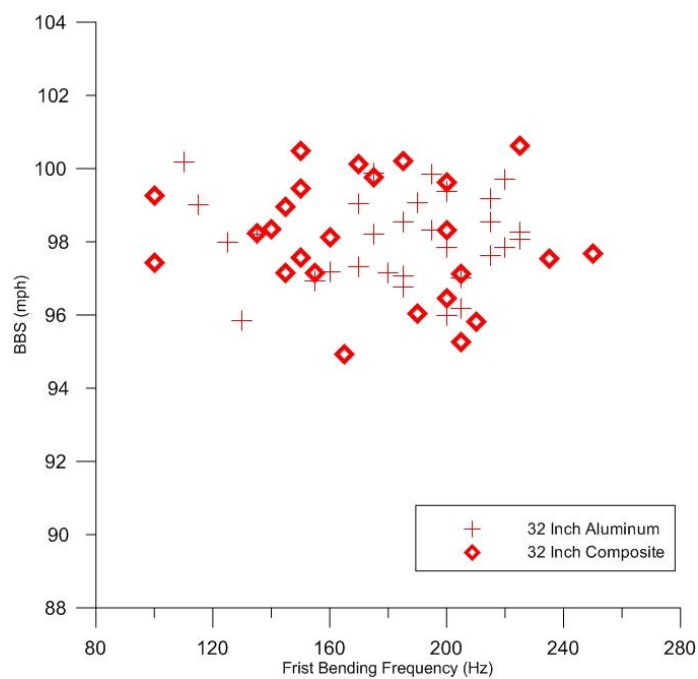


Figure 43: BBS vs. First bending frequency for all 32-in. nonwood bats

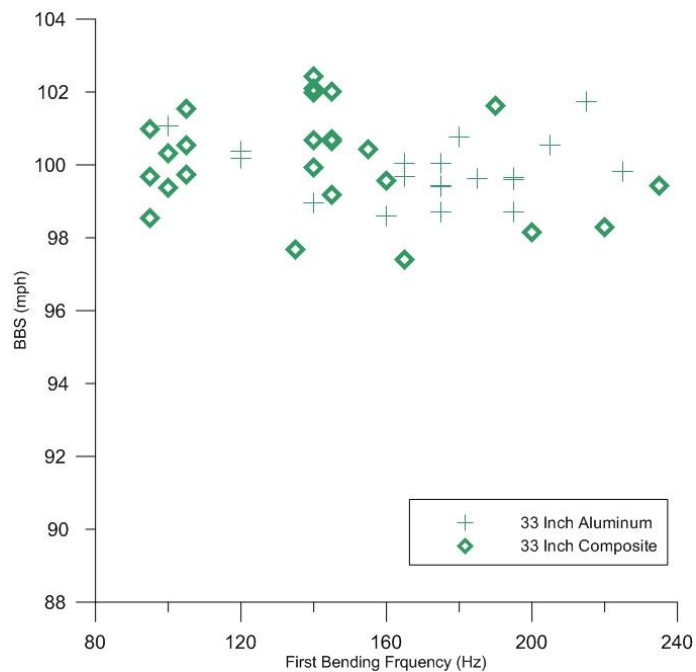


Figure 44: BBS vs. First bending frequency for all 33-in. nonwood bats

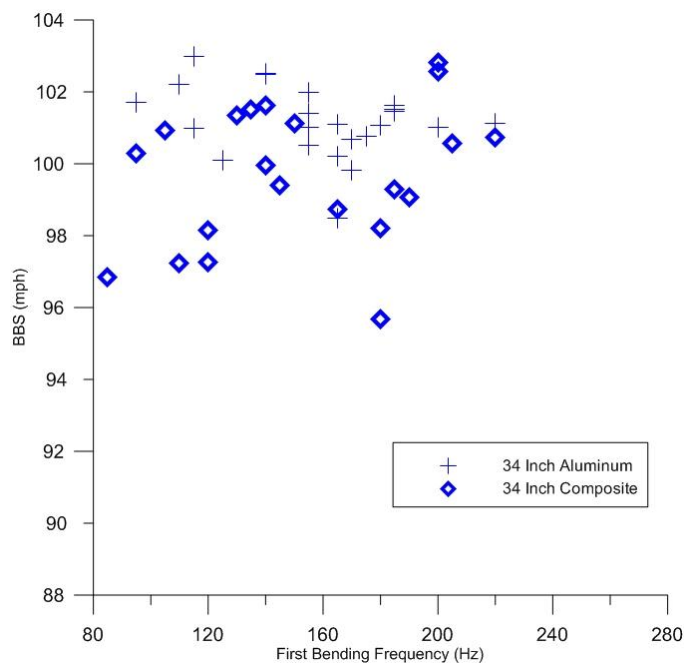


Figure 45: BBS vs. First bending frequency for all 34-in. nonwood bats

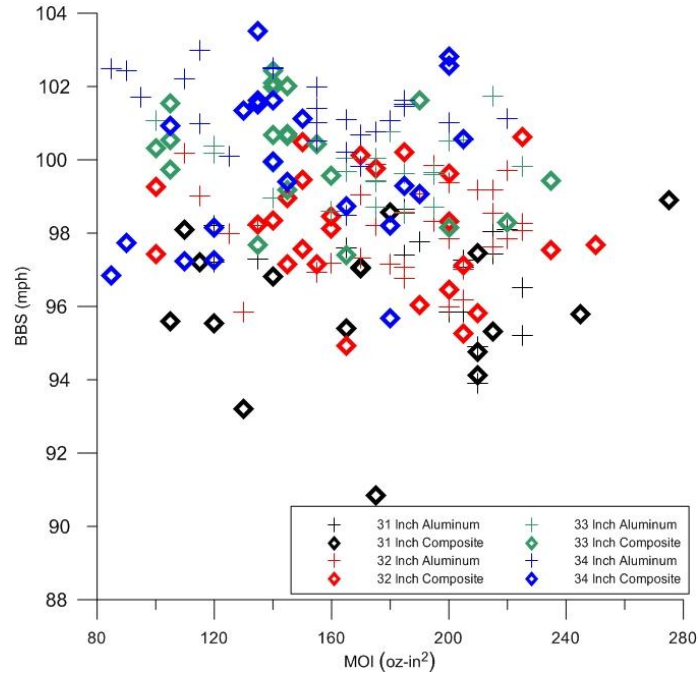


Figure 46: BBS vs. First bending frequency for all nonwood bats

### 4.3.3 BBCOR versus First Bending Frequency

Figures 47 through 51 show BBCOR vs. first bending frequency for the nonwood bats. BBCOR does not exhibit any special trend with respect to the first bending frequency for the nonwood bats. Figure 51 shows a wide range of BBCOR performance for the various bending frequencies. From Figures 47 through 51, BBCOR performance looks to be essentially independent of first bending frequency.



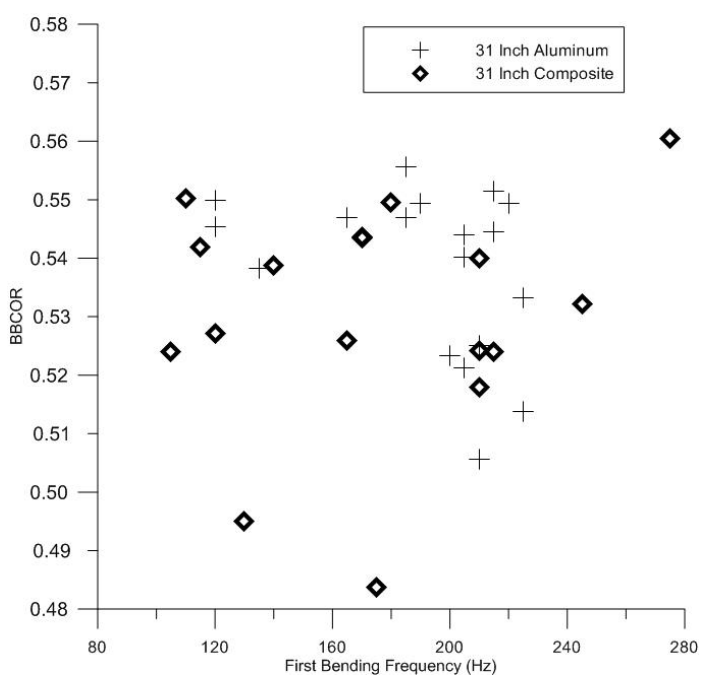


Figure 47: BBCOR vs. First bending frequency for all 31-in. nonwood bats

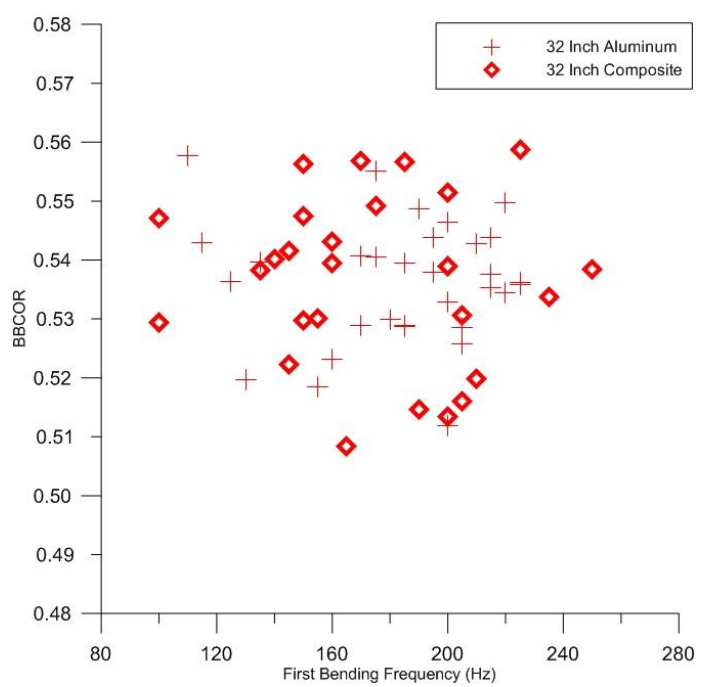


Figure 48: BBCOR vs. First bending frequency for all 32-in. nonwood bats

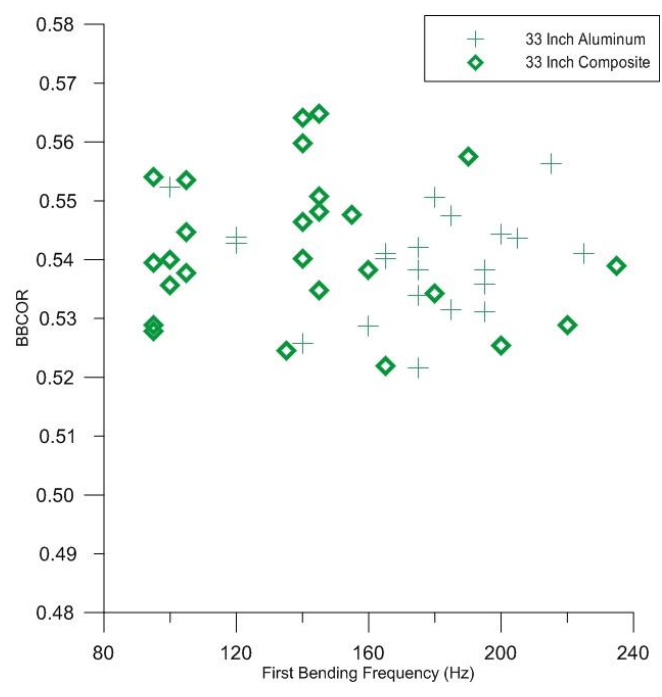


Figure 49: BBCOR vs. First bending frequency for all 33-in. nonwood bats

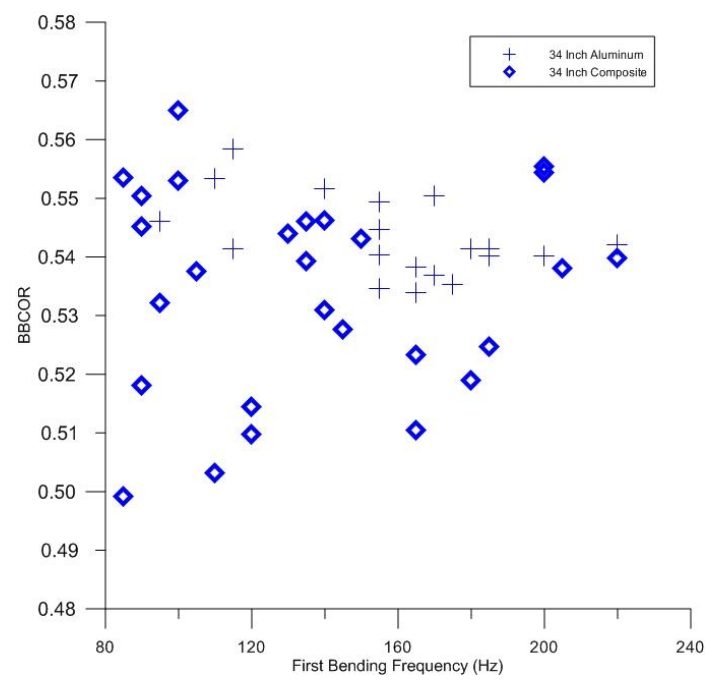


Figure 50: BBCOR vs. First bending frequency for all 34-in. nonwood bats

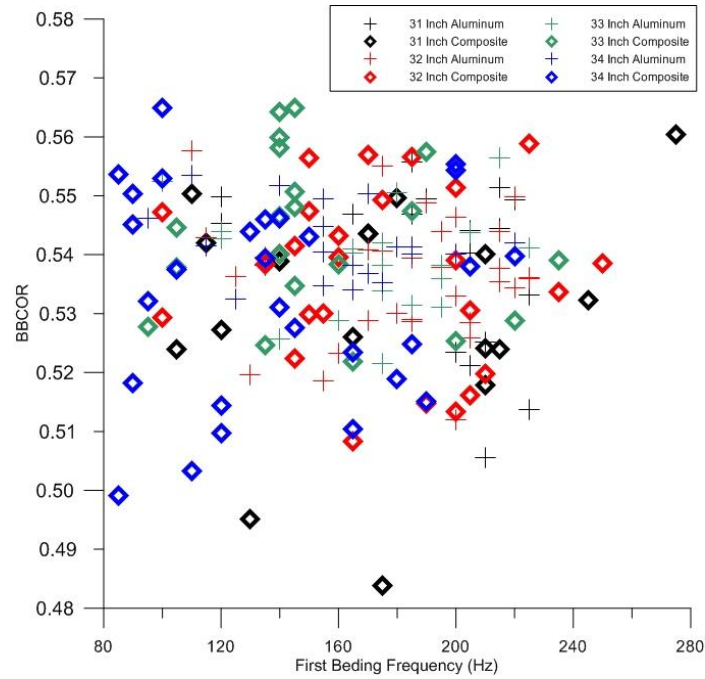


Figure 51: BBCOR vs. First bending frequency for all nonwood bats

## 4.4 Modeling the Trampoline Effect of a Hollow Baseball Bat

### 4.4.1 Bat Model

The nonlinear spring-mass-damper model used by Russell [8], described in Section 2.4.1, was applied to the collision between a baseball and the barrel of a baseball bat. A nonlinear system is needed to capture the nonlinear behavior of the baseball during the collision with the baseball bat to account for the energy loss in the baseball. Figure 52 shows the schematic for the system.

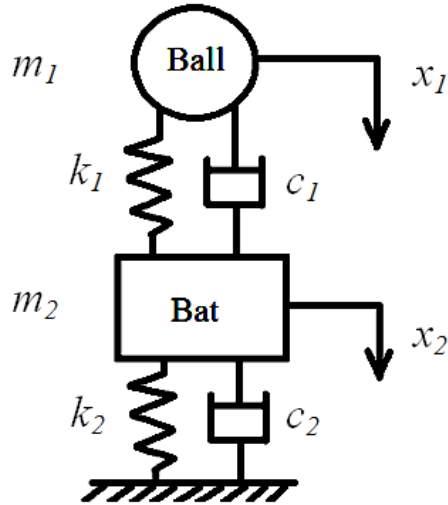


Figure 52: Mass-spring-damper model of the baseball/bat collision

The differential equations used to describe the equations of motion for the nonlinear system are:

$$m_1 \ddot{x}_1 = -k_1(x_1 - x_2)|x_1 - x_2|^a - c_1(\dot{x}_1 - \dot{x}_2)|x_1 - x_2|^b \quad (9a)$$

$$m_2 \ddot{x}_2 = -k_2 x_2 - c_2 \dot{x}_2 + k_1(x_1 - x_2)|x_1 - x_2|^a + c_1(\dot{x}_1 - \dot{x}_2)|x_1 - x_2|^b \quad (9b)$$

where the values of the constants used these equations are given in Table 2.

Table 2: Inputs for spring-mass-damper model

Constant	Description	Value	
		SI units	in-lb-sec units
$m_1$	mass of the ball	0.145 kg	0.32 lb
$k_1$	stiffness of the ball	$60 \times 10^6$ N/m	$3.43 \times 10^5$ lb/in
$c_1$	damping of the baseball	5000 N-s/m	28.6 lb-s/in
$m_2$	effective mass of the baseball bat	0.09 kg	0.1984 lb
$c_2$	damping of the baseball bat	100 N-s/m	0.571 lb-s/in
$k_2$	spring stiffness of the bat	Varied	Varied
$a$	First nonlinear coefficient	0.6495	0.6495
$b$	Second nonlinear coefficient	0.5202	0.5202

The spring stiffness of the baseball bat was determined by the desired hoop frequency and the effective mass of the barrel of the baseball bat. The effective mass of the barrel was determined by investigating several aluminum and composite barrel bats. The volume of the barrel was determined from wall thickness and length measurements over the barrel. Corresponding representative densities for aluminum and composites were used to calculate the mass of the barrel, and the average mass was determined to be the effective mass of the barrel.

The nonlinear constants  $a$  and  $b$  were determined by computing Cylindrical Coefficient of Restitution (CCOR) values using the differential equations (9a and 9b). Cylindrical Coefficient of Restitution is the ratio of the rebound speed to inbound speed off of a rigid cylinder. The mass and stiffness of the baseball bat were changed to represent a “rigid” cylindrical wall. A MATLAB script cycled through different combinations of  $a$  and  $b$  values and computed the CCOR for initial velocities of 60, 80, 90, 100 and 115 mph. The computed CCOR values for each of the combinations of the nonlinear terms and the respective initial velocity were compared to experimental CCOR data. If the computed CCOR values fell within the standard deviation of the measured CCOR data, the  $a$  and  $b$  terms associated with that computed CCOR values were tabulated. The tabulated  $a$  and  $b$  terms were then used again to compute the CCOR values for each of the speeds and plotted against the measured CCOR values. Figure 53 shows the numerically determined CCOR values compared to the experimental CCOR values. From the data, it was determined that  $a=0.6495$  and  $b=0.5202$ . Figure 53 shows the analytical CCOR values fall below the experimental data for 50, 80, 90 and 100 mph and above for 115 mph. The experimental values represent the best fit through the

experimental data given the estimated parameters of the baseball and determined values for the nonlinear exponents  $a$  and  $b$ . A preference to the 115 mph experimental value was selected because it best represents the bat-ball collision speed.

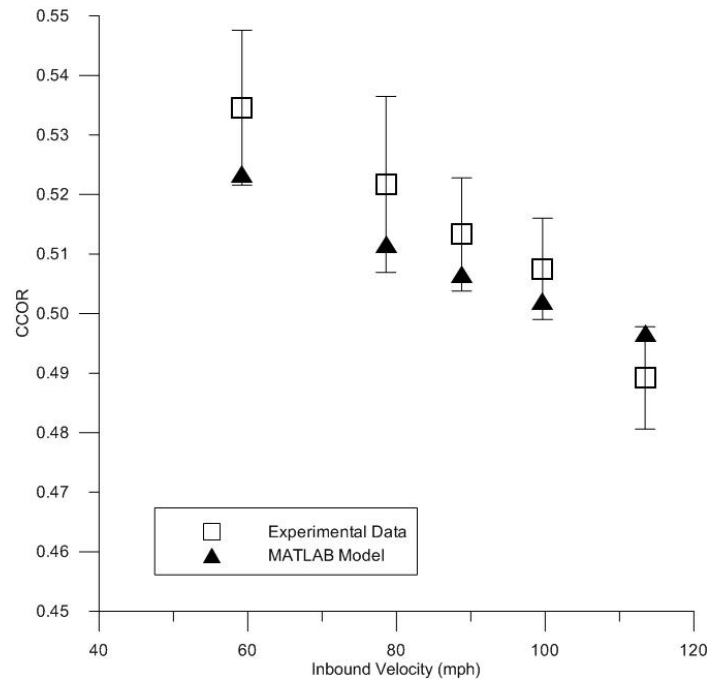


Figure 53: Analytical CCOR data compared to experimental data

With the input values for the spring-mass-damper model known, Equations 9a and 9b could be used to determine the maximum rebound velocity of the baseball for bats with a range of barrel hoop frequencies. An inbound velocity of 136 miles per hour was used as the initial velocity condition, and the hoop frequency of the baseball bat was varied from 0 to 10 KHz. The hoop frequency was used to compute the value of the stiffness,  $k_2$ . The values of CCOR were computed for each discrete value of the hoop frequency and normalized to values for a ball impacting a rigid bat. Figure 53 shows the normalized collision efficiency vs. hoop frequency plot for a baseball bat barrel.

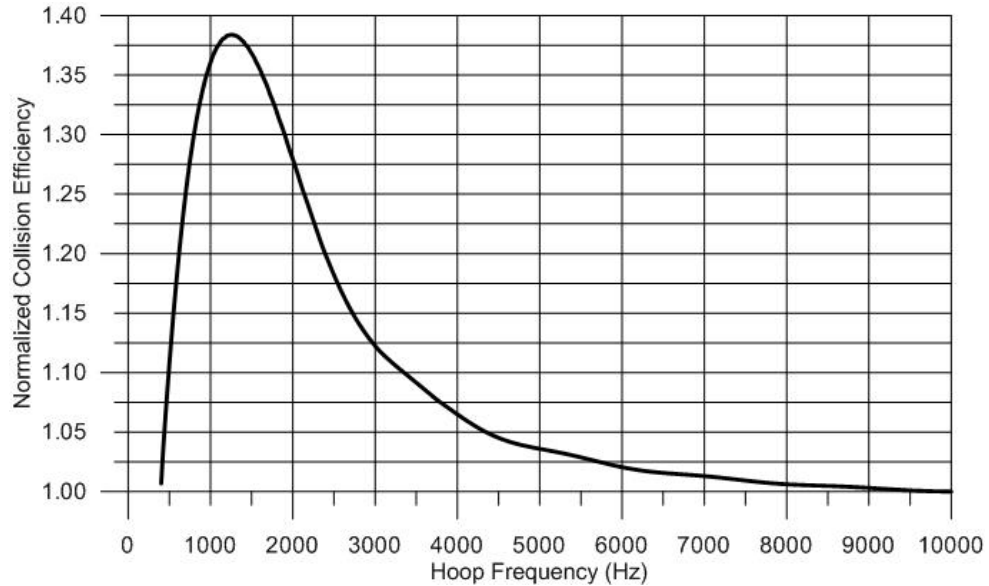


Figure 54: Normalized collision efficiency versus Hoop frequency

Figure 54 shows that the nonlinear mass-spring-damper model predicts a range of 1100 to 1300 Hz in which the hoop frequency would yield the peak batted-ball performance. To the left of this peak, the relative performance of the barrel will drop off quickly with respect to a change in hoop frequency. To the right of the peak, the drop in performance occurs over a range of 1400 to 6000 Hz. As the hoop frequency goes to infinity, the barrel of the bat starts to act as a solid bat, and the bat no longer has a trampoline effect. The MATLAB scripted used in this research is given in Appendix D.

#### 4.5 Performance vs. the First Hoop Frequency for Nonwood Baseball Bats

The first hoop mode frequency was measured and recorded for all nonwood bats according to the procedure in Section 3.6. The following sections will show the BESR,

BBS and BBCOR performance metrics compared to the first hoop mode frequency. Plots are presented by length classification and contain aluminum- and composite-barrel bats.

Composite baseball-bat barrels are more susceptible to damage than aluminum barrels. As a composite-barrel bat is used, the barrel can develop microcracks in the resin and between layers that tend to soften the barrel, i.e. causes the barrel stiffness to decrease. Recall that natural frequency is proportional to the square root of the stiffness divided by the mass. A decrease in the hoop frequency will occur as the barrel softens.

Broe [18] studied the effects of “breaking in” composite barrel bats using an ABI (accelerated break-in) process. The ABI procedure compresses the barrel of the bat by either a prescribed displacement or prescribed load in a rolling device—similar to the pair of rollers used for the ringer on an old washing machine. The rollers apply a pressure to the barrel of the bat, and the bat is rolled back and forth until a change in barrel stiffness is observed due to microcracking induced in the barrel as a consequence of microcracking, delamination and fiber breakage. A similar study performed by Cruz [19] investigated the performance increase in softball bats.

A set of composite-barrel bats that has undergone this ABI procedure was evaluated as part of this research. The hoop frequency was measured prior to each performance test. This ABI procedure was performed according to the NCAA standard [20] and is given in Appendix E. The performance was monitored each time the barrel was rolled. Several of the plots in this thesis show bats that have undergone this ABI procedure, and these bats are denoted in the plots by solid diamond symbols. Bats that have been used in college-level game play and have subsequently been tested at the UMLBRC also fall into this category.



In the following sections, it will be shown that composite bats which have been “used” either in the field or through an ABI process have much lower hoop frequencies and increased performance values in comparison to new composite bats and typical aluminum bats. The composite baseball bats range in hoop frequency from 2800 Hz for new, i.e. “bats right out of the wrapper”, down to 1300 Hz, for bats that have been “used”. The aluminum bats span a relatively narrower range of 1800 to 2400 Hz. Composite bats which have undergone the ABI process are the highest performing and have the lowest hoop frequencies.

In comparison to aluminum-barrel bats, manufacturers have more control over the effective properties of the composite-barrel bats, thereby allowing for the larger range of hoop frequencies occurring for the composite- versus the aluminum-barrel bats. Composite bat designs can differ in wall thickness and in the effective material stiffness along the length of the barrel by varying the directions of the fiber reinforcements. The only variable for aluminum bats is the wall thickness. The effective material stiffness is a consequence of the aluminum alloy used to make the barrel.

#### **4.5.1 BESR vs. the First Hoop Frequency for Nonwood Bats**

Figures 55 through 58 show plots of BESR vs. the first hoop frequency for nonwood bats. It can be seen in all of these figures that as the first hoop frequency decreases the BESR increases. Composite barrel bats have a relatively wide hoop frequency range from 1300 to 2800 Hz, while aluminum-barrel bats have a much narrower range from 1800 to 2400 Hz. Figure 58 also shows that composite bats that

underwent the ABI procedure have significantly lower hoop frequencies and are the higher performing than those that did go through the ABI process.

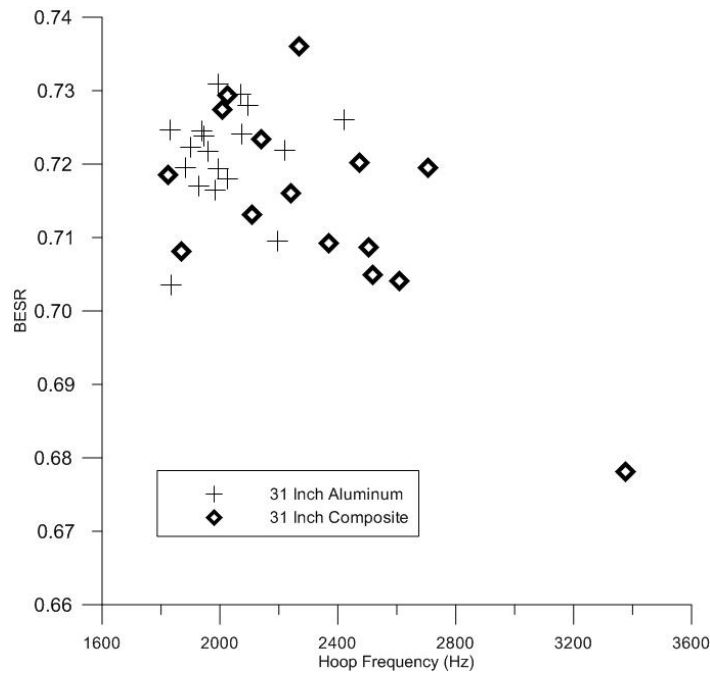


Figure 55: BESR vs. Hoop frequency for all 31-in. nonwood bats

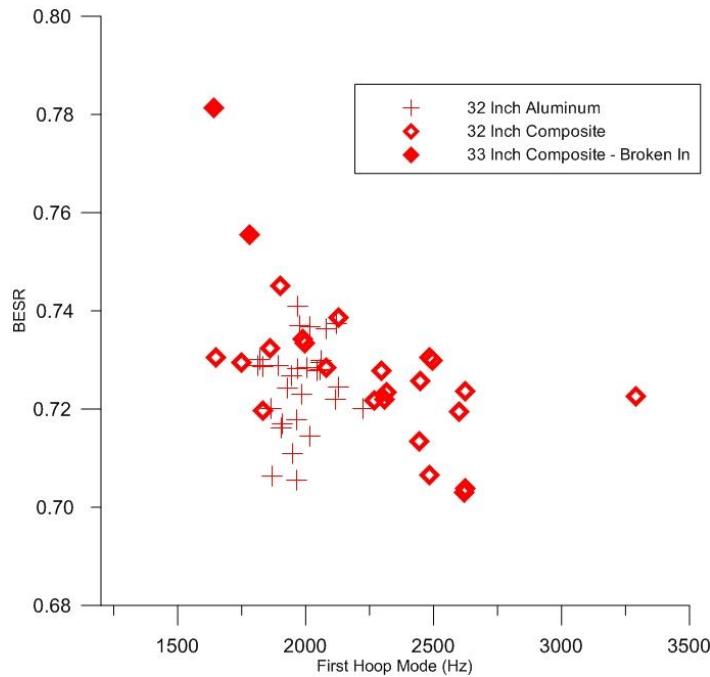


Figure 56: BESR versus Hoop frequency for all 32-in. nonwood bats

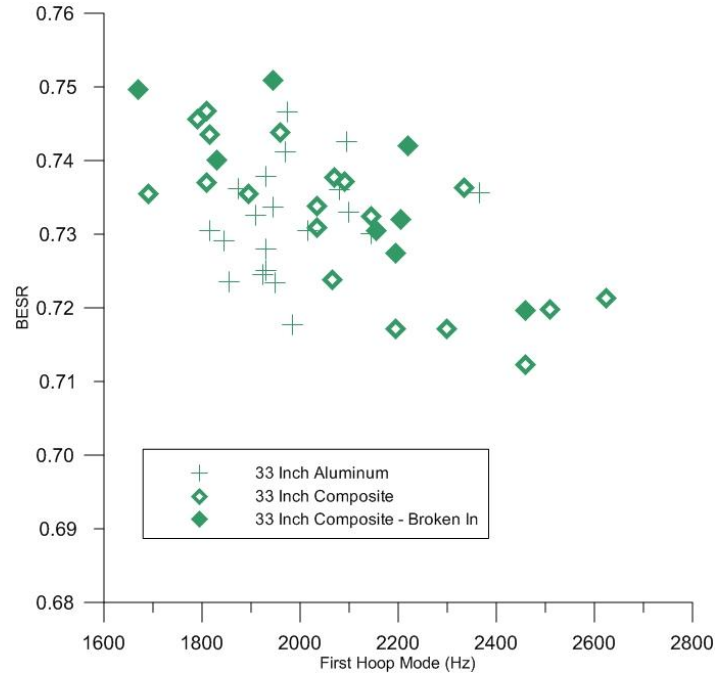


Figure 57: BESR versus Hoop frequency for all 33-in. nonwood bats

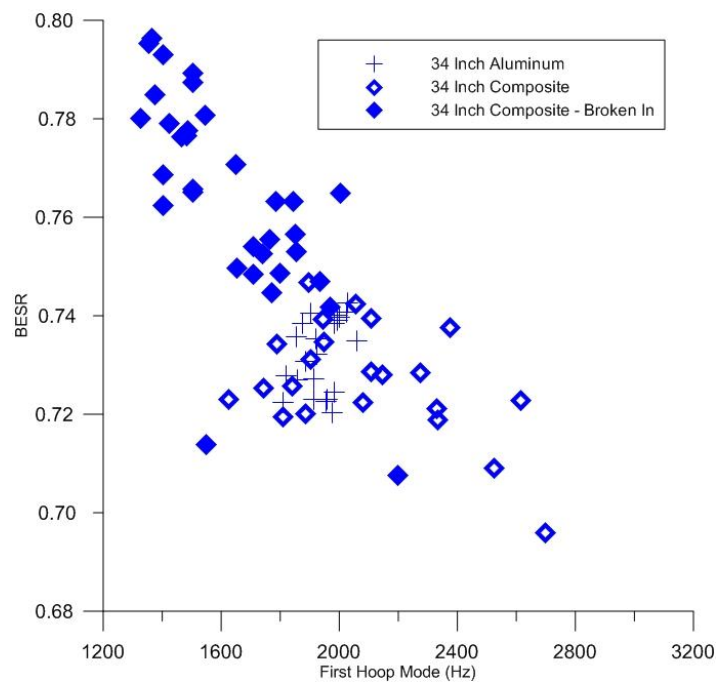


Figure 58: BESR versus Hoop frequency for all 34-in. nonwood bats

#### **4.5.2 BBS versus the First Hoop Frequency for Nonwood Bats**

Figure 59 through 62 shows BBS versus the first hoop frequency for the nonwood bats. Similar to the BESR metric, as the first hoop frequency of the barrel decreases the BBS increases. The composite baseball bats show a wider range of hoop frequency and performance than the aluminum barrels. Similar results were observed for bat lengths of 31, 32 and 33 in.

Figure 62 shows a set of composite baseball bats denoted by the red box that have a hoop frequency range from 1600 to 1900 Hz and have relatively lower performance than the other bats in the hoop frequency range. These bats have relatively high MOI values for the length class, ranging from 10450 to 11000 oz-in<sup>2</sup>, which contribute to a relatively lower swing speed in comparison to the other bats in the frequency range, and hence, relatively lower BBS values. The ABI bat in this red box had shown significant damage which was significantly affecting its BBS performance.

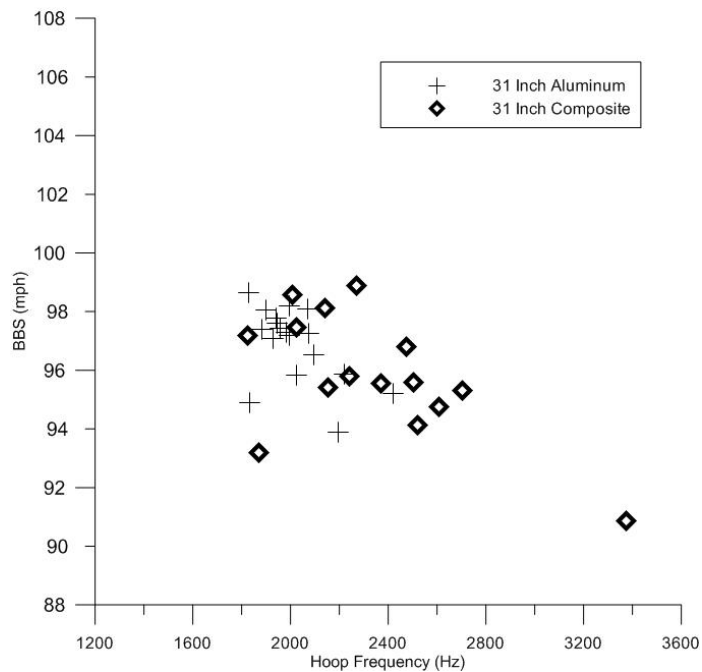


Figure 59: BBS versus Hoop frequency for all 31-in. nonwood bats

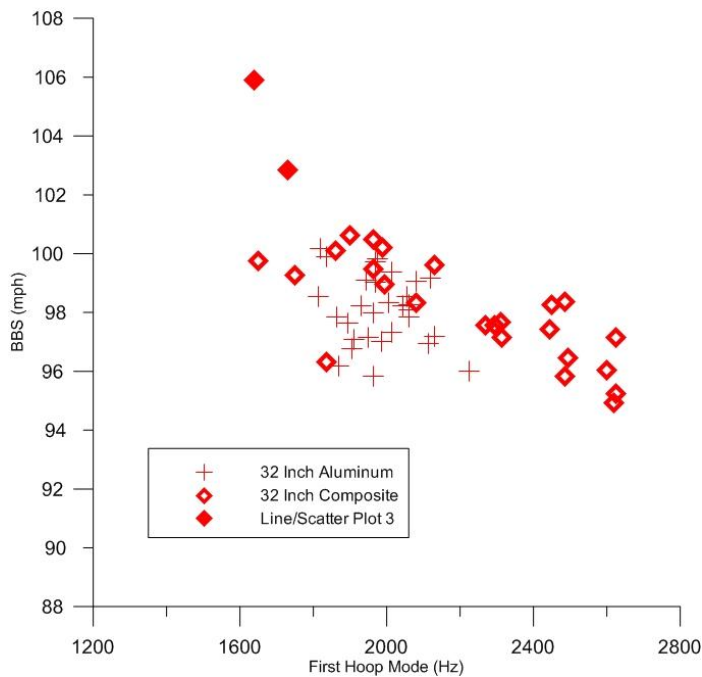


Figure 60: BBS versus Hoop frequency for all 32-in. nonwood bats

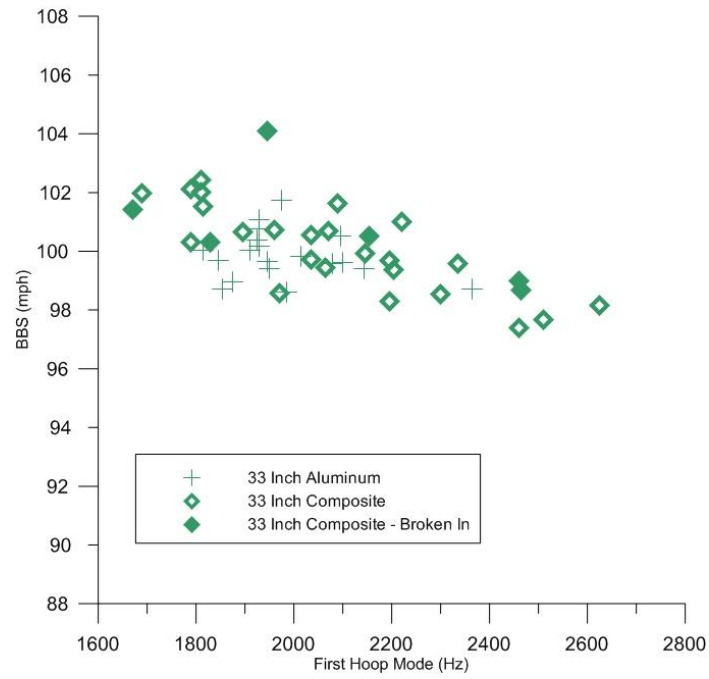


Figure 61: BBS versus Hoop frequency for all 33-in. nonwood bats

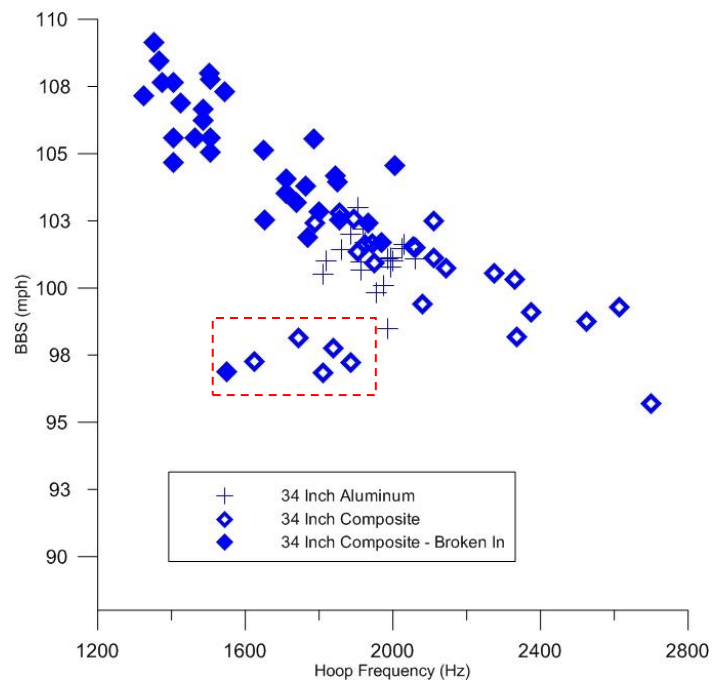


Figure 62: BBS versus Hoop frequency for all 34-in. nonwood bats

### 4.5.3 BBCOR versus Hoop Frequency for Nonwood Bats

Figures 63 through 66 57 shows a plot of BBCOR versus the first hoop frequency for nonwood bats. Similar to BESR and BBS, an increase in BBCOR is observed as the hoop frequency of the barrel decreases. Figure 54 shows a grouping of baseball bats that range in hoop frequency between 1600 and 1900 Hz and values of BBCOR less than 0.520. As mentioned in the previous section, this set of nonwood baseball bats has a relatively large MOI, ranging from 10450 to 11000 oz-in<sup>2</sup>. Again, the bat that underwent the ABI procedure as denoted by the red box had started to break down and form some cracks on the barrel but was still in usable condition.

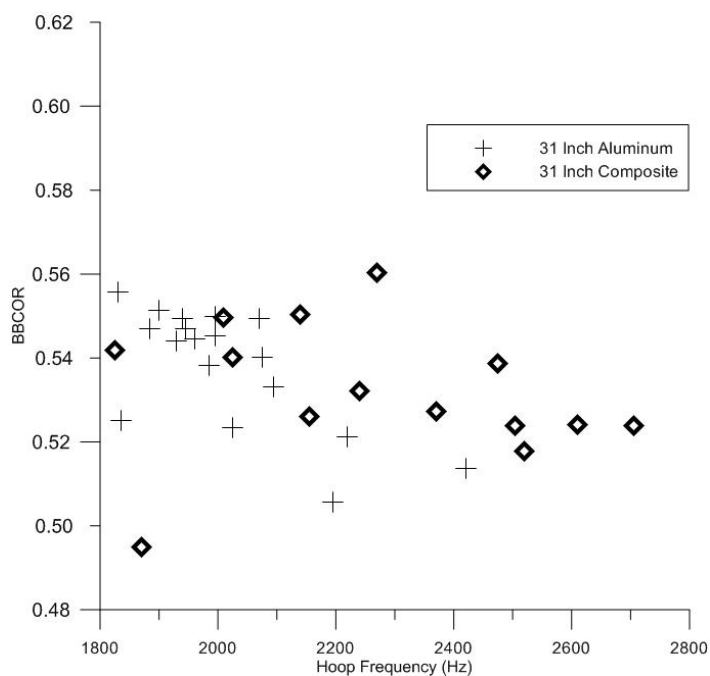


Figure F63: BBCOR versus Hoop frequency for all 31-in. nonwood bats

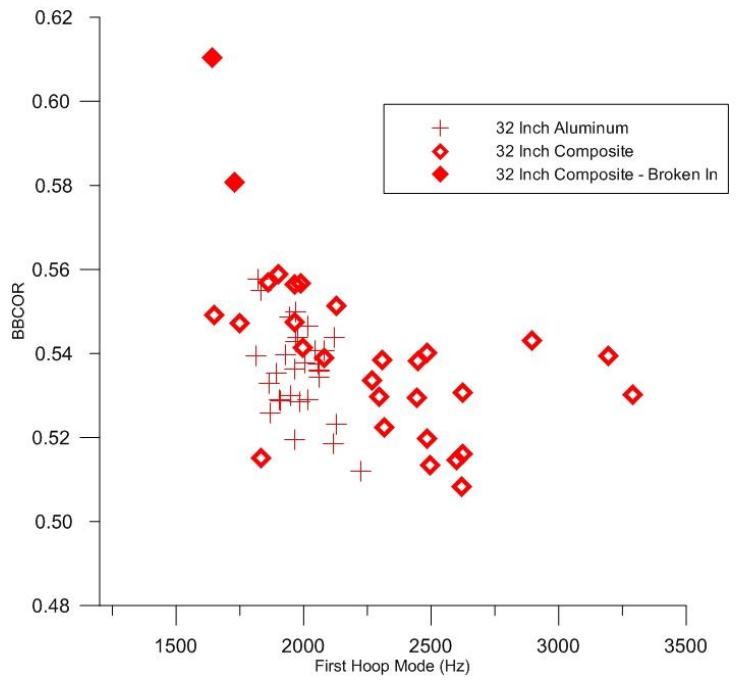


Figure F64: BBCOR versus Hoop frequency for all 32-in. nonwood bats

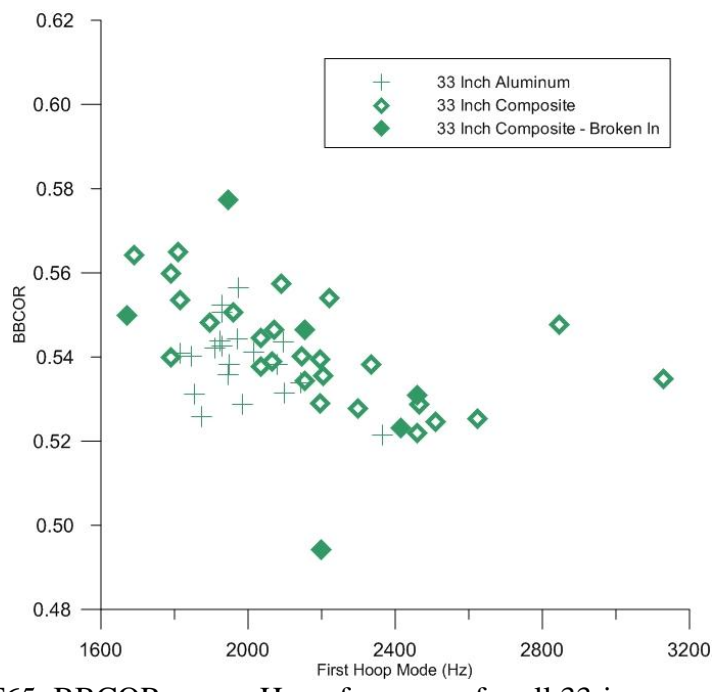


Figure F65: BBCOR versus Hoop frequency for all 33-in. nonwood bats



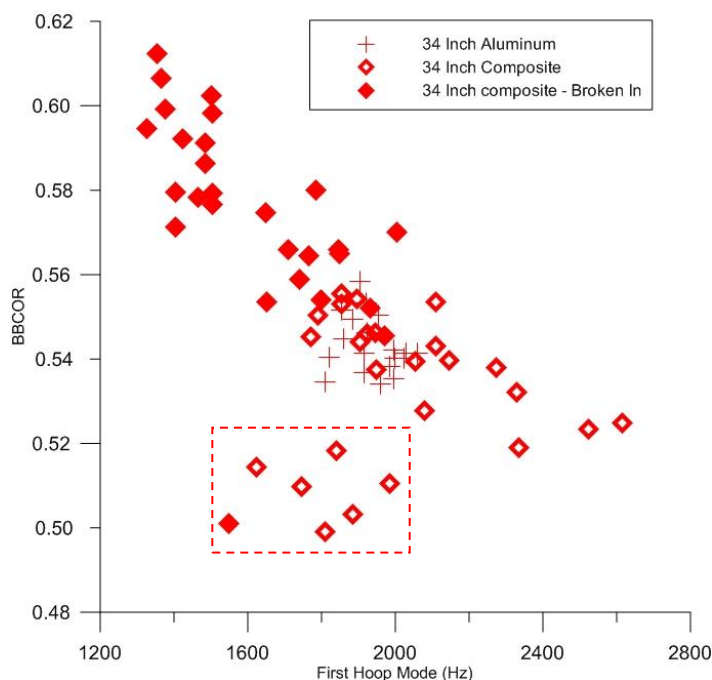


Figure 66: BBCOR versus Hoop frequency for all 34-in. nonwood bats

#### 4.6 Monitoring a Baseball Bat going through an Accelerated Break-In (ABI) Procedure

This section summarizes the performance of a composite bat as it went through the ABI procedure. The hoop frequency was monitored during the ABI procedure before each performance test was conducted. Figures 66 through 68 show the BESR, BBS and BBCOR versus hoop frequency, respectively. For recordkeeping purpose, a new Thesis ID was assigned to the bat for each time the bat was modal tested and then performance tested. Each point is labeled with an increasing Bat ID to denote the progression through the ABI procedure.

Figures 67 through 69 show how the performance of a composite-barrel bat can change over the lifetime of the bat. In these figures, a strong correlation can be observed between the first hoop mode and the performance metric as the bat progressed from the

first performance test through its final test. The bat started with a hoop frequency of 1970 Hz and was relatively low performing compared to its peak level. However, it should be noted that the bat was at the maximum allowable BESR “right out of the wrapper”. The initial test of the bat is identified as AS333, the final test as AS341, and the Bat IDs for the intermediate steps were logically followed. As the bat went through the ABI procedure, the hoop frequency decreased at nearly every step. The bat was at its highest performance at the 8<sup>th</sup> performance test, Bat ID AS340, with a hoop frequency of 1354 Hz. After the AS340 iteration, the barrel of the bat started to deteriorate due to forming large cracks, and the performance started to decrease. During the last test of the bat, the barrel became cracked around the circumference and broke in two pieces.

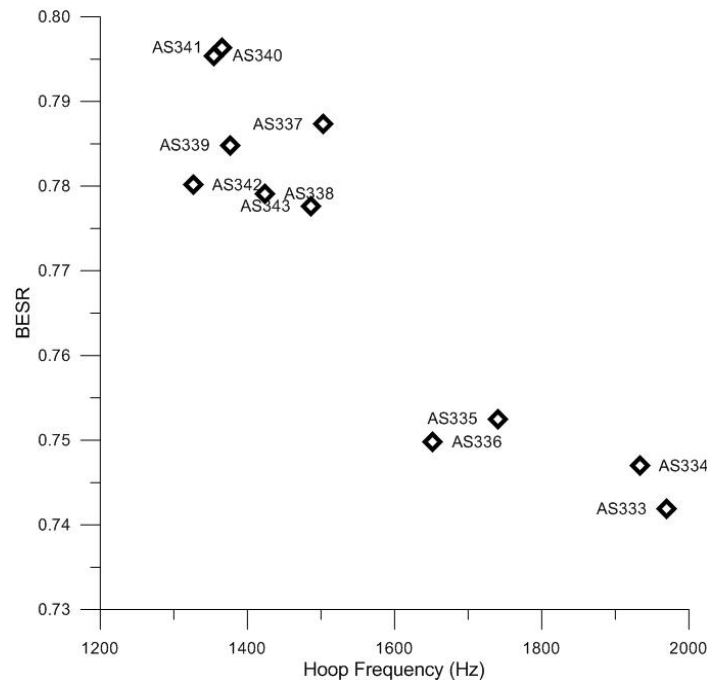


Figure 67: BESR vs. Hoop frequency for ABI test of one bat

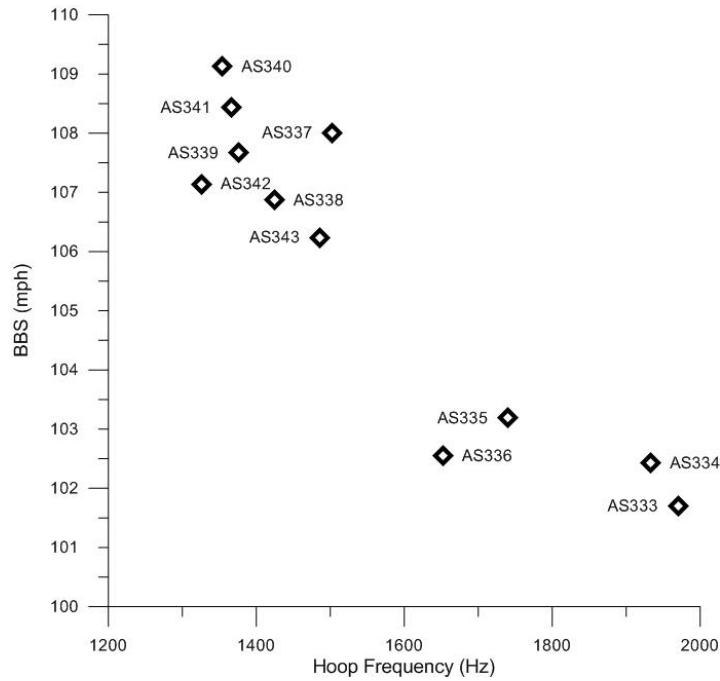


Figure 68: BBS vs. Hoop frequency for ABI test of one bat

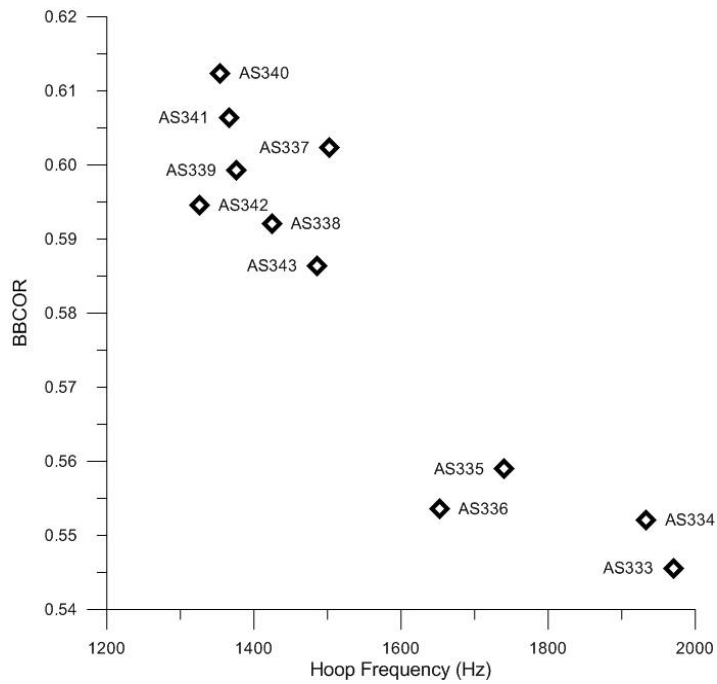


Figure 69: BBCOR vs. Hoop frequency for ABI test of one bat

#### **4.7 The Effect of the Baseball on the Hoop Frequency during the Collision**

The bat ball collision happens in under 0.001 s. During that time, some of the mass of the baseball could be considered to be “part” of bat. This added mass theoretically could cause the natural frequency of the hoop mode to shift. To explore this possibility, a finite element model of a bat-ball collision was investigated using LS-DYNA.

A previous bat-ball model, by Vedula [21], was used to investigate the bat-ball collision in relationship to hoop frequency. Vedula’s finite element model was of a 34-in. aluminum bat and used a homogeneous isotropic viscoelastic baseball. In the finite element model, the bat was swung while the ball was pitched for a combined speed of 136 mph at the point of contact (6 in. from the tip of the barrel).

An iterative eigen-solution option was run with the model. The model was paused at prescribed time steps and an eigen-solution of the bat-ball system was performed within LS-DYNA. It was anticipated that as the ball “wrapped” around the bat, the effective mass of the bat would increase and a measurable shift in the hoop frequency could be quantified. However, a negligible frequency shift was observed, and the results of this model were deemed to be inconclusive.

While the baseball used in the model gave good correlation between batted-ball speeds as measured in the lab by Vedula and the finite element model, the baseball used in the model was relatively stiff in comparison to high-speed video of a real baseball. Thus, visually the baseball does not truly represent the deformation response of a real baseball. If the baseball were to have deformed more like a real baseball, then more mass may have “become” part of the barrel. As more mass is added to the barrel, the hoop

frequency should decrease because of the relationship among natural frequency, mass and stiffness.

Figure 70(a) shows a high-speed video image of a baseball impacting an aluminum-barrel bat, and Figure 70(b) shows the same condition as modeled in LS-DYNA. It can be concluded from these figures that the deformation of the baseball in the model does not fully replicate the deformation seen in the experiment. Research is currently being pursued at the UMLBRC using a layer-by-layer approach to develop accurate finite element models of the Rawlings Major League and R1NCAA baseballs. Implementing one of these more accurate baseball models may show a very different result.

To explore the extreme condition, a finite element model of the baseball “welded” to the bat was investigated using the eigen-solution. With the “welded” ball, the hoop frequency of the bat changed from 2300 Hz to 1600 Hz. This drop in hoop frequency was expected as the mass of the baseball was added to the system. Thus, it is expected that upon the availability of a more credible finite element model of the baseball the frequency shift can be better explored than was done in the current research.

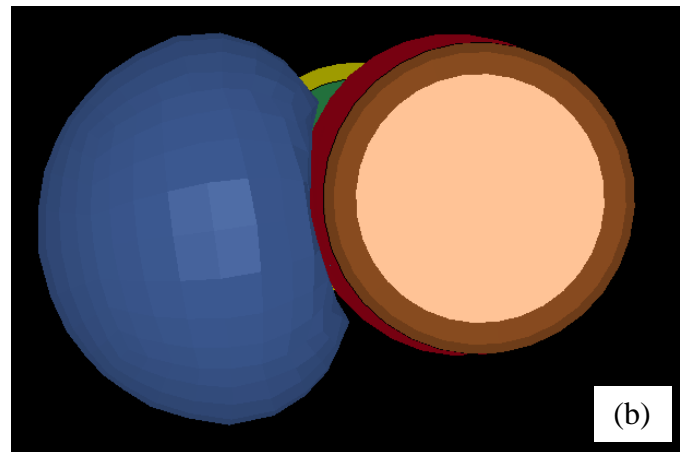
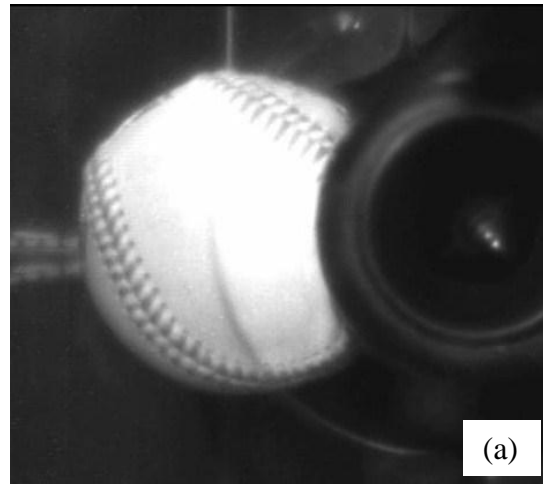


Figure 70: (a) Baseball impacting an aluminum baseball bat  
(b) Finite element model of a baseball impacting an aluminum baseball bat

#### 4.8 Summary

The performance of a baseball bat is a function of the solid properties and dynamic characteristics of the bat. Measurements of the length, weight, MOI and drop were taken for each bat used in this research. Modal analyses were completed on the bats to find the first bending modes of the wood and nonwood bats and the hoop modes of the nonwood bats.

The MOI and the drop of the wood baseball bats were found to contribute to the BESR and BBS performance metrics, but the BBCOR was fairly independent of MOI. As the lengths of the wood bats increased, the linear velocities increased and the BESR and BBS metrics increased with increasing bat length. It was observed that as the first bending modes increased, all performance metrics increased.

For the nonwood bats, it was observed that as the MOI increased, the BESR increased but the BBS and BBCOR decreased. The drop for the nonwood bats was not compared to performance because all of the nonwood bats fell within the -3 classification. A correlation was found that as the first bending mode increased, the BESR and BBS performance metrics increased. Composite bats were found to have a wider range of hoop frequencies than aluminum bats. All performance metrics increased as the first hoop frequency decreased. Composite bats that underwent the accelerated break-in procedure had the lowest hoop frequencies and the highest performance, as quantified by all metrics.

A nonlinear mass-spring model was used to simulate the collision between a nonwood bat and the ball. Model constants were empirically determined using a MATLAB code and experimental CCOR data. The model showed that the maximum batted-ball performance occurred in a hoop frequency range of 1100 to 1300 Hz.

The hoop frequency of a baseball bat was thought to change as the ball impacts the barrel of the bat. A finite element model was used to investigate the evolution of the first hoop frequency during the bat-ball collision. A negligible change in the hoop frequency was observed as the ball moved in and out during the collision. However, the ball used in

this simulation did not accurately represent the characteristic of a real baseball, so the analysis was most likely not representative of a real bat-ball collision.



## 5 Conclusions

The dynamic response of baseball bats has been studied in an effort to develop an understanding of the relationship between the modal characteristics of collegiate and major league bats and their associated batted-ball performance. The physical properties of MOI and drop were also studied to see if and what relationships exist between these properties and bat performance. A simple two degree of freedom mass-spring-damper model was used as a complementary tool for insight into studying these relationships. Several conclusions have been made as result of these studies:

- As the length of the bat increased, the linear velocity increased causing an increase in BESR and BBS for both the wood and nonwood bats.
- As the moment of inertia increased, the BESR and BBS performances increased for both the wood and nonwood bats.
- The BBCOR performance was essentially the same for the wood bats regardless of the MOI. This result is because the barrel of a wood bat is essentially rigid, so these bats do not have a trampoline effect.

- For wood bats, the drop of the wood bat has an effect on the performance metrics of BESR and BBS. As the drop became more positive, the BESR increased. A wood bat with a more negative drop will have an increase in swing speed and therefore will have an increase in BBS.
- As the length of the wood bat decreased, the bending frequencies increased. This result is due to the combination of the decrease in length, which leads to an increase in the effective bending stiffness, and the decrease in mass. As the first bending frequency of the wood bats increased, an increase in performance for all metrics was observed.
- For the nonwood bats, it was found that as the MOI increased, the BESR increased while the BBS and BBCOR values decreased. The drop was not considered because all of the nonwood bats fell within the -3 classification, so this parameter was not varied. The performance metrics of BESR and BBS were found to have a correlation to the first bending mode where the higher the first bending frequency the higher the performance. However, there was no correlation found between the first bending mode and BBCOR.
- A mass-spring-damper model was used to simulate the bat-ball collision for nonwood bats with varying hoop frequencies. The model showed there is an optimal hoop frequency range for the barrel of the bat to produce an efficient collision, and this range is 1100 to 1300 Hz.

- The first hoop mode of the nonwood bats was measured using impact testing and compared to the performance metrics. As the hoop frequency decreased the performance across all performance metrics increased. This phenomenon agrees with the two degree of freedom model used in this research.
- Composite bats were found to have the widest range of hoop frequency and performance. This wide range of hoop frequencies is a reflection of the wide variations that result from the manufacturing processes used for these composite bats.
- A composite bat was tested using the accelerated break in procedure. The hoop frequency of the bat decreased, and an increase in performance was observed.
- A finite element model of the bat-ball collision was used to investigate how the “added” mass of the baseball influences any variation in the hoop mode during the bat-ball collision. The finite element model showed negligible change in the hoop frequency as the ball moved in and out of the collision. However, the stiffness of the ball was not necessarily representative of a real baseball.

## 6 Recommendations

Work done in this thesis gave a good understanding on how the natural frequencies of the baseball bats affect the performance. Recommendations for future research to further this understanding include:

- Investigate baseball bats with hoop frequencies at and below 1300 Hz to try to establish the peak hoop frequency and roll off after 1100 Hz. This study could further validate the nonlinear mass-spring-damper model.
- Another option for exploring the effect of hoop frequency is to use finite element models of bats with hoop frequencies at and below 1300 Hz. However, such a computational study would require the use of a credible and robust finite element model of a baseball, and such a model does not yet exist. However, a qualitative understanding may possibly be developed even with a fairly good finite element model of a baseball.

- A study could be performed investigating how the baseball affects the dynamic response of the baseball bat. As mentioned in the previous bullet, a more accurate finite element model of a baseball than was used in this research would be required.
- Investigate the relationship between durability of a baseball bat as it relates to hoop frequencies. As the hoop frequency drops does the durability drop, too? Before aluminum bats were strictly regulated, it was not uncommon for a very thin-walled aluminum bat to last only 10 impacts.
- Studying the dynamic response of a bat while in the hands of a player may contribute to a better understanding of modal contributions to performance. Accelerometers could be mounted to the baseball bat in several locations so as to measure the frequency response as a player swings and makes contact with the ball.
- Further investigate the hoop modes of wood bats and composite wood bats. Composite wood bats would be constructed of a hollow composite core with a hollow wood shell around the outside.
- Continue investigating the relationship between the breaking in of composite bats to the resulting change in performance. Samples of composite bats from multiple manufacturers should be considered so as to include a representative range of manufacturing methods and a range of qualities. Various techniques for modifying the bat physical properties to change the dynamic response could be performed. Barrel walls could be machined to reduce the wall thickness and hence reduce the hoop frequency (maybe below 1300 Hz).

## 7 Literature Cited

- [1] NCAA, 2009, National Collegiate Athletic Association Standard for Testing Baseball Bat Performance, BESR  
[http://www.ncaa.org/wps/wcm/connect/10e4ff004e0b9c15a2f5f21ad6fc8b25/2006\\_certification\\_protocol.pdf?MOD=AJPERES&CACHEID=10e4ff004e0b9c15a2f5f21ad6fc8b25](http://www.ncaa.org/wps/wcm/connect/10e4ff004e0b9c15a2f5f21ad6fc8b25/2006_certification_protocol.pdf?MOD=AJPERES&CACHEID=10e4ff004e0b9c15a2f5f21ad6fc8b25) (last checked 6/23/09).
- [2] NCAA, 2009, National Collegiate Athletic Association Standard for Testing Baseball Bat Performance, BBCOR  
[http://web1.ncaa.org/web\\_files/rules/baseball/bats/NCAA%20BBCOR%20Protocol%20FINAL%205%2009.pdf](http://web1.ncaa.org/web_files/rules/baseball/bats/NCAA%20BBCOR%20Protocol%20FINAL%205%2009.pdf) (last checked 6/21/10).
- [3] Cross, R, 1998, "Sweet Spot of a Baseball Bat," American Journal of Physics, Vol. 66 No. 9, pp. 772-779.
- [4] Naruo, T. Sato, Fuminobu, 1997 "Performance of Baseball Bat" *Proceedings 5<sup>th</sup> Japan Int. Soc. Adv. Mat. Proc. Eng. Symp.*, pp1311-1316, Tokyo.
- [5] Brody, H 1990, "Models of Baseball bats," American Journal of Physics, Vol. 58, No.8, pp.756-758.
- [6] Noble, L., 1998, "Inertial and Vibrational Characteristic of Softball and Baseball Bats: Research and Design Implications," *Proceedings of the 16th Int. Symp. Biomechanics in Sport*, pp. 86-97.
- [7] Noble, L., 1999, "Softball Bat vibrations During the Swing and Impact: A preliminary Analysis of Empirical Data," *Proceedings of the 17th Int. Symp. Biomechanics in Sport*, pp. 323-326.
- [8] Russell, D. A. 2004 "Hoop frequency as a predictor of performance for softball bats," *Engineering of Sport 5*, Vol. 2, pp. 641-647, *Proceedings of the International Sports Engineering Association*, Davis, CA, September 13-16.
- [9] Fleisig, G.S., Zheng, N, Stodden, DF. and Andrews, J.R. 2002 "Relationship between bat mass properties and bat velocity," *Sports Engineering*, Vol. 5, pp.1-14.
- [10] Adair, R.K 2002, *The physics of baseball*, 3<sup>rd</sup> edn. Harper Collins, New York.
- [11] Nathan, A.M., 2003, "Characterizing the Performance of Baseball Bats", American Journal of Physics, Vol. 71, No.2, pp.134-143.
- [12] Bahill, A. Terry, 2004, "The Ideal Moment of Inertia for a Baseball or Softball Bat," *IEEE Transactions on systems, Man, and Cybernetics—Part A: Systems and Humans*, Vol.34, No.2, pp.197-204.

- [13] Greenwald, R. M., Crisco, J. J., Penna, L.H., 2001, "Differences in batted ball speed with wood and aluminum baseball bats: a batting cage study," *J. Appl. Biomech.* 17: pp.241-252.
- [14] Smith, L, Broker, J, Nathan, A, "A Study of Softball Player Swing Speed," *Sports Dynamics Discovery and Application*, 2003, pp. 12-17.
- [15] Cochran, A. J., 2002, "Development and use of one-dimensional models of a golf ball," *Journal of Sports Science* Vol. 20, pp. 635-641.
- [16] ASTM Standard F2398-04, 2004, Standard Test Method for Measuring Moment of Inertia and Center of Percussion of a Baseball or Softball Bat.
- [17] Jones, J., Sherwood, J., and Drane, P., 2008, "Experimental Investigation of Youth Baseball Bat Performance," *Proceedings of the 7th International Conference on the Engineering of Sport*, July, Biarritz, France.
- [18] Broe, M., 2010, "The Evolution of Composite Baseball Bat Performance," MS Thesis, University of Massachusetts Lowell.
- [19] Cruz, C., 2005, "Characterizing Softball Bat Modifications and Their Resulting Performance Affects," M.S. Thesis in Mechanical Engineering, Washington State University.
- [20] NCAA, 2009, National Collegiate Athletic Association Standard for Accelerated Break-In Procedure,  
[http://web1.ncaa.org/web\\_files/rules/baseball/bats/NCAAABIProcedure.pdf](http://web1.ncaa.org/web_files/rules/baseball/bats/NCAAABIProcedure.pdf)  
(last checked 6/14/10).
- [21] Vedula, G., 2004, "Experimental and Finite Element Study of the Design Parameters of an Aluminum Baseball Bat," MS Thesis, University of Massachusetts Lowell.

## Appendix A: Quick Modal Test Validation

Full modal tests were performed on several nonwood bats and one aluminum cylinder. The purpose of these tests was to validate a procedure to measure the hoop frequencies of nonwood baseball bats without having to perform a full modal test.

A simple structure of an aluminum cylinder was investigated. The cylinder had four lines drawn around the circumference using 1-in. spacing. Eight points were placed on each line spaced evenly around the circumference. The cylinder was hung in a simulated free-free condition as shown in Figure A1.

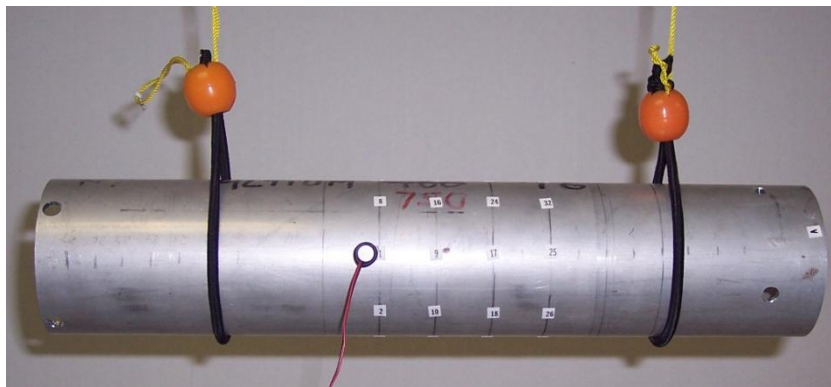


Figure A71: Aluminum cylinder in a simulated free-free condition with points labeled

An accelerometer was placed at one of the points. The average of five impacts was taken at each location. The frequency response function (FRF) data computed by the RT Pro Photon 6.0 data acquisition program was imported into ME-Scope, a computer program used to analyze modal data and animate mode shapes.

A structure of the tested section of the aluminum tube was created in ME-Scope. The imported test data were used to extract the mode shapes. The structure was then animated to visually show an animation of the mode shapes of the section of the



aluminum tube. Figure A2 shows a screen shot of the animation along with the FRF. The first peak of the FRF was determined to be the first hoop mode of the cylinder. Because the cylinder is so short, the first bending mode does not occur until  $\sim 3000$  Hz.

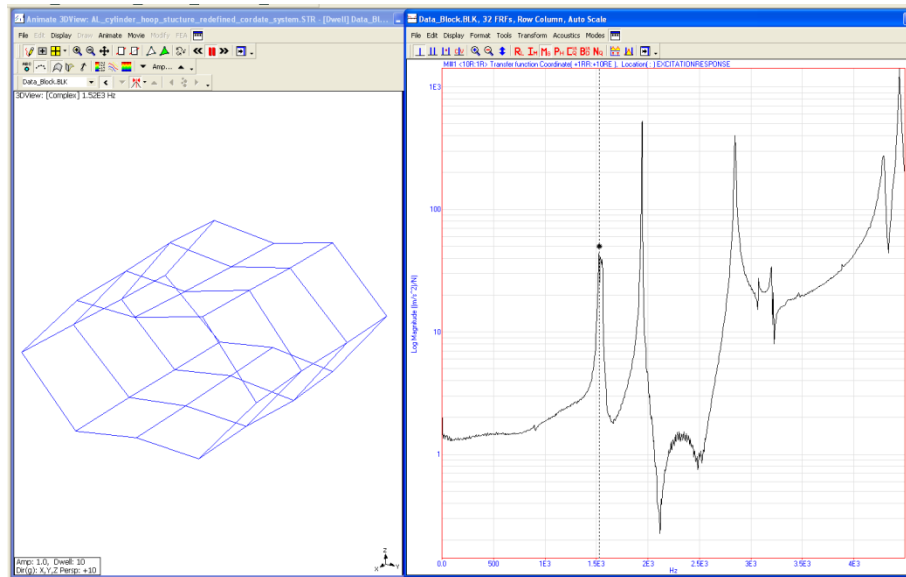


Figure A72: ME-Scope animation of the first mode shape of the aluminum cylinder

A second modal test was performed to help create a fast test for measuring the hoop frequencies. Two accelerometers were placed on the cylinder approximately 90 degrees from one another with the impacts on the same side as one of the accelerometers. The average of five impacts was taken on the barrel. The FRF was computed for each accelerometer and overlaid. Figure A3 shows the overlay plot of the FRF.

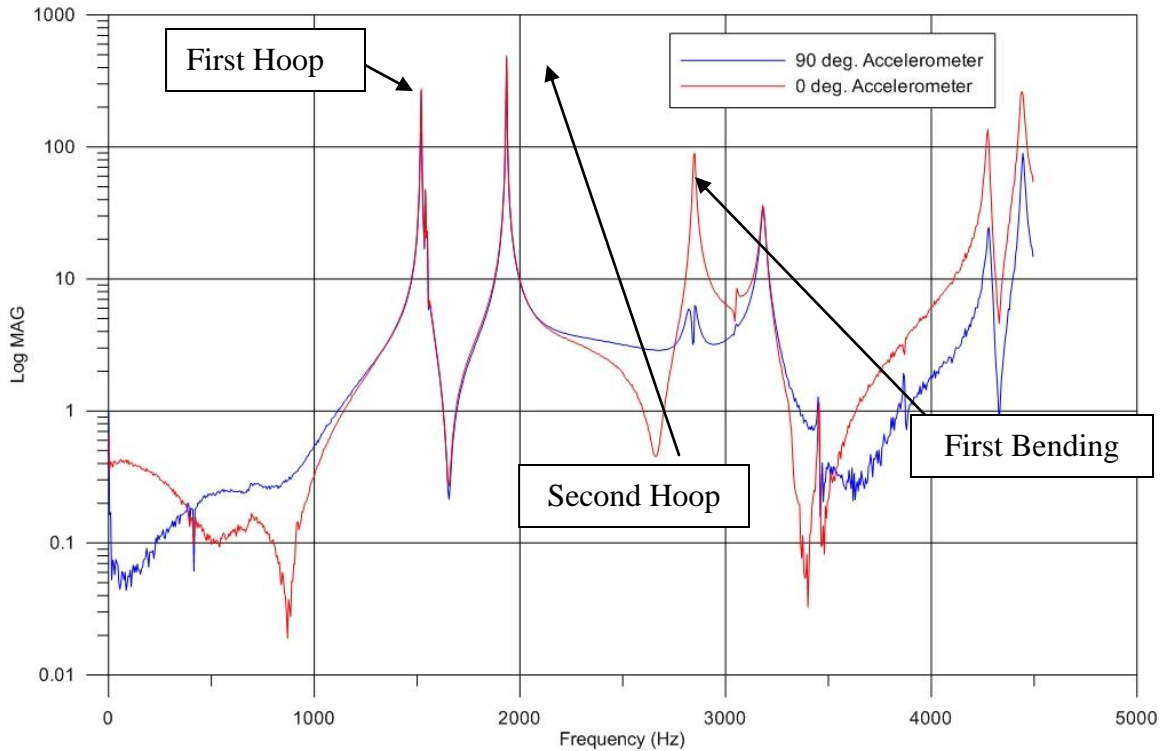


Figure A73: Measured FRF of aluminum cylinder using two accelerometers

As the FRFs for the two accelerometers are overlaid, it is shown that some of the peaks have the same magnitudes. Upon matching up the animated mode shapes from ME-scope to the corresponding peaks, the peaks show the hoop modes of the cylinder. As stated previously, the first hoop mode was found to be the first peak in the FRF, the second hoop mode was found to be the second peak, and the third peak was found to be the first bending mode for this “short” tube. In Figure A3, it can be seen that the hoop mode could be measured using two accelerometers mounted approximately 90 degrees from one another. To check the validity of this test method, a baseball bat was tested using a similar procedure.

Several baseball bats underwent a modal test to evaluate the quick method of measuring hoop frequencies as well as one bat that underwent a complete barrel modal test. For the complete modal test, twelve rings spaced 1.0-in. apart were labeled at ten locations spaced evenly around the circumference. Figure A4 shows the barrel of the bat as labeled.

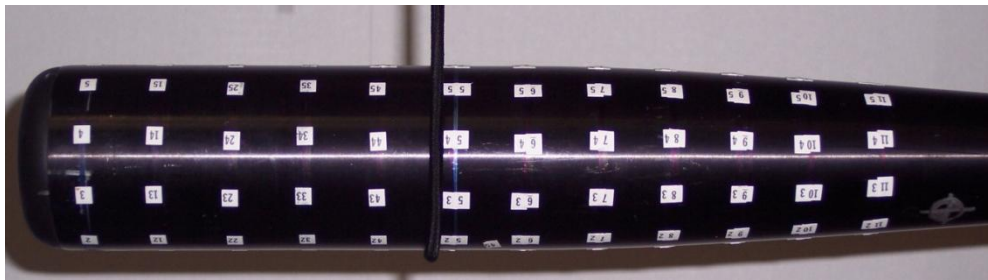


Figure A74: Labeled barrel of baseball bat.

Bats were hung in a simulated free-free boundary condition, and a single accelerometer was placed on one of the numbered locations. The average of five impacts was taken at each of the 120 locations. The data block was imported into ME-Scope, and a cylindrical structure was made representing the barrel of the bat. The data were exported from the RT Pro Photon 6.0 program and imported into the ME-scope program where mode shapes were computed. An animation of the barrel was performed at each of the peaks of the FRF. The first hoop mode of the barrel was found to be at 2100 Hz. Figure A5 shows an image of the ME-scope program with the barrel of the bat animating the first hoop mode.

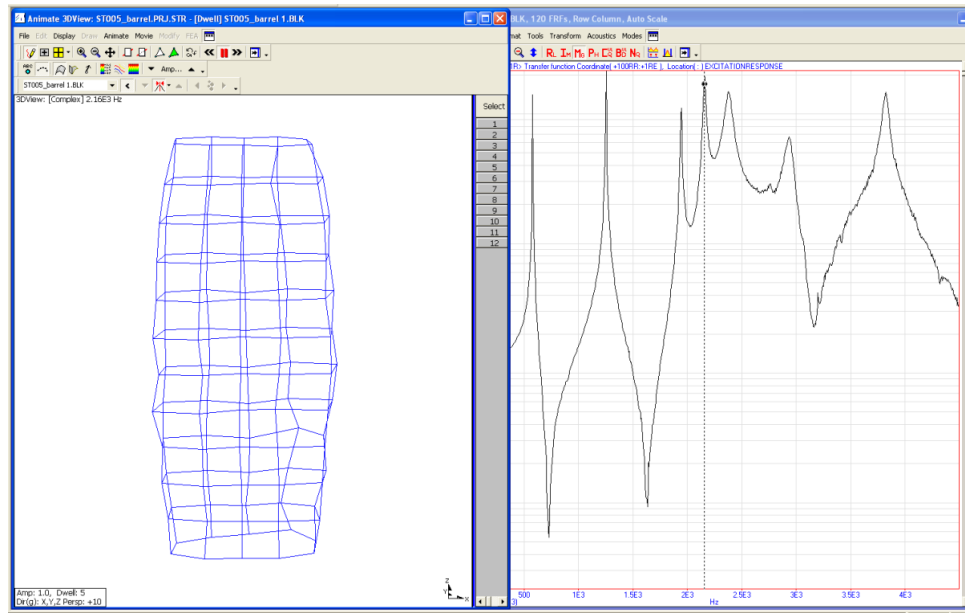


Figure A75: ME-Scope animation of the first hoop mode of a baseball bat barrel

A second test was performed on the bat using two accelerometers placed on the barrel approximately 90 degrees from one another with impacts on the same side as one of the two accelerometers. Figure A6 shows the configuration of the accelerometers.

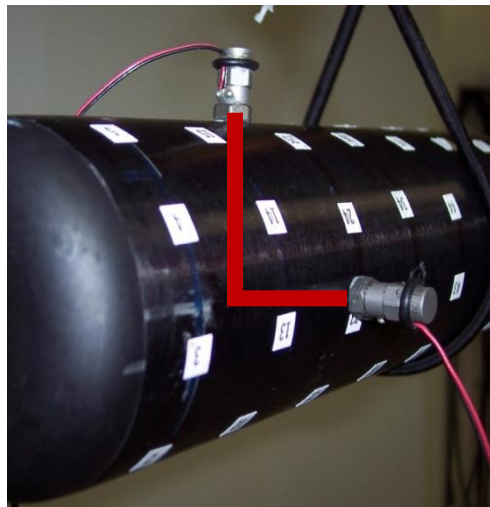


Figure A76: Accelerometers mounted on the barrel of the bat approximately 90 degrees apart

The average of five impacts was taken at the 6-in. location on the barrel of the bat. The FRF was computed from each accelerometer and overlaid. Figure A7 shows the resulting FRF from the impact test. Due to the bat barrel length to diameter being greater than the tube used in the initial part of this study, it can be observed in Figure A7 that the bending modes occur at lower frequencies than the hoop modes for the bat barrel.

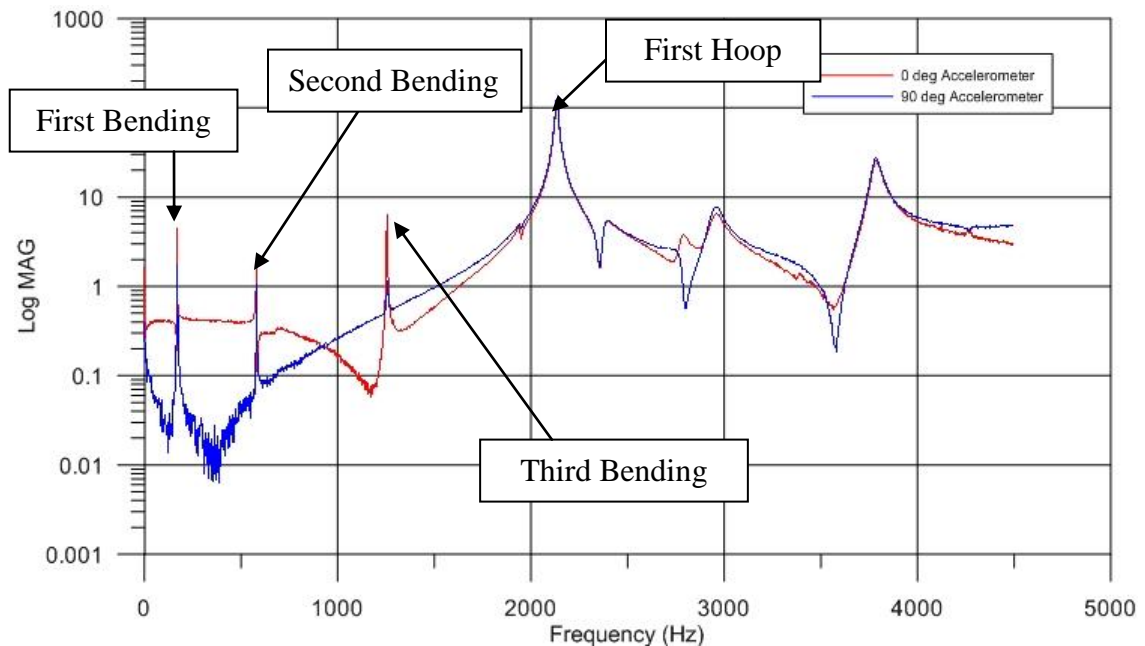


Figure A77: Baseball bat barrel FRF of two accelerometers overlaid

Using ME-scope, each of the peaks in the FRF was determined to be individual modes of the baseball bat. As noted in Figure A7, the first peak was determined to be the first bending mode, the second peak was the second bending mode, and the third peak was the third bending mode. The point where the FRF from both accelerometers overlaid, the fourth peak, is at the same frequency at which the first hoop mode was observed in the ME-Scope animation.

From these results and the aluminum cylinder, it was determined that using two accelerometers to measure the hoop frequency is a valid test methodology to determine the hoop modes.

## Appendix B: BESR vs. Drop Individual Plots for the Wood Bats

Figures B1 through B5 are of BESR vs. drop for each of the various lengths of wood bats investigated in this research. As the drop of the baseball bat becomes less negative, i.e. overall bat weight increases, the performance of the baseball bat increases. As the drop for a bat becomes more negative, the weight of the bat decreases, and the MOI should also decrease. These plots show as that as the drop of the bat becomes less negative the performance of the wood baseball bats for BESR increases.

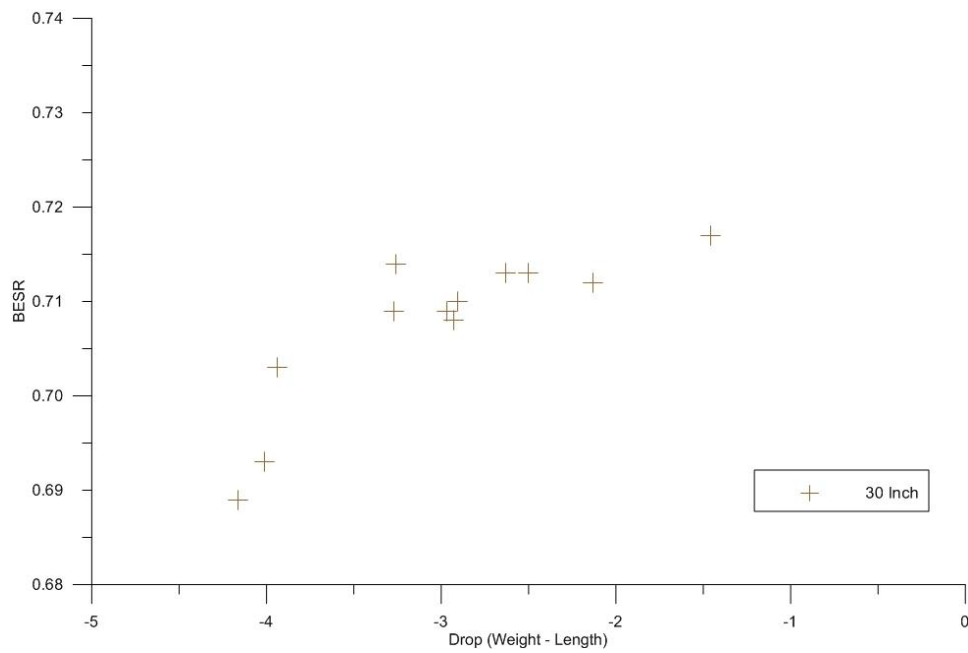


Figure B1: BESR vs. Drop for 30-in. wood

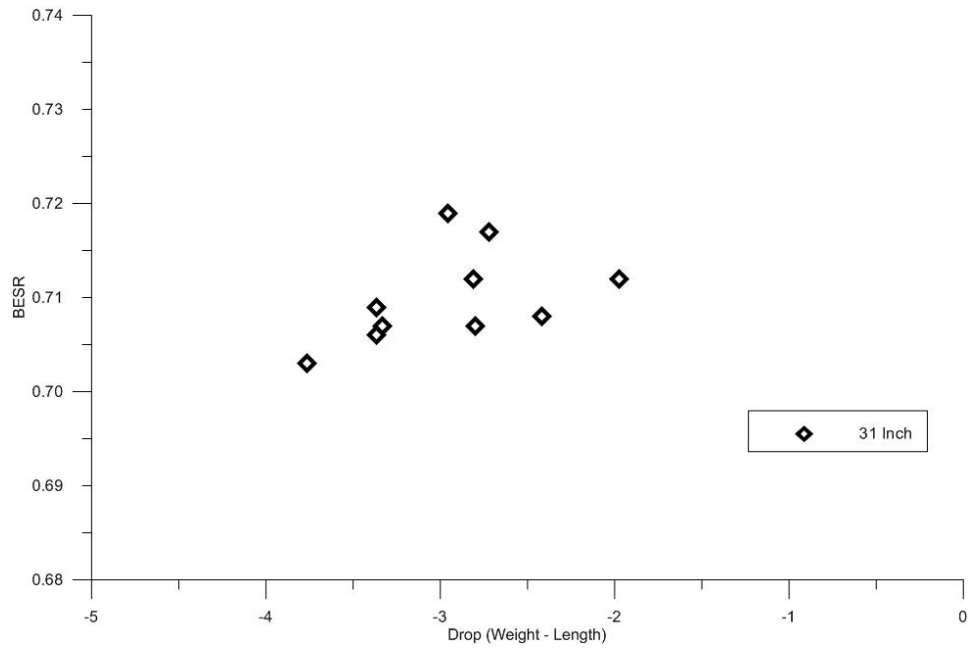


Figure B2: BESR vs. Drop for 31-in. wood

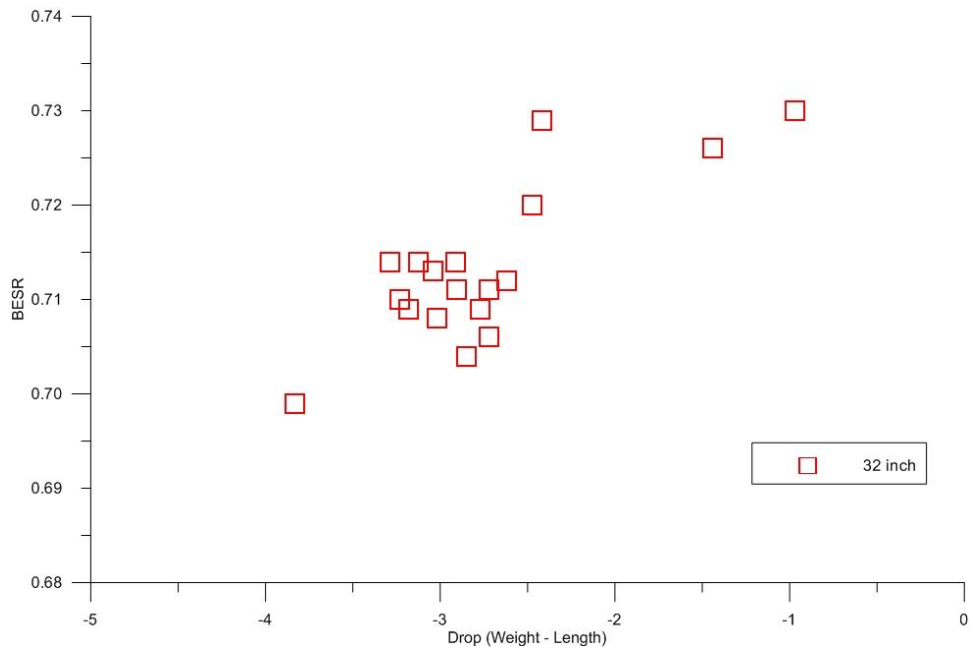


Figure B3: BESR vs. Drop for 32-in. wood



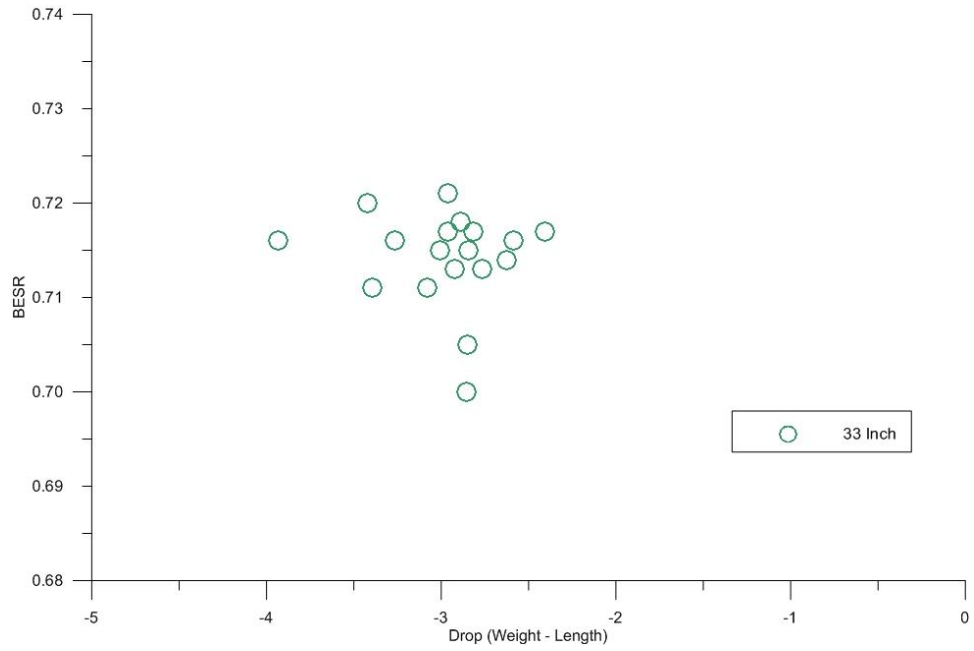


Figure B4: BESR vs. Drop for 33-in. wood

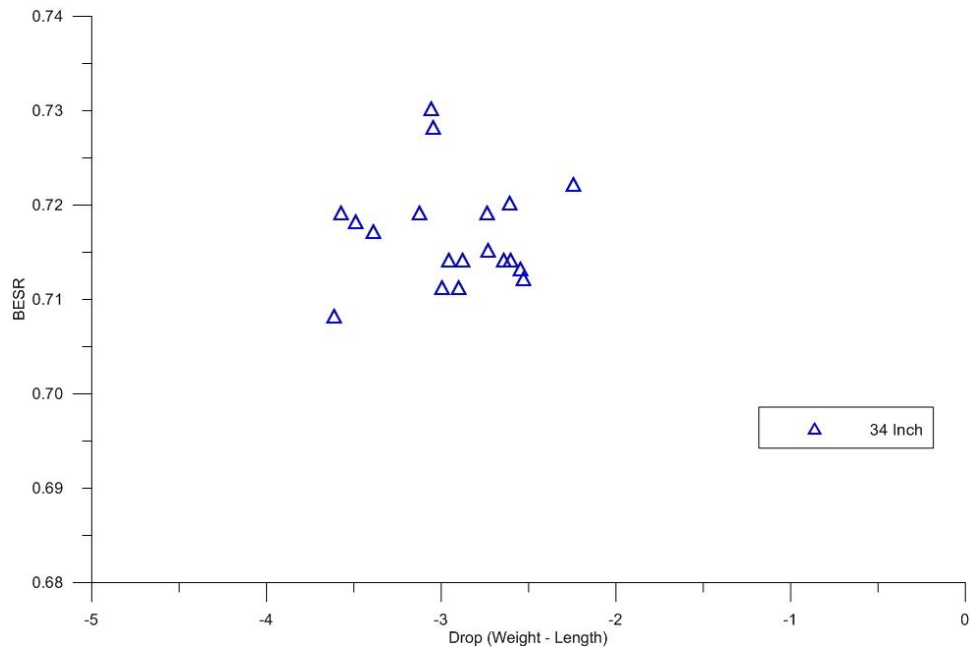


Figure B5: BESR vs. Drop for 34-in. wood

## Appendix C: BBS vs. MOI of Nonwood Bats Submitted for BBCOR Certification

Figures C1, C2 and C3 show plots of BBS vs. MOI for the 32-in., 33-in. and 34-in. bat lengths, respectively. These plots show the data that was previously given in Section 4.2.2 with additional data of bats recently submitted for BBCOR certification. All of these additional bats are aluminum. Each of the bats went through a complete BBCOR certification [2] procedure. The BBCOR procedure is similar to the BESR procedure, however, there are tighter tolerances on the inbound and rebound velocities of the baseball in the BBCOR protocol than in the BESR test protocol. The BBCOR bats tested have relatively high MOI for their length and are lower in performance than the BESR bats.

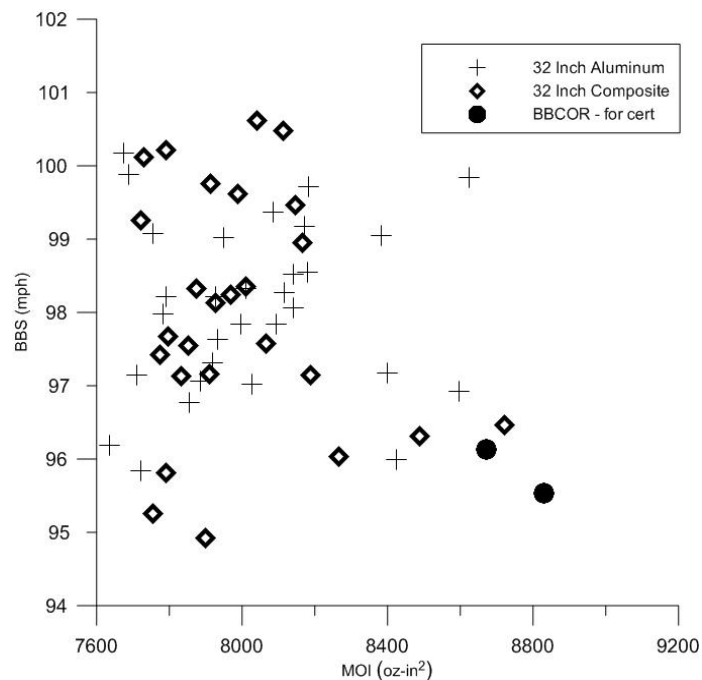


Figure C78 BBS vs. MOI for 32-in. nonwood bats with BBCOR certification bats

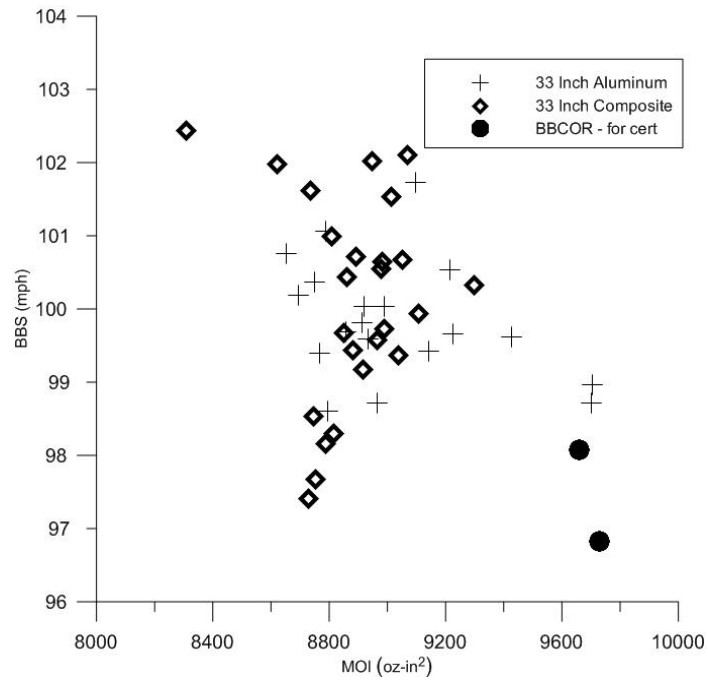


Figure C79: BBS vs. MOI for 33-in. nonwood bats with BBCOR cert bats

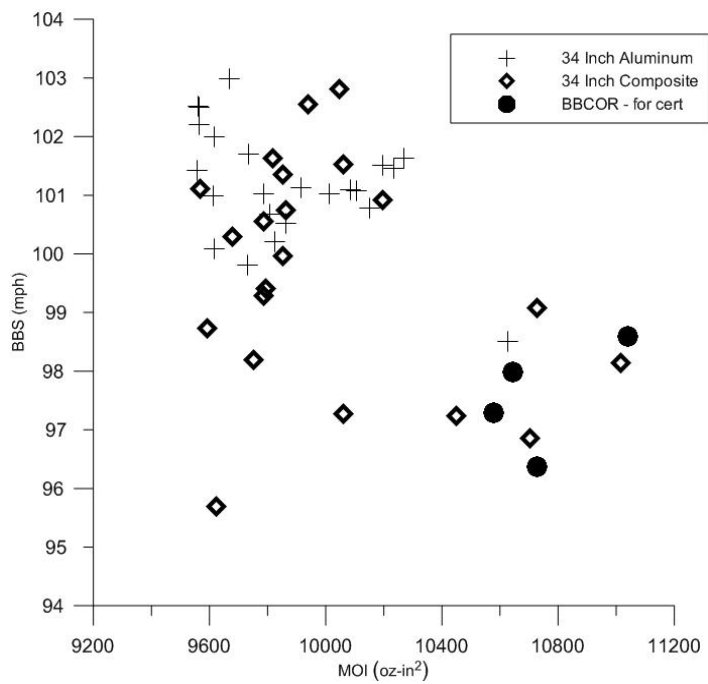


Figure C80: BBS vs. MOI for 34-in. nonwood bats with BBCOR cert bats

## Appendix D: Mass-Spring-Dashpot MATLAB Code

A MATLAB code was used to solve the two degree of freedom system described in Section 4.4.1. The code uses the ODE solver 23t provided in MATLAB to solve the system of equations. The maximum rebound velocity is computed for each hoop frequency, and the COR is computed and normalized to show an improvement in COR. A plot of Normalized COR versus hoop frequency is then created.

```
% Andrew Sutton
% November 24th 2009,
% This script simulates a simple mass-spring-dashpot model of the
trampoline
% effect of the bat ball collision. The ball is modeled as a nonlinear
% system. File battedball.m is needed. The differential equations of
motion
% are solved using ode solver 23t. The bat is considered to be
stationary.
% An inbound velocity of 136 mph is used for the initial condition.
% The code steps through hoop frequencies

% getting started
clear all, close all, nfig=0;
clc
global k1 k2 c1 c2 m1 m2 a b
%

% Softball values
% m1 = 0.180;           % mass of the ball 180 grams
% k1 = 40.6*10^6;      % stiffness of the bat N/m
% c1 = 4700;           % Ball damping coefficient
% a = 0.65;            % non linear spring coefficient
% b = 0.5;              % non linear spring coefficient
% m2 = 0.150           %effective mass in the religion of barrel in
contact with the ball 150 grams

% Baseball Values
m1 = 0.145;           % mass of the ball 145 grams
k1 = 60*10^6          % stiffness of the ball N/m
c1 = 5000;            % Ball damping coefficient
a = .6495;            % non linear spring coefficient
b = .5202;            % non linear spring coefficient
```

```

m2 = 0.090;           % effective mass in the religion of barrel in
contact with the ball 90 grams
c2 = 90.5;           % bat damping constant

% used to check the COR calculation, where the bat is "rigid"
hoop_freq = 100000; % hoop frequency to test for very stiff bat for
COR
k2 = (hoop_freq*2*pi)^2*m2; % Calculation of barrel stiffness based on
mass and hoop frequency

t1=linspace(0,.002);

% Initial Conditions
x1 = 0;               % initial position of the ball (m)
v1 = -60.80;         % initial velocity of the ball (m/s)
x2 = 0;               % initial position of the bat (m)
v2 = 0;               % initial velocity of the bat (m/s)

% tolerance option used in the calculation of the ODE
tol = .000001;
options = odeset('RelTol',tol);

% Calculating COR off of a "rigid" bat

[t,v]=ode23t('battedball',t1,[x1,v1,x2,v2],options);
maxV = max(v(:,2));
COR_WALL= abs(maxV/v1)

%
% Check to see the velocity of the ball rebound speed
% nfig=nfig+1 ;
% figure(nfig)
% plot(t(:,1),v(:,2),'b-.','LineWidth',2)
%

% Solution solving for various hoop frequencies

hoop_frequ = 100:25:10000;

for i = 1:1:length(hoop_frequ)
    k2 = (hoop_frequ(i)*2*pi)^2*m2;
    [t,v]=ode23t('battedball',t1,[x1,v1,x2,v2],options);
    maxV(i) = max(v(:,2)); % Maximum rebound velocity
    COR(i) = abs(maxV(i)/v1); % Calculating the COR
end

% calculation and plot of Normalized COR
COR = COR/.4892;
nfig=nfig+1 ;
figure(nfig)
plot(hoop_frequ,COR)
axis([0 5000 1 1.5])
grid

```

```
xlabel('Hoop Frequency(Hz)'); ylabel('Normalized OR');

% Andrew Sutton
% October 17th, 2009
% This script is used to solve 2 non linear mass, spring, dashpot model
of the simulation of the bat ball collision. The ball is summated to
be non linear while the barrel of the bat is linear. The equations of
motion are in state space.

% k = spring stiffness
% c = damping
% m = mass
% a and b are

function dz = battedball(t,z)
dz = zeros(4,1);
global k1 k2 c1 c2 m1 m2 a b

dz(1)= z(2);
dz(2)=(-k1*(z(1)-z(3))*abs(z(1)-z(3))^a-c1*(z(2)-z(4))*abs(z(1)-
z(3))^b)/m1;
dz(3)= z(4);
dz(4)=(-k2*z(3)-c2*z(4)+k1*(z(1)-z(3))*abs(z(1)-z(3))^a+c1*(z(2)-
z(4))*abs(z(1)-z(3))^b)/m2;
```

## Appendix E: Accelerated Break-In Procedure

The procedure used for the Accelerated Break-in is outlined in this Appendix. The procedure is taken directly from the NCAA protocol for conducting accelerated break in [20]. The roller used during the process is shown in Figure C1.



Figure E81: Roller used in ABI procedure

**NCAA Accelerated Break-In Procedure**  
**30-September-09**

The accelerated break-in procedure is meant to demonstrate how a composite bat will perform during its potential useful life in the field. This test procedure may be used with the NCAA BESR or BBCOR test to quantify the effect that bat usage has on performance and may be used in the certification and compliance testing of composite barrel bats. The procedure is subject to change at anytime.

**Procedure:**

- 1. Measure preliminary properties of the bat per the NCAA BESR or BBCOR Certification Test Protocol and measure an initial barrel compression ( $BC_0$ ).**  
Follow the attached barrel compression procedure.

- 2. Measure bat performance (i.e.  $BESR-i$  or  $BBCOR-i$ , where  $i=1$  to denote the first BESR test cycle).**  
Follow the NCAA BESR or BBCOR test protocol.  
Define  $BESR_{max}$  or  $BBCOR_{max}$  as the average of the six valid hits at the sweet spot.  
If visible damage is observed or the performance limit is exceeded during the first performance test cycle, then stop the test and go to step 8.

- 3. Measure barrel compression ( $BC_{i,j}$ ), where ( $j=0$ )**  
Follow the attached barrel compression procedure and calculate the percent change in barrel compression,  $\Delta BC_0$ , using,

$$\Delta BC_0 = \left( \frac{BC_0 - BC_{1,0}}{BC_0} \right) \times 100\%$$

If the barrel compression change ( $\Delta BC_0$ ) is greater than 15%, then proceed directly to step 7.

- 4. Roll the barrel**  
Follow the attached rolling procedure.  
Increment subscript notation: ( $j=j+1$ , where  $j$  is used to keep track of the roll process)

- 5. Measure barrel compression ( $BC_{i,j}$ )**  
Follow the attached barrel compression procedure.  
Compute the percent change in barrel compression,  $\Delta BC_{i,i}$ , according to

$$\Delta BC_{i,j} = \left( \frac{BC_{i,0} - BC_{i,j}}{BC_{i,0}} \right) \times 100\%$$

- 6. Repeat steps 4 and 5 (Increase rolling depth by increments of ~0.0125 in.) until a barrel compression ( $\Delta BC_{i,j}$ ), reduction of at least 5% is achieved.** The target barrel compression reduction should be as close to 5% as possible.



**7. Measure bat performance (i.e. *BESR-i* or *BBCOR-i*), where ( $i=i+1$ , i.e. set value of  $i$  to denote performance test cycle)**

Follow the NCAA BESR or BBCOR test protocol.

Order of testing axial impact locations may be adjusted by test operator, if necessary.

Define  $BESR_{max}$  or  $BBCOR_{max}$  as the average of the six valid hits at the highest performing location from this test cycle or keep as-is from a previous performance test cycle, whichever is greater.

Check compliance as specified in step 8.

**8. Compliance check**

**The bat fails if:**

- During the performance test, the bat exceeds the performance limit or does not make it through a complete test without visible damage (damage criterion only applies to first performance-test cycle).

**The bat passes if:**

- During a performance test subsequent to the first performance-test cycle, the bat exhibits a sweet spot performance reduction of at least 0.014 in BESR or 0.018 in BBCOR from the maximum bat performance  $BESR_{max}$  or  $BBCOR_{max}$ .

**If the bat has neither passed nor failed**, then proceed to step 9.

**9. Measure barrel compression ( $BC_{i,0}$ )**

Follow the attached barrel compression procedure and calculate the percent change in barrel compression,  $\Delta BC_i$ , using,

$$\Delta BC_i = \left( \frac{BC_{i,0} - BC_{(i-1),j}}{BC_{i,0}} \right) \times 100\%$$

If barrel compression change ( $\Delta BC_i$ ) is greater than 15%, then proceed directly to step 7, otherwise proceed to step 4 and reset  $j=0$ .

**Notes:**

1. This procedure is not necessarily all inclusive and is subject to change at anytime.
2. For purposes of this method, a composite bat uses a fiber reinforced polymer (or similar material whose properties may change with impact) in the barrel portion of the bat.
3. A bat is determined to be broken, during the first performance test only, when a visible crack appears (excluding cracks in the paint or clear coat) or the bat fails the NCAA ring test (as defined in the NCAA BESR or BBCOR bat performance protocol). For subsequent performance test cycles (second, third and so on), damage in the bat is not quantified by the test operator and the bat is tested with respect to the damage criterion until the bat is damaged such that further testing cannot reasonably be accomplished.

4. At the discretion of the test sponsor, the test sponsor may request the test to be continued after failure due to exceeding the performance limit but the bat is still in usable condition. The cost of the continued testing is at the expense of the test sponsor.

#### Barrel Rolling Procedure

Purpose: To accelerate break-in of composite bats.

Apparatus (as described here or similar such device)

- Two nylon wheels – 1.5 to 3.0 in. in diameter
- Fixture to press wheels into barrel in ~0.0125-in. increments
- Device to roll the barrel

Procedure:

1. Place the barrel of the bat in the fixture with the rollers contacting the bat at 6 in. from the endcap and the 0° orientation (as identified during the Barrel Compression Procedure) facing up.
2. Bring roller in contact with the barrel. Displace the rollers ~0.10 in. for initial rolling or ~0.0125 in. greater than the previous time through the Barrel Rolling Procedure.
3. Roll the barrel to within 2.0 to 2.5 in. of endcap and past the taper (no contact between rollers and bat) as shown in Fig. 1. Roll the bat 10 times in each direction. Popping and cracking sounds during this process are normal. (A different number of rolls can be used at the operator's discretion.)
4. Uncompress the bat.
5. Rotate the bat 90° from initial location and repeat steps 1-4.
6. Rotate the bat 45° from initial location and repeat steps 1-4.
7. Rotate the bat -45° from initial location and repeat steps 1-4.
8. For rolling beyond 0.1 in., increase displacement by increments of about 0.0125 in.

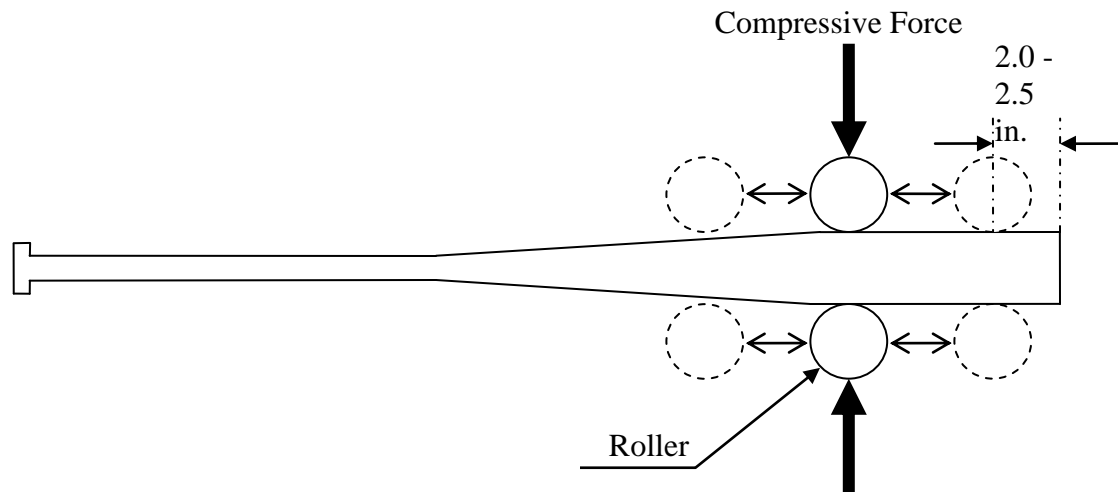


Fig. 1 Rolling parameters

#### Barrel Compression Procedure

Purpose: To measure the barrel compression.

Apparatus:

- Load frame capable of 1000 lbf
- Cylindrical steel loading noses with 3.86 in. in diameter curvature and long enough to maintain proper contact throughout the test
- Means of measuring load and displacement

Procedure:

1. Mark a side on the barrel of the bat that will be the 0° orientation.
2. Set the force gage to zero.
3. Place the bat in the fixture to make contact at 6 in. from the tip of the endcap as shown in Fig. 2 and with the 0° orientation facing up.
4. Activate the fixture until both cylindrical surfaces are in contact with the barrel of the bat.
5. Compress the bat with 5 to 15 pounds of force.
6. Zero the displacement gage.
7. Compress the barrel 0.01 in. at a rate of about 0.15 in/min.
8. Zero the force and displacement gages.
9. Compress the barrel (an additional) 0.03 in.<sup>1</sup> at a rate of about 0.15 in/min.
10. Record the force ( $F$ ).
11. Release the force.
12. Rotate the bat 90° from the initial rotation. Repeat steps 2 through 11
13. Rotate the bat 45° from the initial rotation. Repeat steps 2 through 11
14. Rotate the bat -45° from the initial rotation. Repeat steps 2 through 11.
15. Compute the barrel compression,  $BC$ , from the average of each axis by:

$$BC = \frac{1}{4} \{ (F)_0 + (F)_{90} + (F)_{45} + (F)_{-45} \}$$

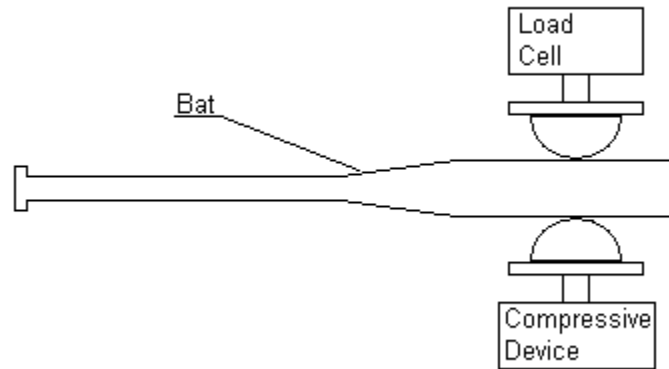


Fig. 2 Compression testing

Note 1: If Force exceeds the load-cell capacity, then the operator may choose to use less displacement (e.g. 0.025 in.). This new displacement must then be used throughout the entire ABI test when measuring barrel compression and be identified in any reports of the tests.